

**ROLE OF NITRIC OXIDE AND MITOCHONDRIA IN
MUSCLE PARALYSIS INDUCED BY ACUTE
ORGANOPHOSPHATE POISONING**

**A THESIS SUBMITTED TO
THE TAMILNADU DR. M.G.R MEDICAL UNIVERSITY, CHENNAI**

For the degree of
DOCTOR OF PHILOSOPHY

By
V. RAGHUPATHY



**THE WELLCOME TRUST RESEARCH LABORATORY
DEPARTMENT OF GASTROINTESTINAL SCIENCES
CHRISTIAN MEDICAL COLLEGE
VELLORE 632 004
TAMIL NADU
INDIA**

JULY 2012

DECLARATION OF THE CANDIDATE

This is to declare that the thesis entitled "ROLE OF NITRIC OXIDE AND MITOCHONDRIA IN MUSCLE PARALYSIS INDUCED BY ACUTE ORGANOPHOSPHATE POISONING" is based on the results of the work carried out by me for the degree of DOCTOR OF PHILOSOPHY under the supervision and guidance of Dr. Anup Ramachandran, Professor, The Wellcome Trust Research Laboratory, Department of Gastrointestinal Sciences, Christian Medical College, Vellore. This work has not formed the basis of any associateship, fellowship, degree or diploma of any other University. This thesis was written on the basis of regulations prescribed by The Tamil Nadu Dr. M.G.R. Medical University, Chennai.


V. Raghupathy,

Ph.D. Candidate,
The Wellcome Trust Research Laboratory,
Department of Gastrointestinal Sciences,
Christian Medical College,
Vellore.

Station: Vellore

Date : 18/07/2012

Department of Gastrointestinal Sciences
Christian Medical College
Vellore - 632 004, Tamil Nadu, India
The Wellcome Trust Research Laboratory



Telephone : 91-416-2282052
Fax : 91-416-2282486, 2232035
E-mail : wellcome@cmcvellore.ac.in

CERTIFICATE

I have the pleasure to certify that V. Raghupathy has worked in the Wellcome Trust Research Laboratory, Department of Gastrointestinal Sciences, Christian Medical College, Vellore from October 2007 and has completed his requirements for the submission of his Ph.D. thesis on "Role of nitric oxide and mitochondria in muscle paralysis induced by acute organophosphate poisoning".

I certify that the thesis represents independent work of the candidate supervised by me during the course of study.

I certify that this thesis is a bonafide record of research work by the candidate during the period of study under me and it has not previously formed the basis for any degree or diploma of any other University.

Anup Ramachandran, Ph.D.
Professor of Biochemistry
(Supervisor / Guide)

Date: July 17, 2012.



DEPARTMENT OF CLINICAL BIOCHEMISTRY

Accredited by NABL / IS / ISO 15189 : 2003

CHRISTIAN MEDICAL COLLEGE

P.O. Box No. 3, VELLORE - 632 004. TAMIL NADU, INDIA.



Telephone : 91 0416 2282170
Fax : 91 0416 2232035 / 2225035
E-mail : clinbio@cmcvellore.ac.in

Certificate No. M - 0036

Dr. R. Selvakumar, Professor & Head
Dr. Joe Fleming, Visiting Professor

Dr. F.S. Geethanjali, Associate Professor
Dr. Victoria Job, Associate Professor

12.07.2012

CERTIFICATE FROM CO-GUIDE

This is to certify that the thesis entitled "Role of nitric oxide and mitochondria in muscle paralysis induced by acute organophosphate poisoning" is based on results of work carried out by V. Raghupathy for the Ph.D. degree under my co-guidance. This work has not been submitted for any degree or diploma of any other university.

Dr F.S. Geethanjali (Co-Guide)
Professor of Biochemistry
Department of Clinical Biochemistry
CMC, Vellore.

**DEPARTMENT OF CLINICAL BIOCHEMISTRY
CHRISTIAN MEDICAL COLLEGE
VELLORE - 632004. SOUTH INDIA**

Christian Medical College
Thorapadi post,
Vellore 632002.
Tamil Nadu, S. India.



Phone: +91 416 228 4268
Fax: +91 416 226 2788, 226 2268
Email: physio@cmcvellore.ac.in

July 12, 2012

To Whomsoever it may concern

This is to certify that the animal studies done by V. Raghupathy as part of his PhD thesis titled "ROLE OF NITRIC OXIDE AND MITOCHONDRIA IN MUSCLE PARALYSIS INDUCED BY ACUTE ORGANOPHOSPHATE POISONING ", was approved by the Institutional Animal Ethics Committee of Christian Medical College, Vellore (IAEC Approval Number 02/2007).

Solomon Sathishkumar
Secretary, Institutional Animal Ethics Committee.
Associate Professor of Physiology

Department of Physiology
Christian Medical College,
Vellore - 632 002, Tamilnadu, India.

ACKNOWLEDGEMENTS

First and foremost I would like to express my gratitude to **Prof. Anup Ramachandran**, my mentor for his patience, encouragement and exceptional moral support throughout the course of this study.

I express my heartfelt gratitude to **Dr. Anna Oommen** for her scientific discussions and support throughout the course of this study. This work would not have been fulfilled without her help.

I would like to thank **Prof. F.S. Geethanjali**, my co-guide for her help and support.

I thank **Prof. Anand Zachariah** and **Prof. K.A. Balasubramanian** for their scientific valuable input and suggestions.

I would like to thank **Mr. Roy Cherian, Mrs. Rebecca Cherian and Mr. S. Jayakumar** for their help and moral support.

I am grateful to **Mr. Jayaraman** and **Mr. G. Jayakumar** for their help and constant support.

I would like to acknowledge my seniors, **Dr. Sathish, Dr. Prabhakar, Dr. Venkatesh, Dr. Parthiban, Dr. Amajad, Dr. Pughaz, Dr. Srikanth, Mr. Jayakanth** and **Mr. Tamil selvan** for their advice and help. I extend my thanks to my colleagues **Mr. Dhanarajan, Mrs. Sophia, Ms. Kavitha Priya,**

Mrs. Kavitha Ruban, Mr. Santhosh and all the neurochemistry lab members for all their help.

My sincere thanks to **Mr. Thirumani** and **Mrs. Kumari** for their secretarial assistance.

I thank **Mr. Antony Raj** and **Mr. Yesudoss** for offering help in conducting experiments with rats.

I express my sincere thanks to the authorities of **The Christian Medical College, Vellore** and **Department of Gastrointestinal Sciences**, for allowing this work to be carried out.

I greatly acknowledge the **Defence Research and Development Organization**, Government of India and **Department of Neurological sciences, Christian Medical College, Vellore** for their financial support.

I thank my **family** and **friends** for their support.

CONTENTS

CHAPTER	TITLE	PAGE NO
	Abstract	1 - 4
1	Introduction and review of literature	5 - 37
	Aims and Objectives	38 - 39
2	Materials and Methods	40 - 53
3	Results	54 - 70
4	General discussion and conclusion	71 - 88
	Bibliography	89 - 114
	Publication	115

List of abbreviations

ACh	Acetylcholine
AChE	Acetylcholinesterase
ATP	Adenosine triphosphate
ADP	Adenosine diphosphate
AMP	Adenosine monophosphate
BIAM	N-(biotinoyl)-N'-(iodoacteyl)-ethylenediamine
BN-PAGE	Blue native polyacrylamide gel electrophoresis
BSA	Bovine serum albumin
CHAPS	3-[(3-Cholamidopropyl)dimethylammonio]-1-propanesulfonate
CNS	Central nervous system
DFP	Diisopropylfluorophosphate
DHPR	Dihydropyridine receptor
DTNB	5, 5'-dithiobis (2-nitrobenzoic) acid
DTT	Dithiothreitol
EDTA	Ethylene diamine tetra acetic acid
EGTA	Ethylene glycol tetra acetic acid
FMO	Flavin-containing monooxygenases
GSH	Reduced glutathione
IEF	Isoelectric focusing
IF ₁	Inhibitor protein
IMS	Intermediate syndrome
INT	2- (p-iodophenyl)-3-(p-nitrophenyl)-5-phenyl tetrazolium
IPG	Immobilized pH gradient
KDa	Kilodalton

LBD	Ligand-binding domain
LMS	Lauryl maltoside
L-NAME	N _w - Nitro-L-arginine methyl ester
MCP	Monocrotophos
Mw	Molecular weight
NAD ⁺	Nicotinamide adenine dinucleotide (Oxidised)
NADH	Nicotinamide adenine dinucleotide (Reduced)
nAChRs	Nicotinic acetylcholine receptors
NO	Nitric oxide
OPP	Organophosphate pesticide
OPIDN	Organophosphorus induced delayed neuropathy
PAGE	Polyacrylamide gel electrophoresis
PAS	Peripheral anionic site
PBS	Phosphate buffered saline
PVDF	Polyvinylidene difluoride
RNS	Reactive nitrogen species
RyR1	Ryanodine receptor 1
SD	Standard deviation
SDS	Sodium doedecyl sulphate
SR	Sarcoplasmic reticulum
TBP	Tributylphosphine
TBS	Tris-buffered saline
TCA	Trichloroacetic acid
UQ	Ubiquinone
UQH ₂	Ubiquinol

**ROLE OF NITRIC OXIDE AND MITOCHONDRIA IN MUSCLE
PARALYSIS INDUCED BY ACUTE ORGANOPHOSPHATE POISONING**

ABSTRACT

Acute organophosphate pesticide poisoning is common in India. Organophosphates inhibit acetylcholinesterase resulting in cholinergic hyper-stimulation of the muscle and significant muscle weakness. Prolonged muscle weakness that is poorly defined with respect to its pathogenesis is a major cause of morbidity and mortality of the poisoning. Although acetylcholinesterase inhibition is the primary event that leads to prolonged muscle weakness of organophosphate poisoning, the absence of accompanying acetylcholine induced muscarinic signs suggests the involvement of additional non-cholinergic pathological reactions. This study explores non-cholinergic pathomechanisms that may contribute to organophosphate induced muscle weakness.

The muscle is a high energy requiring organ and low ATP levels slow contraction and weaken the muscle. Organophosphate poisoning is characterized by intense muscle activity that follows severe inhibition of acetylcholinesterase. This may lead to ATP depletion in the muscle if utilization is faster than generation.

Organophosphate poisoning leads to nitric oxide elevation which is associated with organophosphate induced myopathy. This is by nitric oxide induced mitochondrial dysfunction and decreased ATP production.

We suggest that organophosphate induced nitric oxide inhibits mitochondrial ATP synthase and prevents sufficient ATP synthesis for muscle activity that occurs on poisoning. Inadequate muscle ATP levels, in addition to acetylcholinesterase

inhibition, contribute to muscle weakness following organophosphate pesticide poisoning.

The aim of this study was to examine ATP generation and nitric oxide modulation of mitochondrial function in contributing to muscle paralysis induced by acute severe organophosphate pesticide poisoning.

Methods

The study was carried out in rats orally administered monocrotophos (0.8LD₅₀) and sacrificed over a period of 24 hours at different times, corresponding to paralysis, immediate post paralysis, during recovery and on complete recovery of muscle strength. Monocrotophos is a common organophosphate pesticide poison in India. Cis-monocrotophos levels were measured in blood, muscle, muscle mitochondria and urine over the course of poisoning. Skeletal muscle of each rat was assayed for muscle acetylcholinesterase to determine toxicity. ATP synthesis, by oxidative phosphorylation (ATP synthase activity) and glycolysis (muscle lactate levels), and adenine nucleotides, ATP, ADP and AMP were estimated in skeletal muscle of each rat.

Nitric oxide was estimated in skeletal muscle and ATP synthase examined for nitric oxide induced posttranslational modifications such as nitro-tyrosinylation and nitro-cysteinylation.

The studies were repeated in animals treated with L-NAME, an inhibitor of nitric oxide synthase to confirm the role of nitric oxide modulation of mitochondrial function induced on organophosphate poisoning.

Results

Monocrotophos (0.8LD₅₀) rapidly induced muscle weakness within 15 minutes, and paralysis within 50 minutes in rats. There was complete recovery of muscle power 24 hours later with no treatment. Cis-monocrotophos was cleared from blood and muscle of poisoned rats within 24.0 hours of poisoning.

Severe inhibition of muscle acetylcholinesterase, 67%, occurred within 15 minutes of poisoning that increased significantly to 80% after paralysis and decreased to 55% as muscle regained power. Muscle mitochondrial ATP synthase was inhibited 54% and lactate 40% following paralysis with a recovery in muscle that regained power. Adenylate energy charge of skeletal muscle decreased significantly after paralysis and returned to normal as the muscle regained power.

Monocrotophos (0.8LD₅₀) led to significant induction of nitric oxide in muscle which remained elevated even on recovery of muscle power.

L-NAME treatment of rats significantly delayed onset of cholinergic signs of chewing and body tremor. However, acetylcholinesterase inhibition was not altered by L-NAME treatment of rats.

Posttranslational modification and inhibition of activity of ATP synthase induced by monocrotophos poisoning were reduced in rats treated with L-NAME.

Conclusion

Acute monocrotophos poisoning rapidly induced muscle weakness that progressed to paralysis followed by complete regaining of muscle power in rats. Strong inhibition of muscle acetylcholinesterase was the primary toxicity responsible for induction of muscle weakness, and recovery of enzyme activity was important for

regaining muscle power, which was enabled by a rapid metabolic clearance of monocrotophos from the muscle.

Muscle weakness was also due to nitric oxide induced inhibition of ATP synthesis and inadequate energy. Reversal of this inhibition increased energy generation which may be important in preventing prolonged muscle weakness associated with severe organophosphate poisoning in humans.

CHAPTER 1

INTRODUCTION AND REVIEW OF LITERATURE

1. Introduction

Agricultural communities across the globe depend on pesticides for maintaining their harvests and sustaining their economy. Pesticides play a vital role in food production and approximately 2.5 million tons are used worldwide every year (1). The availability and ease of access to pesticides has led to pesticide self-poisoning being responsible for 30% of all suicides worldwide (2). Pesticide self-poisoning is an important cause of pre-mature death in most agricultural communities of low and middle-income countries (3). The World Health Organization (WHO) estimated in 2006 that 3,000 000 intentional and unintentional pesticide poisoning episodes occur every year in the world, with 600,000 occurring in India (4). Among the pesticides, organophosphates are the most commonly used for suicide. Self poisoning with organophosphate pesticides (OPP) is reported from Asia (5-10), being common in India (11), and also Africa (12-14) and South America (15, 16).

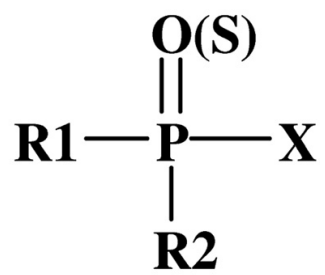
OPP poisoning is fatal as the pesticides rapidly inhibit acetylcholinesterase (AChE), the enzyme responsible for hydrolysis of acetylcholine (ACh) and termination of cholinergic neurotransmission. ACh is evolutionarily conserved as a neurotransmitter from insects to humans and is the most wide spread neurotransmitter in the central and peripheral nervous systems (17). Critical control of ACh action is provided by the catalytic activity of AChE, that hydrolyses ACh at the rate of approximately 5,000 molecules per second, and is therefore important for the nervous system (18). Systems that prevent removal of ACh at this rate lead to accumulation of the neurotransmitter at cholinergic synapses and hyper stimulation and depolarisation of the post-synaptic target. At the neuromuscular junction, severe cholinergic hyper stimulation and prolonged depolarisation of the muscle manifest as weakness and paralysis. Due to this physiology, prolonged muscle weakness is a

characteristic of OPP poisoning and a major cause of morbidity and mortality. The lack of specific and efficient treatment to prevent or reverse muscle weakness contributes to the morbidity.

Treatment for OPP poisoning involves re-activation of the enzyme by displacement of OPPs from the active site of AChE by oximes (19). Re-activation of the enzyme is possible for a short period after OPP inhibition of AChE when the binding is reversible. As the time of contact between OPP and AChE increases, the binding becomes covalent and the enzyme is refractory to re-activation by oximes. In the context of intentional self-harm, when there is delay in access to treatment, oximes have not been found beneficial in preventing muscle weakness (20). These cases would benefit from treatment that does not only address the inhibition of AChE but targets other events in the pathophysiology of OPP induced muscle weakness.

There are several indications that non-cholinergic mechanisms contribute to muscle weakness that occurs in acute OPP poisoning. Prime among these reasons is that despite severe inhibition of AChE all patients do not exhibit delayed prolonged muscle weakness. OPP inhibition of AChE rapidly leads to intense muscle activity that utilises high energy. Utilization rates greater than the generation of energy may deplete the muscle of ATP, and low ATP levels are associated with muscle weakness. This thesis explores non-cholinergic mechanisms, including bioenergetic failure, which may be involved in the patho-physiology of muscle weakness seen in acute severe OPP poisoning. The elucidation of these patho-mechanisms may offer treatment strategies to reduce or prevent muscle weakness that occurs in acute severe OPP poisoning.

FIGURE 1.1 General structure of OPP



(From Ref . (21))

R1 and R2 \longrightarrow Alkylthio, alkyl, alkoxy, or amino groups

X \longrightarrow Halide, cyano, thio or phenol group

The following review of literature provides a background to the questions asked in the thesis under the sections:

- a) OPP - structure, metabolism and toxicity.
- b) How does ACh act on target tissue?
- c) OPP poisoning – clinical profile and treatment.
- d) Muscle structure and physiology and pathology of weakness.
- e) Mitochondrial respiration and energy production.
- f) Nitric oxide induced post translational modifications.

The review will initially focus on structure and metabolism of OPPs as they influence toxicity.

a) OPP structure

OPPs are a large class of chemicals that inhibit AChE and are mainly used as pesticides. They are derivatives of phosphoric, phosphonic, or phosphinic acid and share common chemical properties (**Figure 1.1**). OPPs derived from phosphinic acid do not inhibit AChE (22). OPPs contain a central phosphorus atom with either a phosphoryl ($P = O$) or thiophosphoryl bond ($P = S$) and R1 and R2 groups that are stable alkylthio, alkyl, alkoxy, or amino groups. X is a halide, cyano, thio or phenol group which is more prone to hydrolysis than R1 and R2. (21, 22). There are at least 13 types of OPPs, classified based on the side chains and elements (O or S) attached to the central phosphorus atom. Phosphothioates ($P = S$) are more lipophilic than phosphates ($P = O$). Pure phosphorothioates require desulfuration to oxons to inhibit AChE (22).

Metabolism of OPP

OPPs are mostly lipophilic and non-polar in nature and readily transferred through plasma membranes and absorbed. Once absorbed in the body, they undergo several biotransformations in the liver. Biotransformation reactions of lipophilic OPPs are mainly directed to the production of polar conjugates (23). Bio-transformation reactions include both activation and detoxification of OPPs. Activation of OPPs is defined as conversion of less toxic OPPs to more toxic compounds by metabolic biotransformation. Detoxification of OPPs represents conversion of lipid soluble active OPP to less toxic and more water soluble compounds. The enzymes involved in the biotransformation reactions are divided into two groups namely; phase I and phase II enzymes. Phase I enzymes introduce a polar functional group onto the molecule, which makes them more water soluble (e.g) flavin-containing monooxygenases (FMOs), cytochrome P450-dependent monooxygenase (CYPs) and hydrolases. Phase II enzymes conjugate more bulky hydrophilic molecules (e.g. sulfates, sugars or amino acids) usually at hydrophilic groups introduced by phase I enzymes. This ultimately leads to more water soluble and easily excreted compounds (23).

Activation of OPP compounds

Most OPPs, except the phosphonates and phosphates, do not inhibit AChE in their non-metabolised form. The biotransformations of OPPs to active metabolites that inhibit AChE occur through 5 major reactions.

1. Oxidative desulfuration of thiophosphate that occurs in insects and mammals is carried out by mixed function microsomal monooxygenases specifically the cytochrome P450 system (P450) and flavin-containing monooxygenases (FMO). This enzymatic reaction requires NADPH and molecular oxygen. e.g conversion of

dimethoate (P = S) to dimethoate (P = O). The oxon analog of dimethoate (P = O) is a more potent inhibitor of AChE than dimethoate (P = S) (24). This is due to the greater electronegativity of oxygen compared to sulphur so the polarisation of the P = O bond is greater than the P = S bond. This results in an electropositive phosphorus atom that favours nucleophilic attack of the AChE serine hydroxyl group (25).

2. Oxidation of sulphide groups: Thioester oxidation results in sulfoxides and sulfones, occurs in insects, mammals and plants, and is carried out by the cytochrome P450 system (P450) and FMO; (e.g) oxidation of thioester group of disulfoton. Oxidised disulfoton strongly inhibits AChE and persists in circulation (26).

3. Oxidation of amide groups that involves N-demethylation by the cytochrome P450 system; (e.g) Oxidative N-demethylation of dicrotophos to monocrotophos (MCP), which is a more potent inhibitor of AChE than dicrotophos (26).

4. Hydroxylation of alkyl groups to form cyclic phosphate esters or ketones, carried out by microsomal enzymes and NADPH; (e.g) metabolic activation of triorthocresyl phosphate to *o*-tolyl saligenin phosphate, which has 12 million times more anticholinesterase activity than its parent compound triorthocresyl phosphate (27). In addition to monooxygenases, prostaglandin synthase, present in extra-hepatic tissue functions similar to the cytochrome P450 and is important in the kidney where cytochrome P450 is low. Prostaglandin synthase oxidises parathion into paraoxon (28).

5. Non-enzymatic metabolic conversion results in formation of more potent AChE inhibitors from OPPs; (e.g) metabolic conversion of trichlorfon to dichlorvos via dehydrochlorination (29).

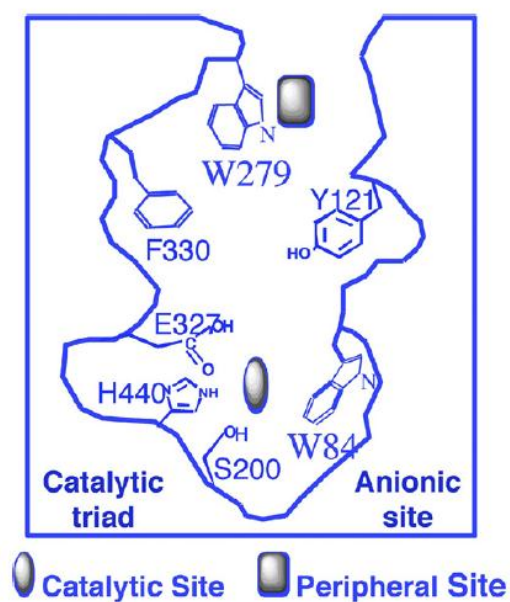
Detoxification of OPP compounds

Detoxification of OPP converts lipid soluble, highly toxic compounds to less toxic or non-toxic and more water soluble compounds by biotransformation. Detoxification of OPP is by cleavage of one of the phosphoryl (P = O) or thiophosphoryl bonds (P = S) or alkylester or aryylester bonds which results in a negatively charged phosphorus molecule that prevents binding to AChE (23). Cleavage of the (P = O) or (P = S) bonds in aryl esters and alkyl esters is achieved by the cytochrome 450 system and NADPH through oxidative dearylation and oxidative O-dealkylation respectively (26).

OPPs are detoxified by A & B esterases. A-esterases are Ca^{2+} dependent and hydrolyse OPP compounds; (e.g) Paraoxonase, somanase and phosphotriesterase (30). Paraoxon is hydrolysed by paraoxonase into the less toxic diethylphosphoric acid and p-nitrophenol. Rabbits express higher A-esterase than rats and show greater protection against paraoxon. This was confirmed by administration of rabbit serum to rats which showed higher protection against paraoxon. Pre-treatment of mice with purified A-esterase significantly decreased AChE inhibition in the brain and diaphragm after administration of chlorpyrifos or its active metabolite chlorpyrifos oxon (31, 32). Paraoxonase knock out mice showed increased susceptibility to chlorpyrifos oxon and diazoxon inhibition (33). These studies illustrate the importance of A-esterase in detoxification of OPPs.

B-esterases are inhibited by OPP compounds; e.g. AChE, carboxylesterase, serum cholinesterase, trypsin and chymotrypsin. They share the common feature of a serine hydroxyl group at the active site, to which OPPs bind. Among the B - esterases, carboxylesterase plays a vital role in detoxification. Carboxylesterase hydrolyses esters and thioesters or amides of carboxylic acids and detoxifies OPPs

FIGURE 1.2A Schematic cross-section through the active-site gorge of TcAChE



(From Ref. (34)) Anionic site and catalytic triad are located at the base of the active site gorge of AChE, which is bordered by ~ 14 aromatic amino acids. The catalytic triad is formed by Serine 200 (S200), Histidine 440 (H440) and Glutamic acid 327 (E327).

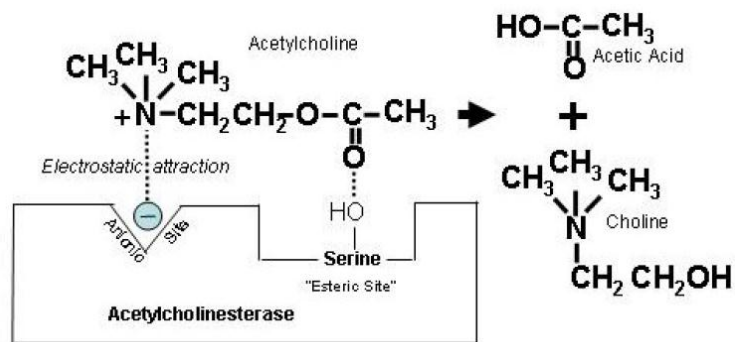
(25). e.g malathion is converted to the less toxic malathion α - monoacid by carboxylesterase, which is highly expressed in humans but not in insects; hence insects are more susceptible to malathion than mammals (28, 35). Carboxylesterase also detoxifies OPPs by binding to them and acting as a scavenger (36).

OPP toxicity

OPP induced toxicity mainly occurs via AChE dependent pathways. AChE is a peripheral membrane-bound enzyme that protrudes into the synapse and rapidly hydrolyses the neurotransmitter ACh at cholinergic synapses. AChE is a highly active enzyme which can hydrolyse approximately 5,000 ACh molecules per second (18). Its high catalytic activity and the high toxicity of OPP compounds are associated with the unique arrangement of amino acids at the active site of the enzyme. Nachmansohn and Wilson in 1951 (37) carried out a kinetic analysis of AChE activity and suggested that AChE consists of two subsites; esteratic and anionic sites. The esteratic site acts as the catalytic site and choline binding occurs at the anionic subsite.

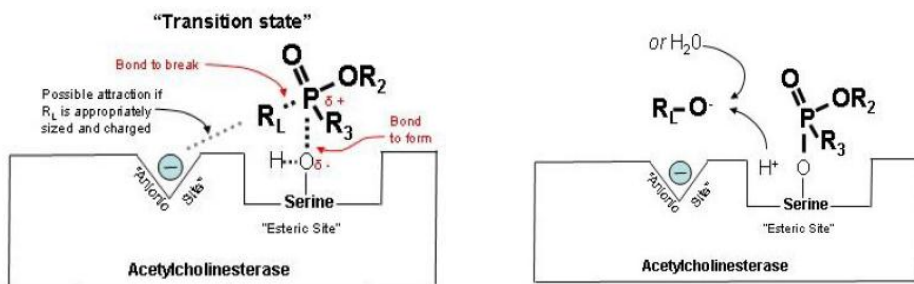
AChE crystals were first obtained from the electric organ of *Electrophorus electricus* in 1966 (38). The first three-dimensional crystal structure of *Torpedo* AChE (TcAChE) was resolved in 1991 (39). Several oligomeric forms of AChE have been identified from the electric fish, *Electrophorus electricus* and *Torpedo marmorata*, which are structurally identical to vertebrate muscle and nerve AChE (40). The active site of TcAChE has serine 200, glutamic acid 327 and histidine 440; these three residues form a planar arrangement, which looks like the catalytic triad of serine proteases; e.g Chymotrypsin (41). The active site of TcAChE and other AChEs is in a gorge, nearly 20Å long and deep which extends into the enzyme almost close to its base (**Figure 1.2A**), with the catalytic triad at the bottom

FIGURE 1.2B ACh hydrolysis



(From Ref. (42)) The positively charged quaternary nitrogen group of choline electrostatically interacts with the catalytic anionic site of AChE, forming a highly unstable intermediate, which liberates choline.

FIGURE 1.2C AChE inhibition by OPPs



(From Ref. (42)) The partial positive charge at the phosphorus atom in OPP favours the electrostatic interaction with the partial negative charge of the serine hydroxyl group at the active site in AChE and inhibits ACh binding.

of the gorge (43). The gorge is lined with 14 aromatic amino acids. Nearly 70% of the gorge is occupied by these amino acids. The gorge can be divided into a catalytic anionic site (CAS) with tryptophan 84 and phenylalanine 330 and a peripheral anionic site (PAS) with tyrosine 70, tyrosine 121 and tryptophan 279. Spectroscopic and chemical modification studies were used to predict the presence of tryptophan at the active site of the enzyme (44, 45). Weise *et al.* in 1991 (46) identified that tryptophan 84 forms part of the putative choline binding site by affinity labelling. ACh is an ester of acetic acid and choline, and is a quaternary amine. Positively charged quaternary nitrogen of choline electrostatically interacts with anionic sites of AChE, which positions ACh at the active site of the enzyme. As shown in **Figure 1.2B**, the ester carbonyl group of ACh covalently interacts with the serine hydroxyl group in the esteric or catalytic site of AChE, forming a highly unstable tetrahedral intermediate, which liberates choline. The covalently bound acetate is spontaneously hydrolysed by a water molecule, resulting in regeneration of free enzyme.

Binding of the ligand to the peripheral anionic site was also evidenced in a 3D structure of TcAChE and thioflavin T complex (47). Binding of any ligand to the peripheral anionic site led to inhibition of enzyme hydrolysis by preventing substrate entry and product exit from the active site (48).

Both ACh and OPPs have high affinity for AChE and readily bind to the enzyme. The partial positive charge at the phosphorus atom in OPP favours a nucleophilic attack by the serine hydroxyl group at the active site in AChE and inhibits ACh binding (**Figure 1.2C**).

The bond between the serine hydroxyl group of the enzyme and the phosphorus atom of OPP is much stronger than the bond with carbonyl carbon in ACh. The

hydrolysis of the carbonyl carbon - enzyme complex occurs very fast, being complete in microseconds, whereas hydrolysis of phosphorus - enzyme complex may take from a few hours to several days, based on the nature of the alkoxy group of the OPP (49). Over time, the bond between the serine hydroxyl group of the enzyme and the phosphorus atom of OPP becomes covalent due to the dealkylation of one of the alkoxy groups from OPP. When this complex formation occurs, the enzyme is irreversibly inhibited by OPP and said to be aged. The rate of aging depends on the dimethoxy and diethoxy structure of OPP; e.g the half-life for aging for various dimethoxyphosphoryl AChE is 2 – 32 hours while for diethoxyphosphoryl AChE it is more than 36 hours (50-52).

Oximes are hydroxylamine derivatives, containing positively charged quaternary nitrogen, which enables them to bind to the anionic site of AChE. They can dephosphorylate AChE bound to OPP and re-activate the enzyme. Reactivation of OP-inhibited AChE by oximes does not occur once the AChE-inhibitor complex has aged (53). Oximes are used in the treatment of OPP poisoning (19).

Toxicity of OPP also occurs in an AChE independent manner. Chan et al. (54) in 2006 used pheochromocytoma (PC 12) cells (noradrenergic clonal cells, devoid of AChE) to demonstrate OPP induced mitochondrial dysfunction and ATP depletion followed by cell death. AChE knockout mice show greater susceptibility to diisopropylfluorophosphate (DFP) with all mice dying within 7 -22 minutes of DFP administration, while none of the control mice died (55). These studies indicate the existence of non-cholinergic toxicity in OPP poisoning.

b) How does ACh act on target tissue?

ACh is released from both the central and peripheral nervous systems by cholinergic neurons (56). ACh, the first known neurotransmitter to be identified, is synthesised from choline and acetyl-CoA by choline acetyltransferase. The newly synthesised ACh is stored in membrane vesicles and transported along the axon (57). Upon neuronal stimulation, membrane vesicles fuse with the plasma membrane and ACh is released at the synaptic cleft, where it interacts with either nicotinic or muscarinic cholinergic receptors to modify postsynaptic cell function.

Action of ACh through nicotinic receptor signaling

Nicotinic ACh receptors (nAChRs) belong to the Cys-loop receptor family, which are ligand - gated ion channels permeable to Na^+ , K^+ and Ca^{2+} ions and give a stimulatory response both at neurons and muscles (58, 59). They are distributed in the central nervous system (CNS) and in the peripheral nervous systems (60). In the muscle, nAChRs are present on the post synaptic membrane, whereas in the brain, nAChRs are localised to the pre and post synaptic membranes (58). The ion channel is made up of 5 subunits. The subunits may be identical or different and share similar structural patterns with an extracellular N-terminal fragment, four transmembrane fragments (M1-M4), a cytoplasmic loop located between the M3 and M4 transmembrane fragments and an extracellular C-terminal fragment (58). The ligand-binding domain (LBD) is formed by the N-terminal end of all the five subunits. A conserved loop of 13 amino acids in the LBD located between two cysteine residues is called the Cys-loop receptor. Binding of ACh or nicotine to the LBD results in channel opening, flow of Na^+ and K^+ ions, membrane depolarisation and finally muscle contraction or excitatory response in the neurons (58).

Action of ACh through muscarinic receptor signaling

Muscarinic receptors are G protein coupled receptors, composed of seven transmembrane domains linked by 3 intracellular and 3 extracellular loops (57). Initially, muscarinic receptors were divided into two sub-groups M₁R and M₂R based on their affinity towards the muscarinic agonist, pirenzepine (61). Bonner et al. (62) in 1987, classified muscarinic receptors into 5 subtypes (M₁-M₅) based on their DNA sequence. Despite extensive homology among subtypes, the receptors differ in their extracellular N-terminal and central portion of the third intracellular loop (63). Muscarinic receptors M₁R, M₃R and M₅R couple with G proteins (Gq/11) and activate phospholipase - C which in turn activates the phosphatidylinositol trisphosphate signalling pathway. Muscarinic receptors M₂R and M₄R couple with Gi/o-type G proteins and inhibit adenylate cyclase activity.

All subtypes are found in the brain and eye (64, 65). In the heart, subtypes M₁R, M₂R, M₃R and M₅R are distributed (66) and M₁R and M₂R activation results in tachycardia and bradycardia respectively (67, 68). M₂R and M₃R regulate smooth muscle contraction (69).

M₂R and M₃R regulate pupillary constriction, bronchoconstriction, urination and defecation. In salivary glands, M₁R controls the release of high-viscosity saliva while M₃R controls flow and volume of secretion (70, 71).

Overactivation of nicotinic and muscarinic receptors by ACh occurs when AChE is inhibited by OPPs. Clinical features of nicotinic and muscarinic receptor overactivation by ACh and medical management of OPP poisoning will be discussed in the following section.

c) **Acute OPP poisoning**

The clinical profile of OPP poisoning is characterised by parasympathetic muscarinic receptor hyperactivity that leads to salivation, lacrimation, vomiting, urination, bradycardia, miosis, bronchospasm, bronchorrhoea and diarrhoea. Sympathetic nicotinic hyper stimulation is characterised by sweating, hypertension, mydriasis and tachycardia. Hyperactivity of nicotinic receptors at the neuromuscular junction results in muscle fasciculation, muscle weakness and paralysis (72-74). The muscarinic receptor antagonist, atropine, controls muscarinic symptoms while the nicotinic symptom of muscle weakness lacks effective treatment and is the main cause of morbidity and mortality of severe OPP in countries where the poisonings occur.

A temporal spectrum of muscle weakness occurs in acute severe OPP poisoning. In the first 48 hours of poisoning, ACh hyperactivation of nicotinic receptors leads to a generalised muscle weakness with hyperreflexia, pyramidal signs and fasciculations, termed Type I paralysis (75).

Type I paralysis overlaps with a cholinergic syndrome of muscarinic receptor hyper stimulation. Type I paralysis may be followed by Type II paralysis or intermediate syndrome - a delayed muscle weakness occurring 48-72 hours after poisoning and characterised by weakness of proximal limb muscles, neck flexors and respiratory muscles (76). Type III paralysis or organophosphorus induced delayed neuropathy (OPIDN), which is not common in India, occurs 1- 4 weeks after ingestion of specific OPP and is due to inhibition of neuropathy target esterase and not to AChE inhibition (77).

Senanayake and Karalliedde (76) in 1987 coined the term intermediate syndrome (IMS) for Type II paralysis as it arose in the gap between the end of the acute

cholinergic crisis and the onset of OPIDN. Morbidity, mortality and high cost of prolonged intensive care of OPP poisoning are associated with Type II paralysis (78).

Medical management of acute OPP poisoning

Medical management of OPP poisoned patients includes atropine treatment, oxime reactivation of OPP inhibited AChE and mechanical ventilation (79). Cholinesterase inhibition is the marker for OPP poisoning. Red blood cell acetylcholinesterase (RBC-AChE), which is readily obtained from poisoned patients, resembles the structure of synaptic AChE and the percentage of its inhibition is associated with neuromuscular transmission failure (80). It also acts as an indicator for atropine (muscarinic antagonist) demand. Patients with 30% and above RBC-AChE activity, were found not to require atropine while patients who had less than 10% RBC-AChE activity needed large doses of atropine (80).

Gastric lavage is the most commonly used method to remove unabsorbed pesticide in the stomach of poisoned patients, although no proof is available about the beneficial effects of gastric emptying in OPP poisoned patients (79).

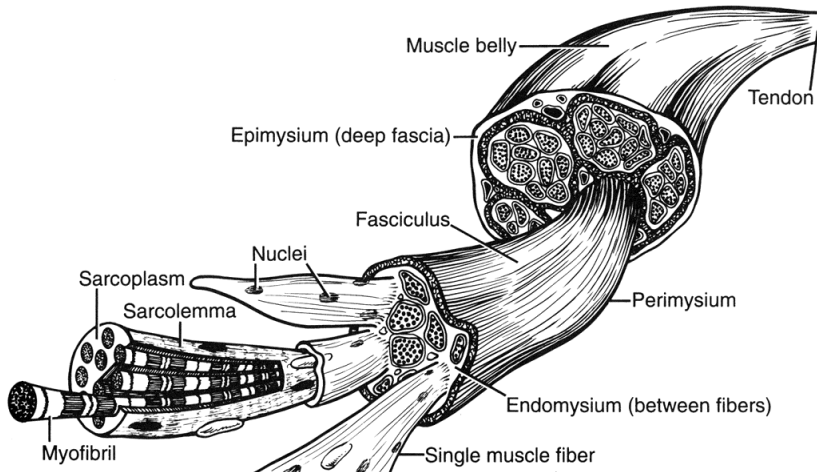
Atropine, glycopyrronium bromide and hyoscine methobromide (scopolamine) are muscarinic antagonists. They differ in their diffusion into the central nervous system (CNS) (81). The entry of atropine into CNS is less than hyoscine. Despite fewer side effects from glycopyrronium, its inability to enter the CNS results in it being ineffective at suppressing coma. OPP poisoned patients who had CNS manifestations responded well to scopolamine (as it penetrates the blood brain barrier more than atropine) (82). Although, atropine produces unconsciousness at high doses; availability, low cost and ability to cross the blood brain barrier (moderately) make it a commonly used muscarinic antagonist world wide (83).

Oximes are hydroxylamine derivatives, used to reactivate OPP inhibited AChE. In 1950, Wilson and colleagues first identified the oxime, pralidoxime, and successfully tested it in parathion poisoned patients (84). In addition to pralidoxime, trimedoxime and obidoxime have been identified for use in OPP poisoning, but pralidoxime remains the commonly used oxime. The reactivation of OPP inhibited AChE by pralidoxime and obidoxime depends on the chemical nature of the OPP ingested. E.g There is better reactivation of AChE inhibited by diethyl compounds like parathion or quinalphos than when AChE is inhibited by dimethyl compounds like monocrotophos (MCP) or oxydemeton-methyl. Reactivation does not occur when AChE is inhibited by S-alkyl-linked compounds like profenofos (19, 85-87).

Diazepam (a benzodiazepine drug) is used to suppress seizures. Although, seizures are not seen in well-ventilated patients with OPP poisoning (85, 88), they are common in poisoning with organophosphorus nerve agents like tabun and soman (89). In animal studies, diazepam decreases OPP induced neuronal damage (90), restores respiration and protects from death (91).

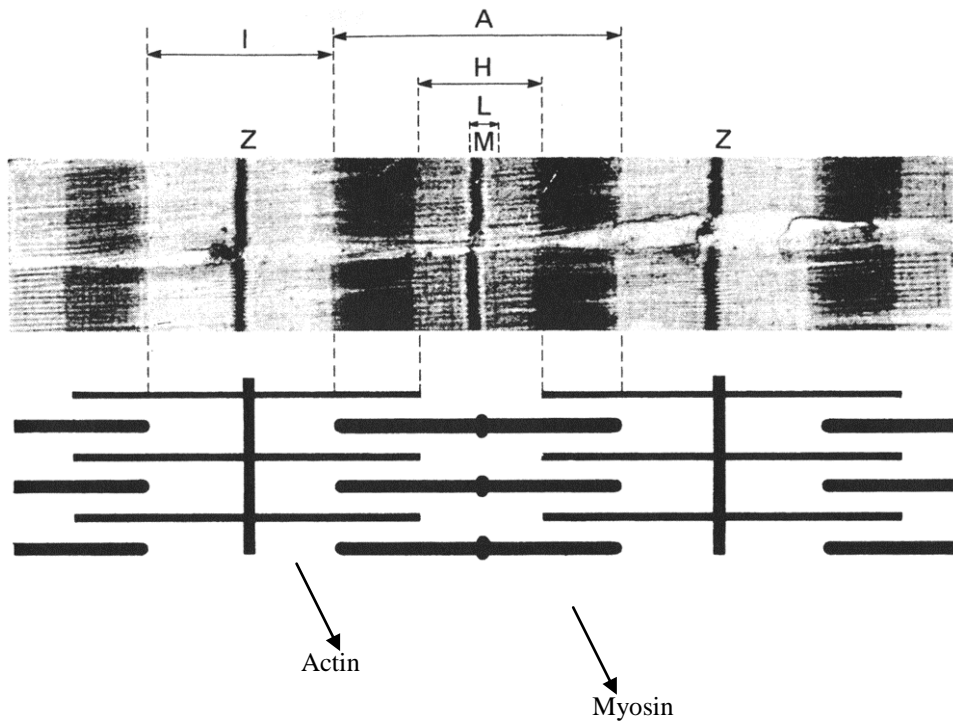
Magnesium sulphate inhibits ligand-gated calcium channels, thereby reduces ACh release from pre-synaptic terminals and protects the function of the neuromuscular junction (92). A reduced mortality rate was observed in OPP poisoned patients treated with 4 gram magnesium sulphate / day (i/v) for just one day after admission (93). OPP in plasma is scavenged by butyrylcholinesterase (present in fresh frozen plasma from healthy individuals), which decreases the availability of OPP to inhibit AChE at synapses (94). Butyrylcholinesterase binds OPP stoichiometrically and a large amount is required to neutralise free OPP. Recombinant phosphotriesterase (A- esterase) from bacteria effectively hydrolyses organophosphorus compounds in animals and protects them (95, 96).

FIGURE 1.3 Basic structure of skeletal muscle



(From Ref. (97)) Structural subunits of skeletal muscle.

FIGURE 1.4 Striation pattern of vertebrate skeletal muscle



(From Ref. (98)) The top panel shows an electron micrograph of vertebrate skeletal muscle fibre striation patterns and the bottom panel shows a simplified representation of the relationship between actin and myosin.

Reactivation of OPP inhibited AChE by oximes is not useful when the AChE-inhibitor complex has aged and no effective antidote is available for nAChRs mediated muscle weakness (19, 20). There is a need to understand non-cholinergic mechanisms that may be involved in the patho-physiology of muscle weakness seen in acute severe OPP poisoning.

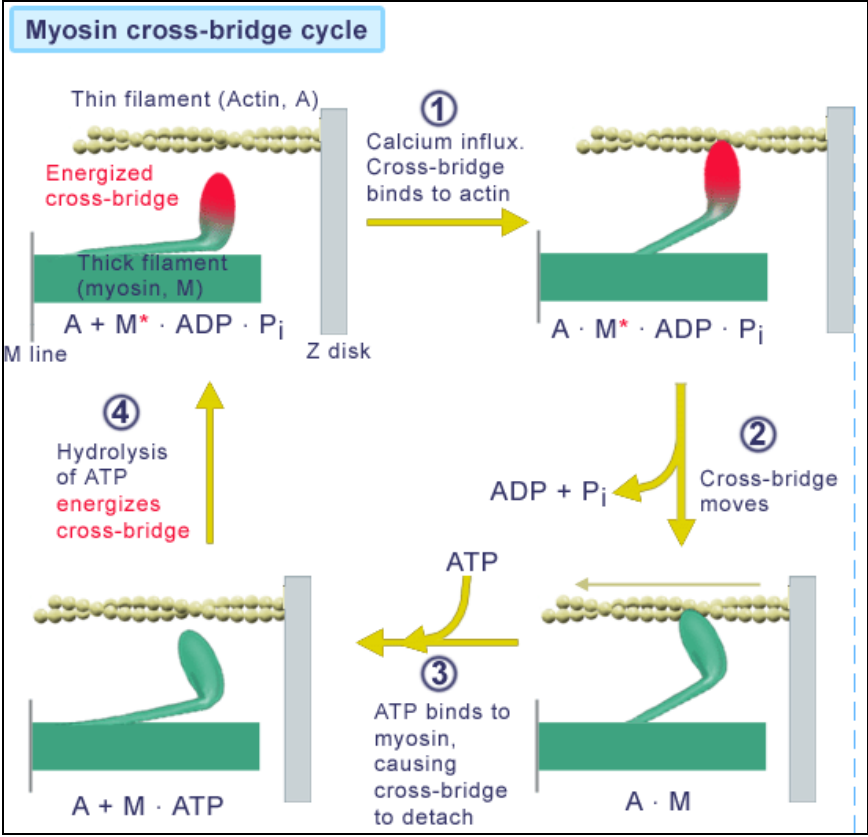
d) Skeletal muscle structure

The structure of the skeletal muscle, the mechanism of muscle contraction, general muscle weakness and OPP induced muscle weakness will be reviewed in the following sections.

The basic structure of the muscle is shown in **Figure 1.3**. The muscle belly is made up of a bundle of bundles: The bigger bundles are named as fascicles and each fascicle is made up of a bundle of muscle fibres. Epimysium, perimysium and endomysium are the coverings of each muscle bundle, fascicle and muscle fibre respectively. Skeletal muscle fibres are formed by fusion of large numbers of individual cells, called the syncytium. The outer cell membrane and the contents are called sarcolemma and sarcoplasm respectively. Contractile units within the fibre are called myofibrils.

Muscle fibres appear striated under light microscopy. An electron micrograph of vertebrate skeletal muscle fibre striation patterns are shown in **Figure 1.4**. Isotropic (I) (consist of actin alone) and anisotropic (A) (consist of actin and myosin) bands are light and dark bands that form the striations. Heller (H) mid-tone is seen within the A band. Dark lines, Mittelscheibe (M) and Zwischenscheiben (Z), are seen in the middle of the A band and the I band respectively. Around the M line a slightly lighter L zone can be seen occasionally. The sarcomere is the distance between adjacent Z lines and is usually 2 to 2.5 μm . Actin and myosin are responsible for the

FIGURE 1.5 Muscle contraction and relaxation



(From Ref. (99)) ATP dependent muscle contraction and relaxation summarised as a four-stroke cycle.

light band (I) and dark band (A) respectively. These proteins are responsible for producing muscle contractions. Nebulin and titin are two proteins which help maintain this arrangement.

Actin is a thin filament, which forms spiral filaments along with troponin and tropomyosin. Myosin is a thick filament, has a globular head and a long fibrous tail. The myosin head binds to actin, as well as adenosine triphosphate (ATP), the energy source for muscle contraction. The myosin tail helps to interact with other myosin subunits. Binding of myosin to actin occurs only when actin binding sites are exposed by calcium ions binding to troponin.

The skeletal muscle is controlled by alpha motor neurons. The muscle cell and its alpha motor neuron form a motor unit. The neuromuscular junction is where the nerve impulses are transmitted to the muscle. Skeletal muscles are stimulated by alpha motor neurons through nerve impulses. ACh carries nerve impulses from the neuron to the muscle cell membrane across the synapse. ACh binds to nicotinic receptors on post-synaptic membranes and opens the Na^+ channels causing membrane depolarisation. AChE hydrolyses ACh, terminates the action of ACh and prepares the muscle for the next nerve impulse. The nerve impulse is passed along the sarcolemma and also into the transverse tubular (t-tubular) system. Dihydropyridine receptor (DHPR), a voltage sensor in the t-tubular system is activated by the nerve impulse. The activated DHPR interact with the ryanodine receptor 1 (RyR1) which is present in the sarcoplasmic reticulum (SR), resulting in calcium release from SR to sarcoplasm (100). Calcium binds to troponin, causing a conformational change which is transmitted to tropomyosin. The myosin heads then bind to actin, and the muscle cell contracts as cross-bridge cycling starts (**Figure 1.5**). The length of actin and myosin themselves do not change during muscle

contraction but the proteins slide over each other. Calcium is released continuously from the SR until motor neuron activity ceases. Calcium is pumped back into the SR continuously by the ATP dependent SR Ca^{2+} pumps. The muscle relaxes as sarcoplasmic calcium concentration decreases (**Figure 1.5**). Muscle excitation and contraction are ATP dependent processes, required by the sarcolemmal Na^+/K^+ channel, for Ca^{2+} sequestration by the SR and actinomyosin cycling. Low levels of ATP (energy charge of the cell) lead to muscle fatigue and decline in force generation and can result in muscle weakness (101, 102).

Energy charge

The energy charge of the cell determines the equilibrium between energy production and expenditure (103).

The energy charge is calculated by the equation:

$$\text{Energy charge} = \frac{[\text{ATP} + \frac{1}{2} \text{ADP}]}{[\text{ATP} + \text{ADP} + \text{AMP}]} \quad (104)$$

The energy charge varies from 0 (when all the adenylate nucleotides are AMP) to 1 (when all the adenylate nucleotides are ATP). Metabolism is regulated by the energy charge of the cell. A low energy charge increases the ATP regenerating reactions by activating the glycolytic enzymes pyruvate dehydrogenase and phosphofructokinase (105), decreasing the rates of ATP consuming biosynthetic enzyme reactions and counteracting the decrease in the energy charge (106). The biosynthetic enzymes phosphoribosyl adenosine triphosphate synthetase, aspartokinase and phosphoribosyl pyrophosphate synthetase are inhibited by low energy charge and product feedback (107).

How does energy charge regulate metabolism? Its influence on metabolic reactions is based on metabolite concentrations of the adenylate pool (ATP + ADP + AMP). For example phosphofructokinase is activated by increased AMP (low energy

charge) and inhibited by increased ATP (high energy charge) (108). AMP-activated protein kinase (AMPK) is activated by high AMP (Low energy charge) (109). The activated AMPK, in turn inhibits ATP consuming pathways such as glycogenesis and biosynthesis of cholesterol and fatty acid (109). Muscle weakness arises at low energy charge when ATP regeneration rates are less than the ATP utilisation rate. Low energy charge is likely to disturb Na^+/K^+ channels, Ca^{2+} sequestration by the sarcoplasm and actinomyosin cycling, resulting in muscle weakness (110).

Skeletal muscle weakness

Skeletal muscle weakness underlies several pathological conditions which include muscle dystrophies, inherited myopathies, cancer and general inflammatory disease. It can also result from normal ageing processes and very little physical activity. Skeletal muscle weakness occurs in the following conditions.

1. Myasthenia gravis in which antibodies produced against ACh receptors result in early onset fatigue and muscle weakness (111).
2. Genetic mutations in the mitochondrial electron transport chain result in defective mitochondrial function, which are responsible for disease. Human mitochondrial myopathies followed by less energy production is associated with exercise intolerance and muscle weakness (112).
3. Muscle weakness also arises from low frequency stimulation. Fatigue arises during intense or persistent activation of skeletal muscle (113). The recovery of contractile function from fatigue can be a slow process; sometimes taking several hours to days, and observed in numerous human muscles (114, 115). This is due to the decreased force induced by low frequency stimulation. This phenomenon is called 'prolonged low-frequency force depression' (PLFFD) (113, 116).

OPP poisoning and prolonged muscle weakness

OPP induced IMS is a major cause of morbidity, mortality and high cost of treatment in hospitalised patients. The patho-mechanisms that lead to development of IMS are not clear. There is no clear correlation between specific OPPs and development of IMS. The OPPs MCP (76), dimethoate (117), fenthion (118), dichlorvos (119), methylparathion (120), methamidophos (76), chlorpyrifos (121) and phosmet (122) are suggested to be involved in the development of IMS. Severe AChE inhibition is the primary event involved in the development of Type II paralysis but not all OPP patients with severe AChE inhibition develop paralysis. This suggests that mechanisms in addition to AChE inhibition are involved in the development of Type II paralysis.

A repeated nerve stimulation study of the proximal muscle of OPP poisoned patients showed clear progression of electrophysiological alterations in association with onset of IMS (121, 123). IMS is also characterised by dysfunction in pre- and post synaptic neurotransmission (76, 120, 124). The reason for neuromuscular transmission failure, which is observed in IMS is probably due to reduced ACh release through pre-synaptic feedback and desensitization of post-synaptic receptors due to persistent nicotinic receptor activation (125, 126).

In acute OPP poisoning, persistent severe AChE inhibition and oxidative stress are associated with development of the IMS (127). A study examining genetic polymorphisms also determined that OPP poisoned patients who had a genetic variant allele at the 55 codon of PON1, null GSTM1 or both GSTM1 and GSTT1 null had considerably higher risk for development of IMS (128).

Toxicant levels and muscle weakness

The pathophysiology of OPP poisoning also depends on tissue distribution and metabolic clearance of the pesticide. Thus pharmacokinetic studies provide important information about the amount of toxicant delivered to the target tissue. Toxicity and pharmacokinetics are integrally related, as the extent of absorption, retention or detoxification ultimately controls the dose delivered to target tissues and the resulting observed effects. OPPs are highly unstable in blood due to the presence of esterases which hydrolyse toxic OPPs to less toxic compounds (129).

OPPs were detected for several days in gastric fluid of patients who exhibited Type II paralysis but not in patients who did not develop prolonged muscle weakness. In patients with Type II paralysis, severe AChE inhibition correlated to continuous circulation of toxicants, as evidenced by the presence of the parent compound and metabolite in gastric fluid and urine respectively (120).

In rats, the rapid detoxification of paraoxon enabled a 50% regain of muscle AChE activity within 24 hours (130). In chick embryo cultures treated with paraoxon, the recovery of muscle AChE activity correlated to newly synthesised AChE as it was not seen in presence of the protein synthesis inhibitor, cycloheximide (131). Rapid metabolic clearance of an OPP would prevent inhibition of re-activated or newly synthesized AChE and aid recovery.

In addition to ACh induced pathology, OPP may interact directly with target tissue and produce injury. This is noted with triazine-based herbicides, atrazine and cyanazine and simazine that bind directly to $F_1 F_0$ ATP synthase but not to other electron transport chain complexes and decrease ATP levels (132). Clearance of the pesticides from tissues would eliminate ACh induced pathology due to direct interactions, enabling recovery from poisoning.

e) **Mitochondria**

As seen in the earlier section, normal muscle function requires ATP. About 90% of cellular ATP is produced by the mitochondria through oxidative phosphorylation (133). Mitochondria utilise the energy from oxidation of substrates to phosphorylate ADP to ATP, a process called oxidative phosphorylation.

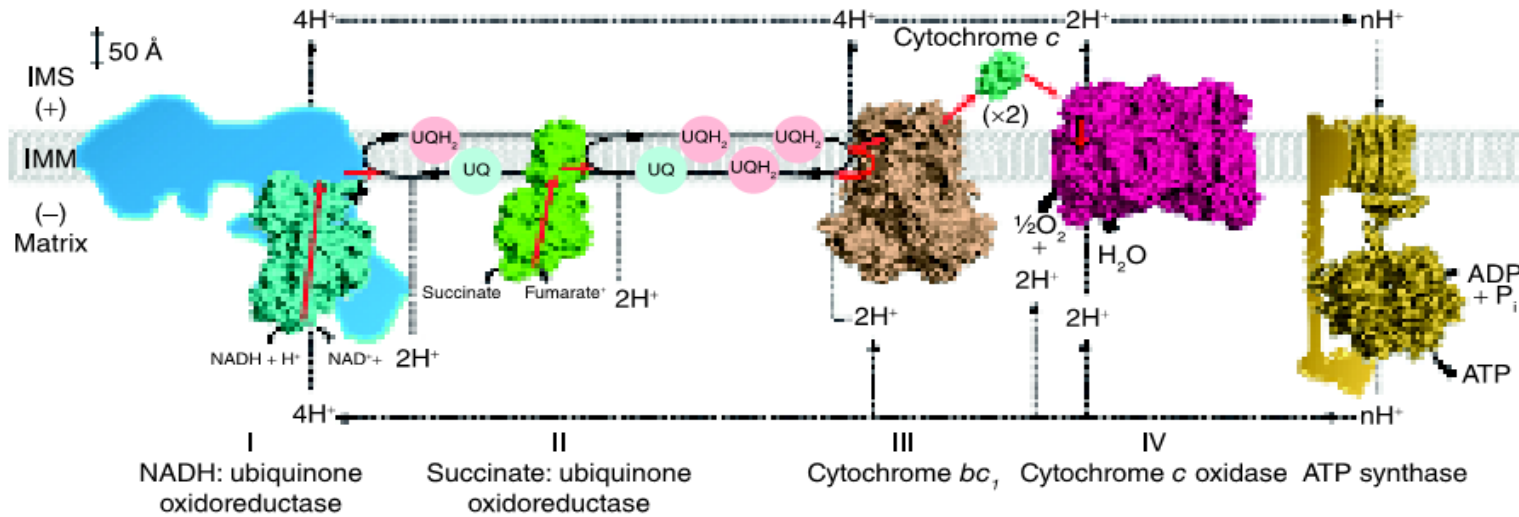
A defect in the mitochondrial function may lead to muscle weakness. The structure of the mitochondria and ATP production by mitochondria will be reviewed below.

Mitochondria are organelles present in all eukaryotic mammalian cells except anucleate red blood cells (134). Mitochondria have two phospholipid membranes that partition the organelle into four biochemically distinct compartments; the outer membrane, inter membrane space, innermembrane and matrix. The outer membrane is freely permeable to ions and small molecules ($M_r < 5,000$) while the inner membrane is impermeable to ions including protons (H^+). The inner membrane is highly folded and forms structures called cristae, which contain the electron transport chain complexes I to IV and complex V. The mitochondrial matrix, surrounded by the inner membrane, is where the tricarboxylic acid cycle (TCA), urea cycle, fatty acid oxidation, mitochondrial DNA replication, transcription and translation, gluconeogenesis, Fe-S biogenesis, protein folding and degradation occur.

Oxidative phosphorylation starts with the entry of electrons into the electron transport chain complexes. These electrons are collected by dehydrogenases from catabolic pathways, which funnel them into either nicotinamide nucleotides (NAD^+ - $NADP^+$) or flavin nucleotides (FAD or FMN).

The respiratory chain comprises electron transport chain complexes I to IV. Electron transport through the respiratory complexes I to IV generate a proton

FIGURE 1.6 An overview of the Electron Transport Chain and ATP synthesis



(From Ref. (134)) The electron transport complex I, II, III, IV and ATP synthase are located in the inner mitochondrial membrane (IMM). Electrons are transported through the complexes, which are responsible for pumping protons from the mitochondrial matrix to the inner membrane space (IMS), generating a proton gradient. Protons are guided back to the matrix through ATP synthase, which utilizes the proton motive force to synthesize ATP from ADP.

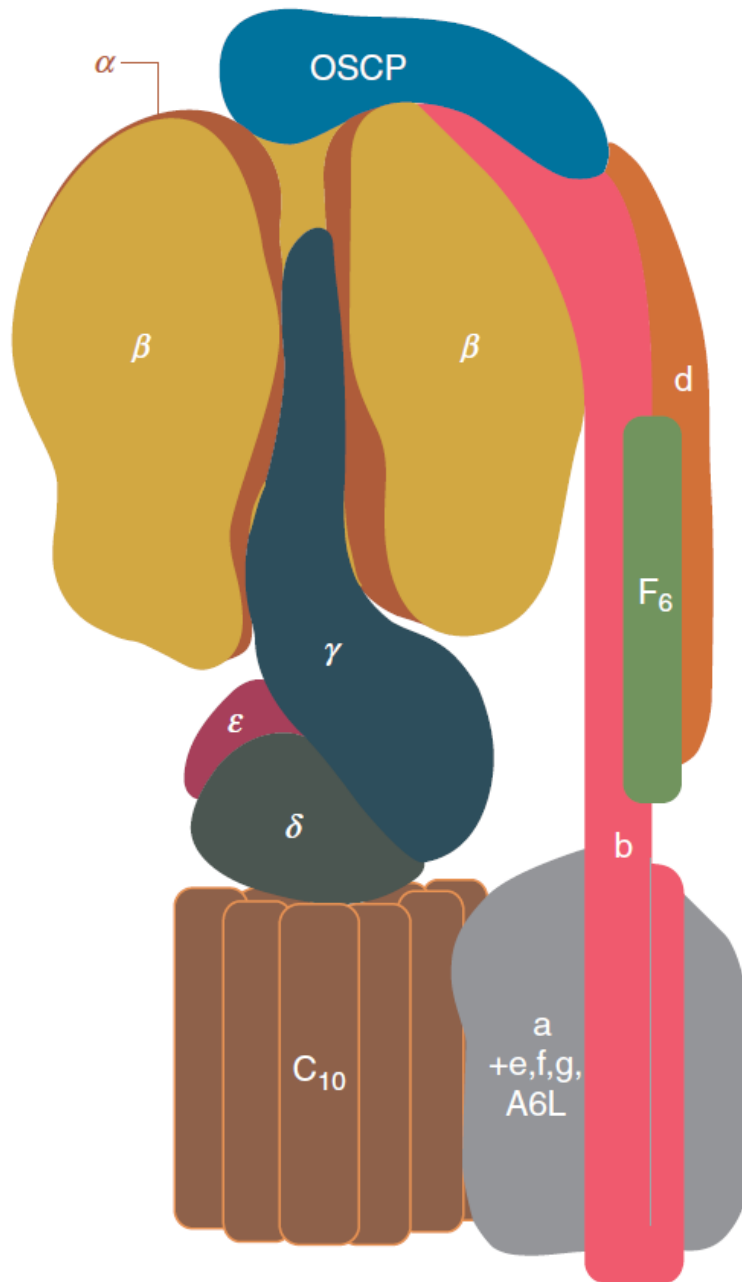
gradient across the inner mitochondrial membrane that drives oxidative phosphorylation at complex V (ATP synthase) and enables synthesis of ATP from ADP and inorganic phosphate (Pi).

A schematic representation of the electron transport chain and complex V is shown in **Figure 1.6**.

Complex I (NADH:Ubiquinone oxidoreductase) consists of 45 subunits with a molecular weight of ~ 980 kDa in bovine mitochondria (135). Electron microscopy of single particles of complex I from different organisms reveal that it possesses an L-shaped structure (136). NADH produced from the TCA cycle and from glycolysis (NADH is transferred from the cytosol to the mitochondrial matrix by a 'substrate-shuttle' mechanism) is re-oxidised by NADH: Ubiquinone oxidoreductase which is coupled with the reduction of ubiquinone (UQ) to ubiquinol (UQH₂) (**Figure 1.6**). This electron transfer is coupled with proton translocation across the inner membrane, which helps generate a proton gradient.

Complex II (succinate:UQ oxidoreductase) is composed of four protein subunits with a molecular weight of 124 kDa in mammalian mitochondria (134). Hydrophilic subunits A and B protrude into the matrix while hydrophobic subunits C and D are attached to the membrane. A number of complexes I, III, IV and ATP synthase protein subunits are encoded by both nuclear and mitochondrial DNA, but all complex II protein subunits are encoded by only nuclear DNA. Complex II directly links to the TCA cycle and catalyses the oxidation of succinate to fumarate which results in reduction of its prosthetic group FAD. Reduced FAD is again reoxidised by UQ in the succinate: UQ oxidoreductase complex (**Figure 1.6**). The activity of the complex does not generate a proton gradient (137).

FIGURE 1.7 Subunit organisation of mitochondrial ATP synthase



(From Ref. (138)) Mitochondrial ATP synthase is composed of the F₁ head piece, a central stalk, the F₀ base and a peripheral stalk. The F₁ head piece consists of a globular domain made up of 3 α and 3 β subunits. The central stalk is made up by the γ , δ and ϵ subunits, while the F₀ base is composed of the c ring subunits and the a subunit. The peripheral stalk consist of the b, d, F₆ (h) and OSCP subunits. The rotary motor is formed by the c-ring and central stalk.

Complex III (cytochrome bc_1 complex or ubiquinone:cytochrome c oxidoreductase) is a homo-dimer and each monomer is composed of eleven subunits in mammalian mitochondria (134). Complex I and II reduce ubiquinone (UQH_2), which can travel in the inner membrane space to reach complex III where it is reoxidised to UQ. During this process, two protons are pumped into the inner membrane space and electrons are transferred to complex IV by the soluble electron carrier cytochrome c (**Figure 1.6**). The overall activity of complex III is oxidation of UQH_2 and cytochrome c reduction (139).

Complex IV (cytochrome c oxidase) is also a homo-dimer and each monomer is composed of 13 subunits with a molecular weight of ~ 200 kDa (140). In addition, it has two heme irons, a and a_3 and two copper centers Cu_A and Cu_B (141). A binuclear centre is formed by a_3/Cu_B metals where oxygen reduction occurs. Complex IV collects two electrons from two molecules of cytochrome c and transfers them to molecular oxygen which results in production of water. During this process, a proton gradient is formed as complex IV also pumps proton to the inner membrane space.

Complex V or mitochondrial ATP synthase or $F_1 F_0$ ATP synthase is a large multisubunit rotary motor enzyme (~ 600 kDa) present in the inner mitochondrial membrane (142). It is encoded by both mitochondrial DNA and nuclear DNA. ATP 6 and ATP 8 protein subunits of ATP synthase are encoded by mitochondrial DNA and the other 14 subunits are encoded by nuclear DNA (143). ATP synthase is composed of two domains, namely the soluble F_1 domain and the membrane bound F_0 domain (**Figure 1.7**). The soluble F_1 domain is composed of 5 subunits α , β , γ , δ & ϵ , in a stoichiometry of $\alpha_3\beta_3\gamma_1\delta_1\epsilon_1$. The F_1 domain comprises a soluble globular domain composed of $\alpha\beta$ subunits and a central stalk, made of subunits $\gamma\delta$ and ϵ . The

F_0 domain is composed of subunits a, b, $c_{(10)}$ (mammalian ATP synthase has 10 copies, this copy number varies in other organisms), d, e, f, g, F_6 , A6L, oligomycin sensitivity-conferring Protein (OSCP) and factor B (144). Subunits b, d, F_6 (h) and OSCP, make up a peripheral stalk that is located to one side of the complex. The F_1 and F_0 domains of the enzyme are connected by the central and peripheral stalks (145). The F_0 domain functions as the proton channel and ATP synthesis and hydrolysis occurs at the F_1 domain by coupling the activities of two rotary motors; one present in F_0 (146) and the other present in F_1 (147). The α and β subunits have regulatory and catalytic activities respectively and the catalytic sites are at the interface between α and β subunits (148). The protons are driven by proton motive force through a channel in F_0 at the interface between the subunit c ring and subunit a . The free energy released during this process causes rotation of the ring (relative to subunit a), along with subunits γ , δ , and ϵ , to which it is attached (149). This favours rotation of γ subunit within the $F_1 \alpha_3\beta_3$ hexamer building torque energy for ATP resynthesis at the catalytic sites (149).

In bacteria, the ϵ subunit C-terminal helices have a high amount of flexibility (150). Movement of the helices between F_0 and F_1 is initiated by proton motive force and nucleotide binding at the catalytic sites (151-153). Tsunoda et al (153) in 2001 pointed out that the ϵ -helical subunit conformation of ATP synthase influences ATP synthesis and hydrolysis differentially. ATP hydrolysis and synthesis occur when the ϵ -helices subunits are situated close to F_0 . The hydrolysis of ATP is inhibited without affecting ATP synthesis when the ϵ -helices subunit lies close to F_1 (153).

Unwanted hydrolysis of ATP is not desirable, and it should be kept low especially during hypoxia. In mitochondria this is regulated by a 10 kDa protein called inhibitor protein (IF_1) which binds to ATP synthase F_1 domain in a stoichiometry of

1:1(154, 155). Hydrolysis of ATP by mitochondrial F₁-ATPase activity is effectively controlled by IF₁ in a pH dependent manner (156, 157).

The complex size and activity of ATP synthase may represent biological strategy to protect the catalytic function of the complex i.e ATP synthesis, from the numerous normal fluctuations of cell metabolism. However, its large and complex structure also offers targets for toxic insults. Modifications of ATP synthase subunits can inhibit enzyme activity. Inhibition of ATP synthesis at complex V can affect mitochondrial electron transport and increase reactive oxygen species generation due to leakage of electrons (158). The resulting mitochondrial oxidative stress can then induce protein modifications which can amplify and worsen damage (158). Thus, in energy intensive tissue such as the muscle, compromised mitochondrial ATP generation can lead to severe injury. It has been demonstrated that OPP poisoning decreases mitochondrial electron transport in rat brain (159) and inhibits complex V activity in the muscle (160). The mechanism of complex V inhibition and its impact on ATP generation in the context of OPP poisoning are not known.

One of the mechanisms for post translational modifications of proteins is by nitric oxide, which is increased in OPP poisoning. Nitric oxide may induce post-translational modifications and alter ATP synthase activity. Nitric oxide signalling, Nitric oxide induced post translational modifications and the influence of OPP poisoning on nitric oxide levels will be reviewed in the following section.

f) Nitric oxide (NO)

NO is a gas and ubiquitous signalling molecule, which acts as a second messenger involved in a number of physiological and pathological processes (161). The Nobel Prize in physiology or medicine was awarded to Robert F. Furchgott, Louis J.

Ignarro and Ferid Murad in 1998 for their discovery "role of NO as a signalling molecule in the cardiovascular system"(162).

NO is a free radical composed of one nitrogen and one oxygen. It is uncharged with an un-paired electron (161). NO is both aqueous and lipid soluble (uncharged). Lipid solubility facilitates its diffusion through phospholipid bilayers and its attack on cells and mitochondria (163, 164). NO is a relatively stable free radical with a half life of 2 to 30 seconds (161).

NO is endogenously generated by NO synthase enzymes (NOS), which exist as neuronal (nNOS), endothelial (eNOS), and inducible (iNOS) isoforms (165). In addition, a mitochondrial NOS species (mtNOS) has been described in a number of tissues (166, 167). Enzyme activities of nNOS and eNOS are induced by increased intracellular calcium. All the isoforms use L-arginine as substrate and produce citrulline as a by-product. This reaction requires the co-factors NADPH, molecular oxygen, tetrahydrobiopterin, heme, flavin mononucleotide and flavin adenine dinucleotide (168, 169).

NO signalling occurs by three major pathways; classical signalling through cyclic GMP (cGMP dependent protein kinases and phosphodiesterases), non-classical signalling (cGMP independent - NO induced post translational modifications) and less classical signalling (inhibition of respiration by competitive inhibition at cytochrome c oxidase and its effects) (170).

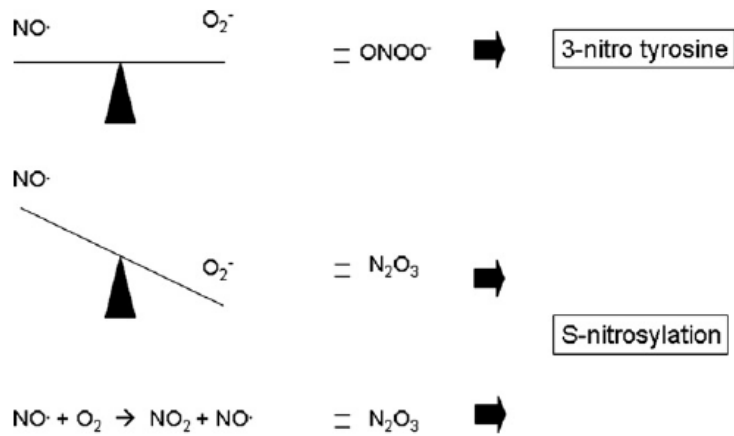
Classical NO signalling: NO is known to regulate a variety of physiological processes such as smooth muscle relaxation, neurotransmission and platelet aggregation by binding to the ferrous iron of soluble guanylate cyclase (sGC), which in turn increases cGMP production.

Cyclic GMP is synthesised by guanylate cyclase from guanosine triphosphate. Guanylate cyclases are of two types, namely particulate guanylate cyclase and soluble guanylate cyclase. Particulate guanylate cyclases are distributed in membranes and can bind to ligands resembling guanylin peptides and natriuretic peptides. (171). Soluble guanylate cyclase (sGC) is a heme-containing heterodimer which binds to NO. Each sGC has three domains, 1) heme-binding domain at the N-terminal, 2) a dimerization domain and 3) catalytic domain at the C-terminal. sGC catalyses the conversion of GTP to cGMP when it binds to NO through its heme prosthetic group. NO carries out most of its biological functions as a signalling molecule through cGMP. NO regulates fluid and electrolyte homeostasis, smooth muscle relaxation and phototransduction through cGMP which directly interacts with its downstream signalling effectors such as cGMP-dependent kinase (PKG), cGMP-dependent phosphodiesterase (PDE) and cyclic nucleotide gated channels (CNGs) (172-174). Increased sGC activity (approximately 200 fold) was observed when bound to NO, but this increased activity is attenuated by phosphodiesterase 5A (PDE5A) (175, 176).

NO produced from the endothelium and in platelets is required for regulating blood pressure, decreasing obstruction in blood vessels and decreasing platelet aggregation (177, 178). Aortic rings isolated from eNOS knockout mice did not show relaxation upon addition of ACh, suggesting that NO derived from eNOS mediates vasodilation (179).

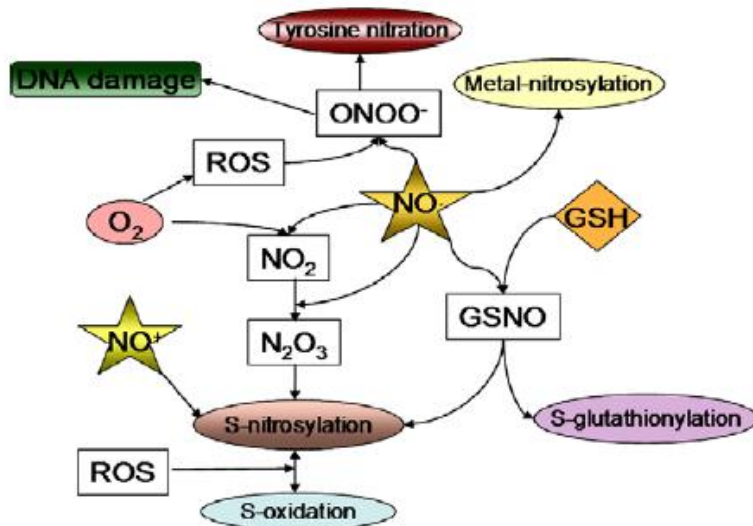
Calcitonin gene-related peptide (CGRP), is highly expressed in kidney and acts as a vasodilatory peptide (180-183). Calcium supplementation (1.4g/day) induces CGRP (184), which in turn activates eNOS and nNOS in kidney. Activation of eNOS and nNOS leads to increased NO followed by decrease in blood pressure. This reaction

FIGURE 1.8A Nitration/S-nitrosylation equilibrium



(From Ref. (185)) Equal concentrations of NO and superoxide (O_2^-) lead to peroxynitrite (ONOO^-) formation, while an increase of 2 to 3 fold in NO concentration relative to superoxide results in formation of dinitrogen trioxide (N_2O_3). Peroxynitrite and N_2O_3 can induce post translational modifications of protein by nitrosylating tyrosine and cysteine residues respectively.

FIGURE 1.8B NO induced post translational modifications



(From Ref. (185)) A schematic representation of NO induced modifications. NO reacts with superoxide to form peroxynitrite, which in turn leads to tyrosine nitration or DNA damage. S-nitrosylation could be mediated by either NO or N_2O_3 or GSNO.

is reversed when calcium supplementation is stopped, which suggests a role for NO role in blood pressure maintenance (181, 186).

NO acts as a neurotransmitter in both the central and peripheral nervous system. Cerebral vasodilatation and blood flow is regulated by NO which is derived primarily from eNOS and preserves the brain during ischemia (187, 188). NO is also a neurotransmitter in neurons that innervate the gut as NOS inhibition inhibits gut mobility (189, 190).

Non-classical NO signalling - NO induced post translational modifications

In addition to cGMP- mediated effects, NO reacts directly with several molecules and brings about an effect. NO reacts with superoxide, yielding “Reactive Nitrogen Species” (RNS). Reaction with GSH leads to nitrosoglutathione (GSNO) formation. NO can modify macromolecules such as DNA and proteins, to alter structure and function (191, 192).

RNS formation is influenced by NO concentration and the oxidative environment. Peroxynitrite (ONOO^-) is formed when NO and superoxide (O_2^-) are present at equal concentrations while a 2 to 3 fold increase in NO concentration leads to formation of dinitrogen trioxide (N_2O_3) (193) (**Figure 1.8A**). Peroxynitrite, a strong oxidant, can induce DNA damage, membrane phospholipid oxidation and post-translational modification of proteins by conversion of tyrosine to nitrotyrosine (192).

NO modifies proteins by direct interaction or by producing reactive nitrogen species, through S-nitrosylation of reduced cysteine residues and by nitration of tyrosine residues (193, 194) (**Figure 1.8b**). S-nitrosylation, the reversible addition of an NO moiety to thiol group of cysteines regulates several enzymes and

signalling pathways (195). Unlike other post translational modification like ubiquitinylation or phosphorylation, S-nitrosylation is not an enzymatic process. It depends on the redox environment which is maintained by the GSH/GSSG ratio, NADPH/NADP⁺ and thioredoxin (191, 196).

Tyrosine nitration occurs by introduction of a nitro triatomic group (-NO₂), at the 3rd position in the phenolic ring of tyrosine (197). Peroxynitrite formation and production of nitrogen dioxide (NO₂) lead to tyrosine nitration in vivo. At physiological pH, superoxide anion (O₂⁻) which is usually kept low by cellular antioxidants, reacts with NO and results in peroxynitrite formation. Nitrogen dioxide (NO₂) is produced by haemeperoxidases, which utilises nitrite and hydrogen peroxide as substrates (198). Increased levels of tyrosine nitration are an indication of nitrosative stress (199).

S-nitrosylation and tyrosine nitration have been associated in many patho - physiological conditions. Glyceraldehyde-3-phosphate dehydrogenase (GAPDH) activity was reversibly inhibited when GAPDH was treated with 200μM NO. This inhibition was associated with S-nitrosylation of GAPDH at Cysteine₁₄₉ residue (200). Increased S-nitrosylation of mitochondrial proteins protected mitochondrial integrity and cells from death even when GSH was depleted. (201). In addition, S-nitrosylation of pro-caspase- 3 inhibits its activity and apoptosis in normal cells (202).

Cell signalling pathways are altered by tyrosine nitration as it blocks the phosphorylation of tyrosine residue (192). Apoptosis is induced by nitration of manganese superoxide dismutase (MnSOD), which is present in the mitochondria and helps in removal of superoxide. MnSOD is inactivated upon tyrosine nitration.

Inactivation of MnSOD leads to more peroxynitrite formation which finally triggers the signal for apoptosis (203).

Apoptosis is induced by high concentrations of NO; generally produced by iNOS, while low concentrations of NO produced from eNOS and nNOS inhibit apoptosis and protect the cells (204). In addition, there is a strong correlation of cancer and iNOS expression and tyrosine nitration. Higher levels of iNOS activity and nitrated proteins were observed in lung cancer (205, 206), human metastatic melanoma (207), gastric cancer (208) and pancreatic cancer (209).

Neurodegenerative diseases such as Alzheimer's disease, amyotrophic lateral sclerosis and Parkinson's disease are associated with protein tyrosine nitration and mitochondria dysfunction (210-212).

Less classical NO signalling – NO induced mitochondrial damage

Major cellular targets for the action of NO are the mitochondria. The inhibition of mitochondrial respiration by NO is a well-studied phenomenon (213).

Complex I activity and respiration were inhibited in murine macrophage J774 cells when they were treated with high NO concentrations (approximately 1.5 μ M) for 6 hours (214). Riobo et al (215) suggested that this inhibition was due to NO causing an increased production of superoxide anion and peroxynitrite, but not due to a direct effect of NO. This was confirmed by addition of superoxide dismutase (SOD) (which scavenges superoxide) and uric acid (peroxynitrite scavenger), which protected complex I enzyme activity and inhibited tyrosine nitration (215). NO and calcium induced complex I inhibition was reversed by reduced glutathione or light. GSH selectively removes NO from s-nitrosothiol, and high intensity light destroys

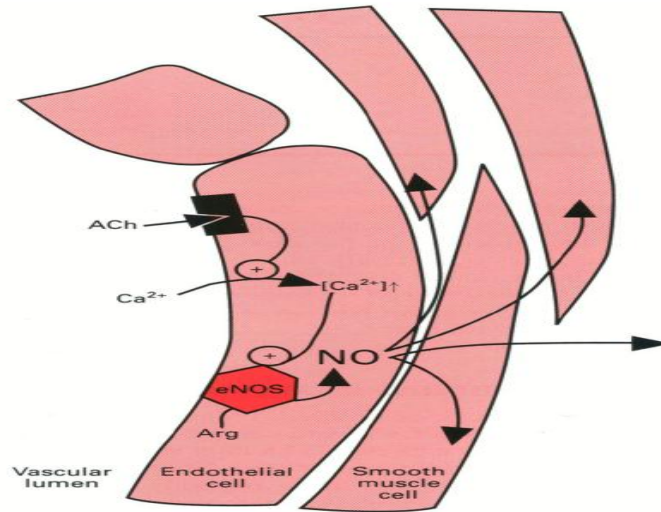
s-nitrosothiol; suggesting that complex I inhibition was through s-nitrosylation or Fe-nitrosylation (216).

NO binds to iron-sulfur clusters present in mitochondrial complex II and disrupts them, which occurs only at high NO concentrations (217, 218). As Fe-S clusters present in complex II are not readily oxidized, inactivation occurs only with a strong oxidant like peroxynitrite. Inhibition of complex II by peroxynitrite probably occurs through the oxidation of a critical thiol (cysteine 252 of subunit A) in the dicarboxylate binding region of succinate dehydrogenase (219, 220).

Complex IV or cytochrome c oxidase has 2 haems (cyt *a* and *a*₃) and 2 copper centers (Cu_A and Cu_B). A binuclear center is formed by *a*₃ (Fe²⁺) and Cu_B (Cu⁺), where oxygen reduction occurs (221). NO competes with oxygen for binding at the binuclear centre of cytochrome c oxidase and reversibly inhibits respiration (213, 222, 223). Maximal inhibition of mitochondrial respiration occurred at 10-100nM NO and normal tissue oxygen levels (20 - 40μM) (222). The binding of NO at the binuclear centre of cytochrome c oxidase, which prevents molecular oxygen reduction, results in higher amounts of reduced electron chain compounds (217). Thus superoxide generation from molecular oxygen by monovalent reduction is indirectly promoted by NO at various sites of the electron transport chain (224, 225). These superoxide radicals react with NO, produce peroxynitrite, a potent oxidant in the mitochondria and inhibit other electron transport chain complexes I, II and V (213, 215, 226, 227).

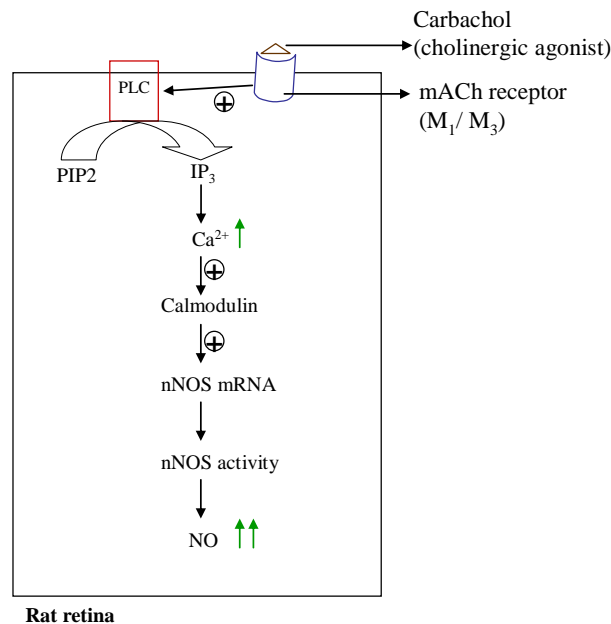
In contrast to complexes I, II and V, complex IV is not inhibited by peroxynitrite, as it is more resistant to oxidative damage (217, 226, 228, 229).

FIGURE 1.9A NO synthesis by eNOS in vascular endothelial cells induced by ACh



(From Ref. (230)) ACh binds to the muscarinic receptor in the endothelial cell and activates the inositol triphosphate (IP₃) signalling cascade, which results in increased intracellular calcium. The increased calcium activates calcium dependent nitric oxide synthase (eNOS).

FIGURE 1.9B NO synthesis by nNOS in retina induced by cholinergic agonist



(Modified from Ref. (231)) Carbachol, a cholinergic agonist binds to the muscarinic receptor in the rat retina and activates the IP₃ signalling cascade, which produces increase intracellular calcium and activation of nNOS, resulting in increased NO production.

Complex V is also a target for modification by NO in the brain (232). Cellular excess of NO production as well as peroxynitrite, result in formation of nitrotyrosine and inhibition of complex V activity (217, 226, 233). ATP synthase α subunit is nitrotyrosinylated in Alzheimer's disease (232). The activity of ATP synthase decreases in aging when the β subunit of the enzyme is nitrated (234). S-nitrosylation of the α subunit of ATP synthase also leads to loss of activity (235).

OPP poisoning and NO levels

ACh binds to the muscarinic receptor in the endothelial cell and activates phospholipase C and the inositol triphosphate (IP₃) signalling cascade which in turn increases the release of calcium from endoplasmic reticulum. Increased intracellular calcium activates calmodulin and protein kinase C (PKC), stimulating eNOS which results in NO production in endothelial cells (**Figure 1.9A**) (230, 236).

As shown in **Figure 1.9B**, in the rat retina, carbachol treatment (cholinergic agonist) also increases NOS activity by increasing the expression of nNOS mRNA (231). Increased levels of NO were also observed when rat atria and rat cerebral frontal cortex were treated with carbachol (236, 237). Thus, increased levels of NO are a natural consequence in OPP where AChE is inhibited and ACh levels are increased.

Animal studies have shown that NO is involved in OPP induced myopathy. Paraoxon induced muscle necrosis in rats was reduced by 80% when animals were administered NOS inhibitors with the OPP (238). Increased citrulline levels (as a marker of NO/NOS) were noted in skeletal muscle after administration of the OPP diisopropylphosphorofluoridate (DFP) to rats, which correlated to myotoxicity (239). High dose DFP induced seizures were suppressed and mortality reduced by L-N^G-nitroarginine methyl ester (L-NAME - NOS inhibitor) pre-treatment of rats

(240). OPP induced NO toxicity is also observed in the brain as rats treated with AChE inhibitors exhibit increased citruline and decreased ATP (241). In rodent muscle, MCP toxicity is associated with complex V inhibition, sparing the activity of respiratory complexes I–IV (160).

With this background, it is suggested *that NO may modify and inhibit ATP synthase in acute severe OPP poisoning. This would compromise ATP generation and contribute to muscle weakness that occurs in the poisoning in rats.*

AIMS AND OBJECTIVES

The aim of the study was to examine ATP generation and NO modulation of mitochondrial function in contributing to muscle paralysis induced by acute severe OPP poisoning.

The objectives of the study were:

1. To determine muscle energy charge over the course of acute severe OPP poisoning.
2. To determine muscle mitochondrial ATP synthase activity over the course of acute severe OPP poisoning.
3. To determine the role of NO in ATP synthase inhibition following acute severe OPP poisoning.
4. To correlate OPP induced muscle weakness and recovery of muscle power to clearance of pesticide.

Outline of the Study

Rodents administered OPP at high doses exhibit clinical profiles of OPP poisoning with cholinergic symptoms and muscle weakness leading to paralysis. Animals recover from poisoning with no treatment. Rats are therefore a suitable model to study the pathogenesis of muscle weakness induced by severe OPP poisoning and recovery of muscle power from poisoning.

The following study was carried out to determine if a compromise in energy generation and NO modulation of mitochondrial function contribute to muscle paralysis induced by severe OPP poisoning.

Wistar rats (female, 150 ± 5 g) were administered MCP by gavage at a dose of $0.8LD_{50}$ to induce severe but not fatal poisoning. MCP is an OPP commonly used

for intentional self-harm in India. The animals were evaluated for poisoning by onset and duration of cholinergic signs, as well as muscle weakness and were sacrificed at different stages during the development of paralysis and on recovery of muscle power. Skeletal muscle, muscle mitochondria, blood and urine were obtained from these animals.

The muscle was studied for AChE activity to confirm OPP poisoning, adenine nucleotides to determine energy levels and lactate to determine the role of anaerobic glycolysis in contributing to the energy status of the muscle. NO was estimated in muscle to determine its involvement in muscle weakness of OPP poisoning and iNOS and nNOS estimated to delineate the source of nitric oxide. Reduced glutathione (GSH) levels were measured in the muscle to determine the oxidative status of the cell.

The muscle mitochondria were evaluated for integrity and ATP synthase activity (Complex V). Biotin iodoacetamide (BIAM) labelling of ATP synthase was done to identify sulfhydryl group modifications. Nitrosylation of ATP synthase at cysteine and tyrosine moieties was explored as a mechanism of ATP synthase inhibition and NO modulation of mitochondrial function leading to OPP induced muscle weakness. The studies were repeated in rats treated with the NOS inhibitor, L-NAME, to confirm the role of NO induced by OPP poisoning in modulating mitochondrial function.

MCP exists as cis and trans isoforms. Cis-MCP inhibits AChE more strongly than the trans isoform (242). Cis-MCP levels were estimated in blood, muscle, muscle mitochondria and urine of rats through the course of poisoning and on recovery from poisoning to determine the role of metabolic clearance in contributing to muscle weakness and recovery of muscle power.

CHAPTER 2

MATERIALS AND METHODS

2.0 Materials

2.1.1 Chemicals

Acrylamide, adenosine diphosphate, adenosine monophosphate, β -mercaptoethanol, biolyte ampholytes (pH 3 – 10), bis-acrylamide, bovine serum albumin fraction V (BSA), 3[(3Cholamidopropyl)dimethylammonio]-1-propanesulfonate (CHAPS), Coomassie Brilliant Blue G-250, Coomassie Brilliant Blue R-250, dithiothreitol (DTT), 5, 5'-dithiobis (2-nitrobenzoic) acid (DTNB), n-Dodecyl β -D-maltoside (lauryl maltoside), eserine hemisulfate, lactate dehydrogenase, reduced glutathione, Nagarase (proteinase enzyme III), N-(1-Naphthyl)ethylene-diamine dihydrochloride, nicotinamide adenine dinucleotide (Reduced) (NADH), *N*_ω-Nitro-L-arginine methyl ester hydrochloride (L-NAME), oligomycin, phenylmethylsulfonyl fluoride, phospho(enol) pyruvate, pyruvate kinase, rotenone, sulfanilamide, tetrabutylammonium hydrogen sulfate, N,N,N',N'-tetramethylethylenediamine (TEMED), Tricine, thiourea, Tween 20 and urea were from Sigma-Aldrich Chemical Co., USA.

MCP (36% SL) was from Syngenta India Pvt. Ltd. India. Acetylthiocholine iodide, adenosine triphosphate, 6-aminocaproic acid, ammonium persulfate, Bis(2-hydroxyethyl) iminotris (Hydroxymethyl) methane (Bis-Tris), ethylene glycol tetra acetic acid (EGTA), 2- (p-iodophenyl)-3-(p-nitrophenyl)-5-phenyl tetrazolium (INT), nicotinamide adenine dinucleotide oxidised (NAD⁺) and sodium dodecyl sulphate (SDS) were from Sisco Research Laboratories Pvt. Ltd.. India. Lithium lactate was from BDH Chemicals Ltd. England. Ethylene diamine tetra acetic acid (EDTA), HPLC-grade acetonitrile, methanol and sodium dihydrogenphosphate were from Qualigens Fine Chemicals Pvt. Ltd. India. N-(biotinoyl)-N'-(iodoacetyl)-ethylenediamine (BIAM) was from Invitrogen, USA. Immobilised pH gradient

(IPG) strips were from Bio-Rad Laboratories, Inc. USA. Immobilon – P membrane (polyvinylidene fluoride (PVDF) was from Millipore Corporation, MA, USA. Protein molecular weight standards were from Bangalore Genei, India. Chemiluminescence substrate luminol and stable peroxide were from Pierce Biotechnology, Thermo Scientific, USA. All other chemicals were Analar Grade. Water was Milli-Q ultrapure.

Antibodies

Antibodies to glyceraldehyde 3-phosphate dehydrogenase (GAPDH), nNOS, nitrotyrosine and nitrotyrosine were from Sigma-Aldrich Chemical Co., USA. Antibody to iNOS was from Santa Cruz Biotechnologies Inc, USA. Antibodies to ATP synthase α subunit and mouse ATP synthase β subunit were from Invitrogen, USA. Anti-mouse IgG-horseradish peroxidase was from Cell Signalling Technology, Inc. USA. Goat anti-rabbit IgG- horseradish peroxidase was from Bangalore Genei, Bangalore, India. Streptavidin horseradish peroxidase conjugate was from Pierce Biotechnology, Thermo Scientific, USA.

Table 2.2.1 Grading of muscle power in OPP poisoned rats (246).

Grade	Muscle power
Grade I	Ataxic gait due to hind leg weakness
Grade II	Voluntary movements only after tail stimulation
Grade III	No voluntary movements even after tail stimulation

2.2 METHODS

2.2.1 MCP poisoning:

MCP is an OPP commonly used for intentional self-harm in South India (243). Female and male rats differ in levels of AChE and activity of the detoxifying enzyme carboxylesterase (244). To avoid these gender differences only female rats were used in this study. Wistar rats (female, 150 ± 5 g) were administered MCP by gavage at a dose of 0.8 LD₅₀ in 1.0ml water (MCP 0.8 LD₅₀ = 6.4 mg / kg body weight) (245). Control rats were administered 1.0ml water by gavage. The study was approved by the Institutional Review Board and Institutional Animal Ethics Committee of the Christian Medical College, Vellore.

Rats were observed after exposure to MCP for cholinergic hyperstimulation and signs of chewing, tremor, salivation and lacrimation. Cholinergic signs were documented by time of onset and duration. Animals were also evaluated for muscle power according to method De Bleecker et al. (246) as given in **Table 2.2.1**.

Rats were sacrificed, under ether anesthesia, at the following times after poisoning: 1 hour; i.e. during complete paralysis, 2.5 hours; i.e. soon after paralysis, 8 hours; i.e. during recovery of muscle power and 24 hours; i.e. on complete recovery of muscle power.

In studies that estimated cis-MCP in tissue, animals were also sacrificed at 15 and 30 minutes after poisoning to determine the absorption rate of MCP, at 40 minutes; i.e. immediately prior to paralysis, and after paralysis at 75 minutes.

L-NAME treatment of rats

L-NAME was administered to rats to inhibit NOSs.

L-NAME (20 mg /Kg body weight / day) was administered to rats in drinking water for 14 days (247, 248) following which rats were subjected to MCP poisoning and sacrifice at 2.5 hours after poisoning as described above.

Animals were weighed on day 0; i.e before L-NAME treatment, day 7; i.e during L-NAME treatment and day 14; i.e at the end of L-NAME treatment to determine the effect of L-NAME on body weight, as the compound influences food intake.

2.2.2 Sample collection and storage

Blood (500 µl) was collected on sacrifice. Muscle (intercostal, upper and lower limb) (5gm) was collected within 10 minutes of sacrifice in cold phosphate buffered saline. Urine was collected for 24 hours after MCP administration.

Muscle obtained at sacrifice was processed immediately for isolation of mitochondria and estimation of adenine nucleotides. An aliquot of the muscle was also stored at -70°C until used for other assays.

For estimation of Cis-MCP, blood, urine and muscle were deproteinized on collection with 2 volumes of acetonitrile, centrifuged at 10,000 rpm for 7 min and the supernatant stored at -70°C until assay.

2.2.3 Acetylcholinesterase assay

Muscle was homogenized in 10 volumes of 10mM Tris HCl pH 7.5 containing 1M NaCl, 1% Triton X-100, 5mM EDTA, stirred for 1 hour at 4°C and centrifuged at 10,000g for 30 min (249). Muscle acetylcholinesterase was assayed in the supernatant by the method of Ellman et al (250) using acetylthiocholine iodide as substrate. In a reaction of 0.5 ml, 2mM DTNB, 3mM acetylthiocholine iodide, 0.1M

potassium phosphate buffer pH 7.0 and 10µl muscle supernatant were incubated for 10 minutes at 37°C. The reaction was stopped with 0.5 ml of 2mM eserine sulphate and absorbance read at 412 nm. Enzyme units were calculated from the molar extinction co-efficient of 5-mercapto-2-nitro benzoic acid of 13.6×10^3 at 412nm and expressed as nmoles acetylthiocholine iodide hydrolyzed/min/mg protein. Protein was estimated by the method of Lowry *et al* using BSA as standard (251).

2.2.4 Skeletal muscle mitochondria isolation

Upper and lower limb skeletal muscle were finely minced and homogenized in eight volumes of 50mM Tris HCl pH 7.4 containing 100mM KCl/2mM EGTA, Nagarase (2.1 U/ml), 1mM ATP, 5mM MgCl₂, 0.5% BSA and centrifuged at 490×g for 10 min at 4 °C to obtain the post nuclear supernatant. This was filtered through nylon cloth and the filtrate spun at 10300×g for 10 min at 4°C. The pellet of mitochondria was washed twice by re-suspension in 50mM Tris HCl pH 7.4/100mM KCl (30 ml) and centrifugation at 10300×g for 10 min at 4°C. The mitochondrial pellet was suspended in 0.5 ml of buffer containing 50mM Tris HCl, 100mM KCl, 2mM EGTA, pH 7.4.

Enrichment of the mitochondrial fraction was assessed by measuring the mitochondrial marker enzyme succinate dehydrogenase (252). Oxidation of succinate to fumarate by succinate dehydrogenase releases electrons that are taken up by 2-(p-iodophenyl)-3-(p-nitrophenyl)-5-phenyl tetrazolium to form formazan crystals and estimated at 490 nm. The assay mixture of 500µl contained 100µg mitochondrial protein, 50mM dipotassium hydrogen phosphate buffer pH 7.4, 50mM succinate and 0.1% 2-(p-iodophenyl)-3-(p-nitrophenyl)-5-phenyl tetrazolium (w/v). The assay mixture was incubated at 37° C for 15 minutes and the reaction stopped with 0.5 ml of 10% trichloroacetic acid. Formazan formed was extracted

into 2 ml of ethyl acetate and measured at 490 nm. Enzyme units were calculated from the molar extinction co-efficient of formazan in ethyl acetate of $20.1 \times 10^3 \text{ M}^{-1}$ at 490nm and expressed as $\mu\text{moles /min/mg protein}$.

2.2.5 Mitochondrial integrity

The integrity of isolated mitochondria was assessed by evaluating mitochondrial swelling by following the reduction in absorbance at 540nm over 7 minutes as described by Takeyama *et al* (253). Mitochondrial suspension (100 μg protein) was added to the buffer (50mM Tris HCl and 100mM KCl/2mM EGTA pH 7.40) and change in absorbance observed at 540 nm for 7 minutes in a dual beam spectrophotometer noted. Decrease in absorbance at 540nm indicates mitochondrial membrane damage and loss of membrane integrity.

2.2.6 Complex V assay (ATP synthase)

Mitochondria contain several membrane bound ATP dependent ion pumps and it is necessary to measure mitochondrial ATPase activity specifically. Oligomycin which specifically inhibits mitochondrial ATPase activity, was used in the assay.

Complex V was assayed in mitochondria by an ATPase coupled reaction measuring oxidation of NADH at 340nm at 30°C in the presence and absence of oligomycin (254). Assay mix contained 100 μg mitochondrial protein, 50mM Tris pH 8.0, 5mM MgCl_2 , 10mM KCl, 2mM phospho (enol) pyruvate, lactate dehydrogenase (4 units), pyruvate kinase (4 units), 5mg BSA, 0.2mM NADH, 10 μM rotenone and 2mM KCN in 1ml. The reaction was initiated by addition of 0.5mM ATP and the oxidation of NADH to NAD, measured at 340 nm for 7 minutes. Oligomycin (2 $\mu\text{g/ ml}$) was then added to the same cuvette and NADH oxidation measured for an additional 7 minutes. Mitochondrial specific ATPase activity was measured from the difference in reduction of NADH oxidation in the presence and absence of

oligomycin. Enzyme units were calculated from the molar extinction co-efficient of NADH of 6.22×10^3 at 340nm and expressed as $\mu\text{moles NADH oxidised/min/mg}$ protein.

2.2.7 Lactate estimation

Lactate was measured in the muscle as an indirect indicator of glycolysis, source for ATP. Muscle obtained on sacrifice was immediately deproteinized with 0.8 volumes of 0.4M perchloric acid, neutralized with 2M potassium carbonate, centrifuged for 10min at 3000g and lactate estimated in the supernatant.

Lactate was assayed by following the oxidation of lactate to pyruvate by lactate dehydrogenase measuring the reduction of NAD at 340nm (255). In a reaction of 1.0ml, 280mM hydrazine, 467mM glycine, 2.6mM EDTA, 2.5mM β -NAD and 20 μl of deproteinised sample were incubated at 25°C for 5 minutes to stabilise the reaction and the reaction started by addition of 20 units lactate dehydrogenase. The increase in absorbance at 340nm was followed for 5 minutes and lactate estimated from a lactate standard and expressed as $\mu\text{moles/gram wet tissue}$.

2.2.8 Estimation of muscle adenine nucleotides

ATP, ADP and AMP were estimated simultaneously in each muscle sample by ion pair reversed-phase HPLC (256). Muscle (50 mg) was homogenized immediately on collection at sacrifice in 500 μl of cold 0.4M perchloric acid to precipitate protein and the supernatant (200 μl) neutralized with 2M potassium carbonate (25 μl), spun at 12,000 \times g for 5 min and filter sterilised through 0.4 μm filter. Twenty μl was analyzed for ATP, ADP, and AMP by HPLC on a Hypersil ODS column followed by detection at 254 nm.

Standards of ATP, ADP and AMP 50 µl (1mM each) were added to 150µl of 0.4 M perchloric acid, neutralized with 2M potassium carbonate (25µl), spun at 12,000×g for 5 min and filter sterilised through 0.4 µm filters. Twenty µl filtrates were analyzed for ATP, ADP and AMP. The nucleotides were separated in 0.2 g% tetrabutylammonium hydrogen sulfate in 0.1M sodium hydrogen phosphate pH 5.5 (Buffer A) and Buffer A with acetonitrile 77:25 (v/v), at a flow rate of 1.2 ml / minute at 25°C for 40 minutes. The column was equilibrated with buffer A for 20 minutes prior to application of the next sample. The detection limit of the assay was 5µM adenine nucleotide. Elution profiles were integrated using LC solution software provided by the manufacturer (Shimadzu Corporation, Kyoto, Japan). The retention time of AMP, ADP and ATP were 17, 23 and 29 respectively. ATP, ADP and AMP levels were expressed as nmoles/mg protein read from the corresponding standard.

2.2.9 Energy charge

Energy charge is a measure of metabolically accessible energy transiently stored in the adenylate pool. The adenylate pool is a sum of the concentrations of all the adenylate nucleotides (i.e) ATP + ADP + AMP in the cell. The energy charge of the muscle was calculated as given by Atkinson and Walton (104).

Energy charge = $[(\text{ATP} + \frac{1}{2} \text{ADP})] / [(\text{ATP} + \text{ADP} + \text{AMP})]$.

2.2.10 Nitrate levels in the muscle

Nitrate the stable end product of NO was estimated as an indicator for NO. Nitrate was reduced to nitrite and estimated by the Greiss reaction in muscle homogenates (257). Skeletal muscle was homogenised in 10 volumes phosphate-buffered saline (PBS), pH 7.4, containing 1% (v/v) Triton X-100 and 1mM phenylmethylsulfonyl fluoride, spun at 3,000 rpm for 3 minutes and nitrate estimated in the supernatant

(258). To 100µl supernatant, 150 mg of copper/cadmium alloy was added and incubated for 1 hour at 25°C with shaking. The reaction was arrested by addition of 100µl 0.35M sodium hydroxide and 400 µl 120mM zinc sulphate. After incubation for 10 minutes at 25°C the tubes were spun at 4,000g for 10 minutes. To 500µl supernatant, 250µl 1% sulphanilamide in 3N HCl and 250µl 0.1% naphthylethylene diamine were added and the color developed measured at 545 nm. Nitrate levels were expressed as nmoles/mg protein read against a NaNO₃ standard.

2.2.11 Western blots of nNOS and iNOS

nNOS and iNOS levels were estimated in muscle on western blots. Muscle supernatant (100µg protein) was added to two volumes of protein dissociation buffer (v/v) containing 0.0625M Tris HCl pH 6.8, 1% SDS, 5% β- mercaptoethanol, 10% glycerol and 0.001% Bromophenol blue and heated at 100°C for 10 minutes, cooled to 25°C and centrifuged at 3500 g for 2 minutes. The muscle supernatant was subject to SDS-PAGE (5-12% gels) (259). Molecular weight markers (9µg) were run in parallel.

Following SDS-PAGE, the resolved proteins were electro transferred to PVDF membranes at 80V for 120 minutes at 4°C (260). Membranes were blocked with 5% BSA in PBS/0.02% Tween 20 (PBS/T) for 1 hour at 25°C and incubated with antibodies to rabbit anti-nNOS (diluted 1:1000 in 5% BSA) or rabbit anti-iNOS (diluted 1:1000 in 5% BSA) for 12 hours at 4°C, followed by goat anti-rabbit IgG-HRP (1:1000 diluted in 5% BSA) for 2 hours at 25°C.

As nNOS and iNOS are of 156 kDa and 130 kDa respectively, the lower half of the blots were probed for glyceraldehyde 3-phosphate dehydrogenase as loading control. The blots were incubated with mouse anti-glyceraldehyde 3-phosphate

dehydrogenase (37 kDa) (1:1000 diluted in 5% BSA) for 12 hours at 4°C, followed by goat anti-mouse IgG-HRP (1:1000 diluted in 5% BSA) for 2 hours at 25°C.

Blots were washed between each step for 3 x 5 minutes with PBS/T. Bound HRP on western blots was detected by the chemiluminescence reagent luminol and peroxide (HRP oxidises the luminol in the presence of peroxide to emit light). This emission of light was enhanced and captured using an image capture system (Vilber, Lourmat, France). The molecular weight markers were visualised with amido black 10B. The blot images were subjected to densitometric analysis using Scion image software (Scion Corporation, Frederick, MD, USA).

2.2.12 2D Blue Native Gel electrophoresis to separate mitochondria electron transport chain complexes I to V

Mitochondrial electron transport chain complexes I to V were separated by Blue Native polyacrylamide gel electrophoresis (BN-PAGE) performed according to the method of Schagger and von Jagow (261, 262) modified by Brookes *et al* (263). Mitochondrial proteins (0.5 mg) were extracted with 80 µl of 0.75 M aminocaproic acid, 50 mM BisTris, and 1% *n*-dodecyl-β-D-maltoside and centrifuged at 14,000 rpm for 5 min. The supernatants containing extracted mitochondrial complexes (250µg protein) were treated with 2.5µl of Coomassie Brilliant Blue G-250 (5% w/v suspension in 0.5 M aminocaproic acid) and subjected to non-denaturing PAGE (5–12% gels) to separate the individual respiratory complexes intact.

The identity of the ATP synthase (complex V) band of mitochondria subjected to BN-PAGE was confirmed by electro-transfer of the gel to PVDF membranes and probing the blots with antibodies to mouse anti-ATP synthase α subunit (diluted 1:1000 in 5% BSA) for 12 hours at 4°C, followed by goat anti-mouse IgG-HRP (1:1000 diluted in 5% BSA) for 2 hours at 25°C. Bound HRP in western blots was

detected by chemiluminescence as described in section 2.2.11. The blots were subject to densitometric image analysis using Scion Image software.

2nd dimension TRIS-TRICINE-SDS-PAGE and western blots to detect nitrosylated ATP synthase subunits

In further experiments, the band corresponding to ATP synthase in BN-PAGE gels was excised from the gel and equilibrated with 0.375M Tris pH 8.8 containing 6M urea, 2% SDS, 20% glycerol and 30mM DTT for 30 minutes prior to separation by second dimension Tris-Tricine-SDS-PAGE (10-14% gels) with β -mercaptoethanol to separate individual proteins of the complex (264). Following Tris-Tricine-SDS-PAGE, the resolved proteins were electro transferred to PVDF membranes at 80V for 120 minutes at 4°C. Membranes were blocked with 5% BSA in PBS/0.02% Tween 20 (PBS/T) for 1 hour at 25°C and incubated with antibodies to mouse anti-ATP synthase α subunit (diluted 1:1000 in 5% BSA) for 12 hours at 4°C, followed by goat anti-mouse IgG-HRP (1:1000 diluted in 5% BSA) for 2 hours at 25°C.

Membranes were also probed with either rabbit anti-nitrotyrosine (diluted 1:1000 in 5% BSA) or rabbit anti-nitrocysteine (diluted 1:1000 in 5% BSA) for 12 hours at 4°C, followed by goat anti-rabbit IgG-HRP (1:1000 diluted in 5% BSA) for 2 hours at 25°C. Bound HRP on western blots was detected by chemiluminescence as described in section 2.2.11. The blots were subjected to densitometric image analysis with Scion Image software.

2.2.13 Biotin -iodoacetamide labelling of free sulfhydryl groups

To evaluate free sulfhydryl groups on ATP synthase subunits, mitochondria were incubated with biotin-iodoacetamide (BIAM) (100 μ M) for 15 minutes at 25°C in the dark, following which the labelling reaction was stopped with 20mM β -mercaptoethanol. The BIAM labelled mitochondria were subject to BN-PAGE and

the band corresponding to ATP synthase in BN-PAGE was excised from the gel and subjected to second dimension Tris-Tricine-SDS-PAGE (10-14% gels) with β -mercaptoethanol to separate individual proteins of the complex as given in section 2.2.12. (264). Following Tris-Tricine-SDS-PAGE, the resolved proteins were electro transferred to PVDF membranes at 80V for 120 minutes at 4°C. Membranes were blocked with 5% BSA in PBS/0.02% Tween 20 (PBS/T) for 1 hour at 25°C and incubated with streptavidin- HRP (diluted 1:10,000 in 5% BSA) for 2 hours at 25°C. Bound HRP in western blots was detected by chemiluminescence as described in section 2.2.11. The blots were subjected to densitometric image analysis with Scion Image software. Free thiol groups react with idoacetamide and give a signal on treatment with streptavidin - HRP. Thus signals on the BIAM blot membranes indicate free thiol groups while loss of signal compared to control indicates modification of sulfhydryl groups on the corresponding protein.

2.2.14 Blue Native PAGE, Isoelectric focusing and Tris-Tricine-SDS PAGE for analysis of ATP synthase subunit modifications:

The following protocol was carried out to improve protein resolution and identify ATP synthase subunits that undergo thiol group modification on MCP poisoning.

BIAM labelled mitochondria were subject to BN-PAGE to separate respiratory complexes I to V. Complex V was excised from the gel and extracted with 125 μ l rehydration buffer containing 0.875M urea, 0.25M thiourea, 2% CHAPS, 0.5% lauryl maltoside, 0.63 μ l Biolyte ampholytes (pH 3 – 10), 80 μ M tributylphosphine (TBP) and 33mM dithiothreitol (DTT)). The extracted proteins were applied on strips with an immobilized pH gradient (IPG strips) (pH 3-10) for 12 hrs at 25°C and subject to isoelectric focusing. Isoelectric focusing was carried out at 20°C using a gradient program with steps of 200 volts (until 100 volt-hours (V-hrs)), 450

volts (till 150 V-hrs), 750 volts (till 250 V-hrs), 1200 volts (till 400 V-hrs) and 2000 volts (till 3100 V-hrs), finally being held at 500 volts.

After isoelectric focusing the strips were equilibrated with 0.375M Tris pH 8.8 containing 6M urea, 2% SDS, 20% glycerol and 30mM DTT for 30 minutes prior to separation in the third dimension by Tris Tricine SDS-PAGE (10-14% gel) as given in section 2.2.12. (264). Following Tris-Tricine-SDS-PAGE, the resolved proteins were electro transferred to PVDF membranes at 80V for 120 minutes at 4°C. Membranes were blocked with 5% BSA in PBS/0.02% Tween 20 (PBS/T) for 1 hour at 25°C and incubated with streptavidin horseradish peroxidase (diluted 1:10,000 in 5% BSA) to determine free thiol groups.

Membranes were also probed with antibodies to mouse anti-ATP synthase α subunit (diluted 1:1000 in 5% BSA) or antibodies to mouse anti-ATP synthase β subunit (diluted 1:1000 in 5% BSA) for 12 hours at 4°C, followed by goat anti-mouse IgG-HRP (1:1000 diluted in 5% BSA) for 2 hours at 25°C. Bound peroxidase was visualized by chemiluminescence as given in section 2.2.11. and 2D blot images analyzed with MELANIE software (265), which enables pI and molecular weight analysis of the proteins on gels and blots.

2.2.15 Muscle GSH estimation

GSH levels were estimated in muscle homogenised in 10 volumes of 5% trichloroacetic acid /5 mM EDTA at 4°C. The homogenate was spun at 15000 $\times g$ for 10 minutes at 4°C and GSH estimated in the supernatant. Briefly the supernatant (200 μ l) was mixed with 0.8ml of 0.4mM EDTA pH 8.9 and 20 μ l of 10mM DTNB and absorbance read at 412nm after 5 minutes in the dark at 25°C (266). GSH was expressed as μ mol/gram wet tissue read from a standard of GSH.

2.2.16 Cis-MCP estimation in blood, muscle, muscle mitochondria and urine

Cis-MCP was estimated in blood, muscle, muscle mitochondria and urine by reverse phase HPLC. Blood, urine, muscle homogenate and muscle mitochondria were deproteinised with 2 volumes of (v/v) acetonitrile and centrifuged at 10,000 rpm for 7 minutes. The supernatant (100µl) mixed with 400 µl of eluent ((water: acetonitrile) (87:13, v/v)), filter sterilised through a 0.4 µm filter and 20µl of filtrate analyzed for cis-MCP.

Standard cis-MCP 1.6mM in 100µl was added to 200µl acetonitrile and mixed, 100 µl added to 400µl of eluent ((water: acetonitrile) (87:13, v/v)), filter sterilised through a 0.4 µm filter and 20µl of filtrate analyzed for cis MCP.

Separation was on a Hypersil ODS column, using water-acetonitrile (87:13 v/v) at a flow rate of 1.0 ml /min for 15 minutes at 25°C and detection at 218nm (242). The column was regenerated with water-acetonitrile (87:13 v/v) for 15 minutes prior to application of the next sample. The limit of detection of the assay was 40nM. Elution profiles were integrated using LC solution software provided by the manufacturer (Shimadzu Corporation, Kyoto, Japan). The retention time of cis-MCP was 12 minutes. Cis-MCP levels were expressed as µg/ml in blood, ng/mg tissue in muscle and as micrograms in urine, read from the standard.

2.2.17 Statistical analysis

Data are expressed as mean \pm SD. Tests of significance were performed by the Student's t test for parametric data (Normal distribution or non-skewed data) and by Mann-Whitney test for non-parametric data using statistical software SPSS version 16.0. A probability of < 0.05 was considered significant.

CHAPTER 3

RESULTS

Table 3.1.1 Clinical profile of MCP poisoned rats

Symptom	Start of symptom (Minutes) (Mean \pm SD) (n = 18)	Duration of symptom (Mean \pm SD) (n = 18)
Chewing	3.3 \pm 2.1	25.0 \pm 10 min
Body tremors	7.9 \pm 1.9	3 \pm 1 hour
Salivation	20.1 \pm 5.7	90 \pm 30 min
Lacrimation	20.4 \pm 4.2	90 \pm 30 min
Muscle power		
1) Grade I power	10.6 \pm 1.9	10 \pm 5 min
2) Grade II power	22.1 \pm 6.5	25 \pm 5 min
3) Grade III power	51.5 \pm 22.3	20 \pm 5 min

Table 3.1.2 Muscle AChE activity of control and MCP poisoned rats

	Control	Time after MCP poisoning							
		15 min	30 min	40 min	1 hour	75 min	2.5 hours	8.0 hours	24 hours
nmoles acetylthiocholine iodide hydrolysed min / mg protein (Mean \pm SD)	13.56 \pm 1.0	4.55 \pm 1.1	3.14 \pm 0.1	4.33 \pm 0.4	5.82 \pm 0.4	2.70 \pm 0.3	3.72 \pm 0.35	4.87 \pm 0.8	6.13 \pm 0.7
Sample size	n = 5	n = 3	n = 3	n = 3	n = 3	n = 4	n = 3	n = 4	n = 5

3.1.1 MCP poisoning – clinical profile in rats

Rats subjected to 0.8 LD₅₀ (6.4 mg / kg body weight) MCP poisoning manifested nicotinic signs of chewing within a mean of 3.3 min and body tremors within a mean of 7.9 minutes. Chewing continued for upto 30 minutes and tremors were evident until 4 hours after poisoning. Muscarinic signs of salivation occurred within a mean of 20.1 minutes and lacrimation in a mean time of 20.4 minutes after poisoning and continued for upto 2.5 hours after poisoning (**Table 3.1.1**).

Muscle weakness observed as ataxic gait (Grade 1 power) was seen in rats within a mean of 10.6 min after MCP administration that progressed to Grade 2 power within a mean of 22.1 min. Paralysis (Grade 3 power) occurred in the rats within a mean of 51.5 min after MCP administration and continued for a mean duration of 20 min. The rats regained partial muscle power 8 hours after poisoning and normal muscle power 24 hours later (**Table 3.1.1**).

Muscle AChE activity

Muscle AChE activity was inhibited 67% within 15 minutes of 0.8LD₅₀ MCP administration to rats. The inhibition increased to 80% 75 minutes after poisoning, followed by a decline of inhibition to 55% 24 hours later, indicating recovery of enzyme activity (**Table 3.1.2**).

Table 3.1.3 Adenine nucleotide levels in muscle of control and MCP poisoned rats

Adenine nucleotide	Controls	Time after MCP poisoning			
		1 hour	2.5 hours	8.0 hours	24 hours
ATP (nmoles / mg protein) (Mean \pm SD)	8.49 \pm 4.81	10.14 \pm 2.54	0.70 \pm 0.64 (p < 0.0001)	9.07 \pm 4.46	17.06 \pm 5.23 (p < 0.01)
ADP (nmoles / mg protein) (Mean \pm SD)	4.37 \pm 0.93	3.29 \pm 0.91	1.6 \pm 1.46 (p < 0.01)	4.41 \pm 3.77	7.09 \pm 2.11 (p < 0.01)
AMP (nmoles / mg protein) (Mean \pm SD)	0.72 \pm 0.28	0.83 \pm 0.26	0.32 \pm 0.20 (p < 0.01)	1.22 \pm 0.95	2.37 \pm 1.16 (p < 0.01)
Sample size	n = 9	n = 6	n = 6	n = 6	n = 6
p compared to control muscle					

Table 3.1.4 Energy charge of skeletal muscle following MCP administration to rats

	Control	Time after MCP poisoning			
		1 hour	2.5 hours	8.0 hours	24 hours
Energy charge (Mean \pm SD)	0.75 \pm 0.1	0.82 \pm 0.04	0.56 \pm 0.08 (p < 0.002)	0.76 \pm 0.1	0.78 \pm 0.06
Sample size	n = 9	n = 6	n = 6	n = 6	n = 6
p compared to control muscle					

Adenine nucleotide levels in skeletal muscle of rats subject to MCP poisoning

Adenine nucleotide levels in rat skeletal muscle are shown in **Table 3.1.3**. The adenine nucleotides; namely ATP, ADP and AMP were normal for 1 hour after MCP poisoning (i.e) during paralysis.

Two and a half hours after MCP poisoning the levels of muscle ATP, ADP and AMP decreased. ATP levels decreased significantly by a mean of 12-fold, ADP levels by a mean of 2.74-fold and AMP by a mean of 2.25-fold compared to controls ($p < 0.01$).

Levels of all the adenine nucleotides in muscle returned to normal 8 hours after poisoning when rats had regained muscle power.

Twenty-four hours after poisoning, when rats had regained complete muscle power, muscle ATP levels were 2.0-fold higher, ADP levels 1.62-fold higher and AMP levels 3.3-fold higher than normal ($p < 0.05$) (**Table 3.1.3**).

Energy charge of skeletal muscle of rats subject to MCP poisoning

The mean adenylate energy charge of skeletal muscle of control rats was 0.75 and of skeletal muscle 1 hour, 2.5 hours, 8 hours and 24 hours after poisoning was 0.82, 0.56, 0.76 and 0.78 respectively. The energy charge of skeletal muscle 2.5 hours after poisoning decreased significantly in comparison to controls ($p < 0.002$) (**Table 3.1.4**).

Table 3.2.1 Integrity of skeletal muscle mitochondria isolated from control and MCP poisoned rats

Parameter	Control	Time after MCP poisoning			
		1 hour	2.5 hours	8.0 hours	24 hours
Mitochondrial swelling (Decrease in absorbance at 540nm/min/mg protein) (Mean \pm SD) (n = 6)	0.002 \pm 0.001	0.002 \pm 0.002	0.004 \pm 0.004	0.003 \pm 0.002	0.003 \pm 0.004

Table 3.2.2 ATP synthase activity of skeletal muscle mitochondria isolated from control and MCP poisoned rats

Parameter	Control	Time after MCP poisoning			
		1 hour	2.5 hours	8.0 hours	24 hours
ATP synthase activity (μ moles NADH oxidised/min/mg protein) (Mean \pm SD)	0.31 \pm 0.05	0.27 \pm 0.04	0.14 \pm 0.09 (p < 0.0002)	0.22 \pm 0.05 (p < 0.01)	0.27 \pm 0.03
Sample size	n = 11	n = 6	n = 9	n = 6	n = 6
p compared to control muscle mitochondria					

Table 3.2.3 skeletal muscle lactate levels in control and MCP poisoned rats

Parameter	Control	Time after MCP poisoning			
		1 hour	2.5 hours	8.0 hours	24 hours
Lactate (μ moles /gram wet tissue) (Mean \pm SD) (n = 6)	3.44 \pm 1.04	3.56 \pm 0.52	2.07 \pm 0.92 (p < 0.05)	2.79 \pm 1.15	3.48 \pm 0.66
p compared to control muscle					

3.2 Muscle mitochondrial ATP synthase activity over the course of acute severe

OPP poisoning

3.2.1 Skeletal muscle mitochondria – integrity

Mitochondrial swelling was assessed as an indirect measure of mitochondrial integrity. The decrease in absorbance at 540nm/min/mg protein of mitochondria isolated from control rats (0.002 ± 0.001 ; n=6) did not differ from that of mitochondria isolated from rats after MCP treatment for 1 hour, 2.5 hours, 8 hours and 24 hours (**Table 3.2.1**).

Skeletal muscle mitochondrial ATP synthase activity of rats subject to MCP poisoning

ATP synthase (Complex V) was inhibited 12%, 54%, 28% and 12% in muscle mitochondria 1 hour, 2.5 hours, 8 hours and 24 hours respectively after MCP poisoning compared to non-treated control animals. This inhibition was significant at 2.5 hours and 8.0 hours after poisoning ($p < 0.01$) (**Table 3.2.2**).

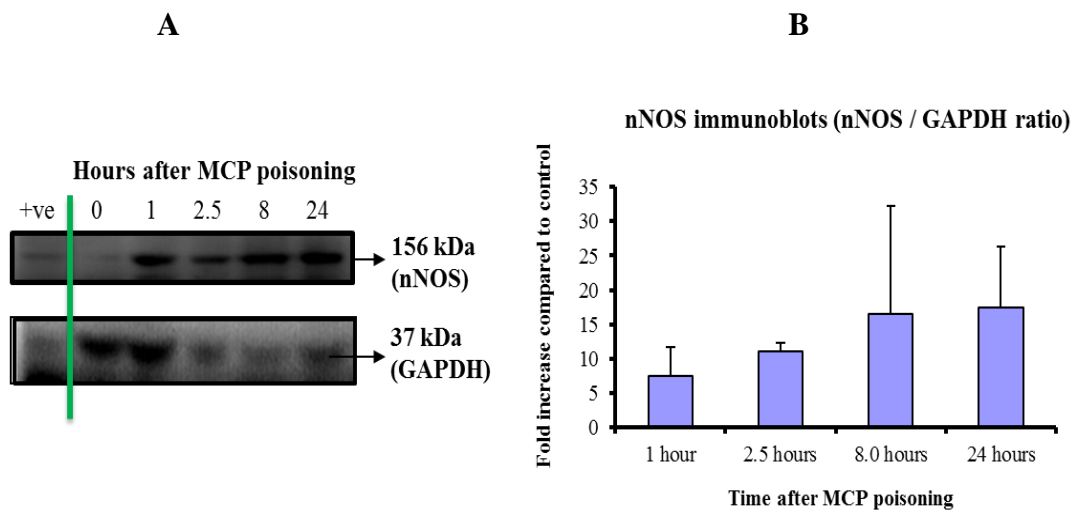
Muscle lactate levels

As shown in **Table 3.2.3**, muscle lactate levels were normal for 1 hour after MCP poisoning, decreased significantly 2.5 hours after poisoning by 40% ($p < 0.05$) and by 19% 8 hours after poisoning. The levels were normal 24 hours after poisoning.

Table 3.3.1 Muscle nitrate levels in control and MCP poisoned rats

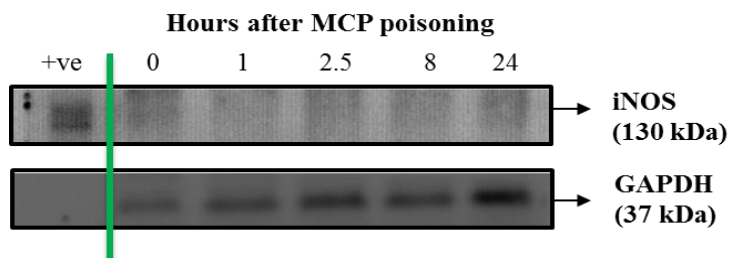
Parameter	Control	Time after MCP poisoning			
		1 hour	2.5 hours	8.0 hours	24 hours
Nitrate (nmoles /mg protein) (Mean \pm SD) (n = 6)	0.48 \pm 0.06	1.21 \pm 0.16 (p < 0.0001)	1.36 \pm 0.23 (p < 0.0001)	1.23 \pm 0.38 (p < 0.003)	1.23 \pm 0.33 (p < 0.002)
p compared to control muscle					

Figure 3.3.1 Representative Western blot of nNOS in control and MCP poisoned rat skeletal muscle



A. Western blots of nNOS of skeletal muscle excised from un-poisoned control (0 hours) and MCP poisoned rats. **B.** Densitometric analysis of nNOS Western blot (Mean \pm SD, n = 3).

Figure 3.3.2 Representative Western blot of iNOS in control and MCP poisoned rat skeletal muscle



Western blots of iNOS of skeletal muscle excised from un-poisoned control and MCP poisoned rats. (n = 3).

3.3 The role of NO in ATP synthase inhibition following acute severe OPP poisoning

3.3.1 Nitrate levels in skeletal muscle

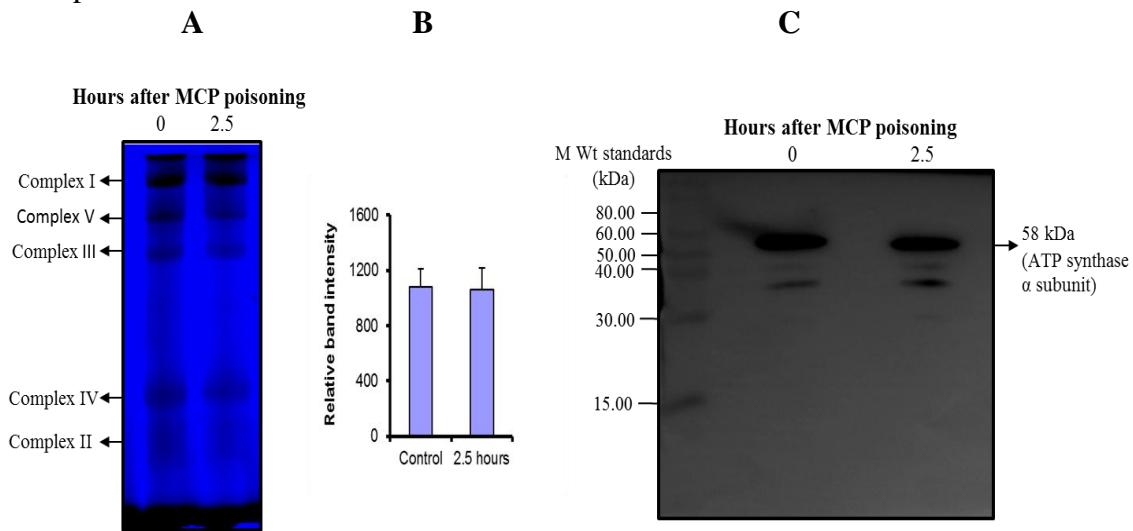
Nitrate levels in skeletal muscle of rats are shown in **Table 3.3.1**. MCP poisoning led to significant increase in nitrate levels in skeletal muscle within 1 hour, which remained elevated on recovery of muscle power (i.e) 24 hours after MCP poisoning.

Source of muscle NO in acute severe MCP poisoning

nNOS protein expression was increased in MCP poisoning. Densitometric analysis of nNOS to GAPDH band intensities on western blots showed that nNOS increased 7.5 ± 4.1 fold in muscle of MCP poisoned rats 1 hour after poisoning and remained at this elevated level for 24 hours compared to muscle of non-poisoned rats (n =3) (**Figure 3.3.1 (A & B)**).

iNOS protein was not detected in muscle of MCP poisoned rats (n =3) (**Figure 3.3.2**).

Figure 3.3.3 A representative BN-PAGE of mitochondria isolated from control and MCP poisoned rat skeletal muscle

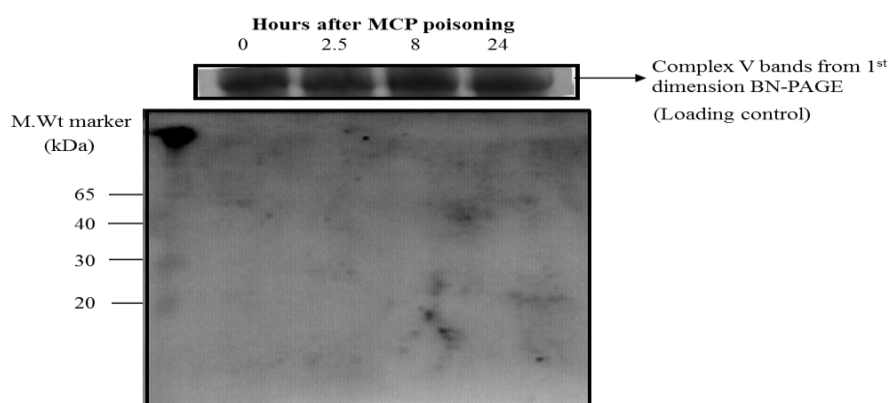


A. Representative BN-PAGE. Mitochondrial complex V protein separated by BN-PAGE from unpoisoned control rat (0 hours) and from MCP poisoned rat (2.5 hours).

B. Densitometric analysis of mitochondrial complex V protein separated by BN-PAGE from control and MCP poisoned rats (2.5 hours) (Mean \pm SD, n = 15).

C. Representative ATP synthase α subunit blot. Mitochondrial complex V excised from BN-PAGE of control and MCP poisoned rat mitochondria were subjected to Tris-Tricine-SDS-PAGE, electroblotting and probed with ATP synthase α subunit antibodies.

Figure 3.3.4 Representative nitrotyrosine blot of complex V from mitochondria isolated from control and MCP poisoned rat skeletal muscle



Representative nitrotyrosine blot. Mitochondrial complex V excised from BN-PAGE of control and MCP poisoned rat mitochondria were subjected to Tris-Tricine-SDS-PAGE, electroblotting and probed with anti-nitro-tyrosine antibodies.

NO induced post-translational modification of muscle mitochondrial ATP synthase

To identify NO induced post-translational modifications of ATP synthase (complex V), the mitochondria were subject to Blue native polyacrylamide gel electrophoresis (BN-PAGE) to separate respiratory complexes I to V followed by Tris-Tricine-SDS-PAGE for separation of complex V subunits. The complex V protein was electro transferred to PVDF membranes. Membranes were probed with nitrotyrosine or nitrocysteine antibodies to check NO induced post-translational modifications.

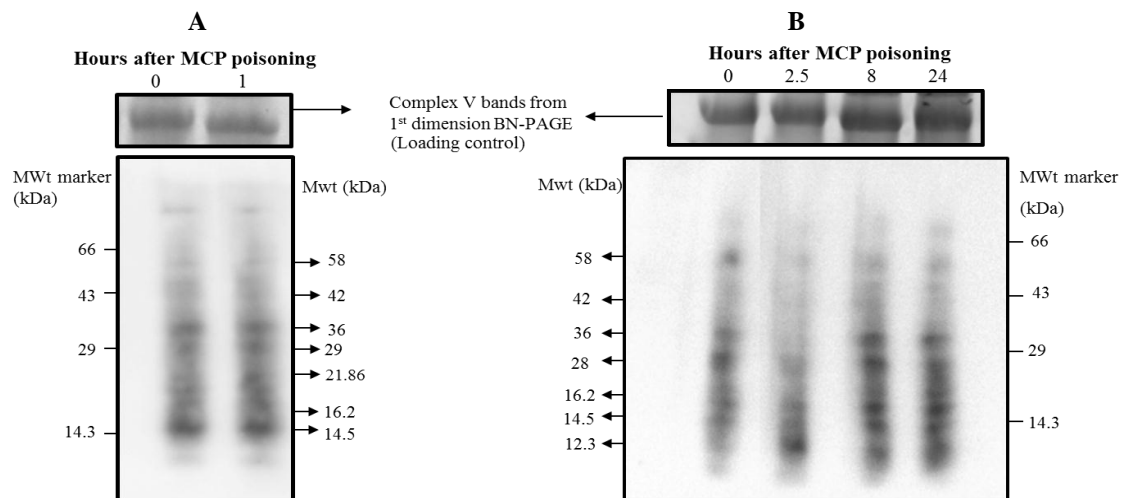
BN-PAGE was used to separate complex V in native form. No difference in level of complex V protein was noted between control and MCP poisoned rats after 2.5 hours on 1D BN-PAGE (n = 15) (**Figure 3.3.3. A & B**).

In further experiments, the band corresponding to ATP synthase in BN-PAGE was excised from the gel and subjected to second dimension Tris-Tricine-SDS-PAGE to separate individual protein subunits and transferred to PVDF membranes. Then membranes were probed with ATP synthase α subunit, which confirmed that the excised protein complex was ATP synthase. (**Figure 3.3.3. C**).

Nitrotyrosinylation of complex V in MCP poisoned rats

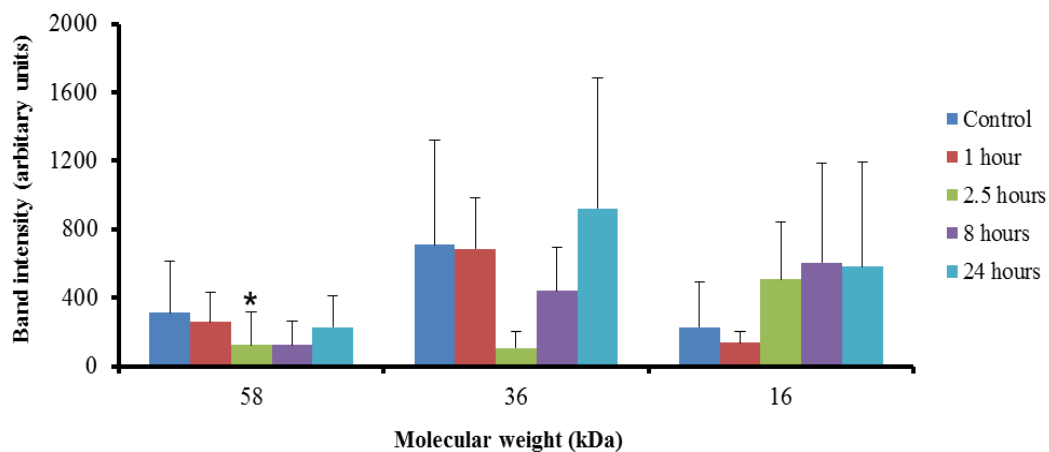
The complex V protein band from BN-PAGE was excised from the gel and subjected to 2nd dimension Tris-Tricine-SDS-PAGE to separate individual proteins of the complex. Following Tris-Tricine-SDS-PAGE, the resolved proteins were electro transferred to PVDF membranes. Membranes were probed with rabbit anti-nitrotyrosine antibodies. Western blots showed that MCP poisoning did not lead to tyrosine nitration of ATP synthase (n = 3) (**Figure 3.3.4**).

Figure 3.3.5 A A representative sulphhydryl group labeling of complex V from mitochondria isolated from control and MCP poisoned rat skeletal muscle



A & B. Representative BIAM labelling of ATP synthase from control and MCP poisoned rats. BIAM labelled mitochondria were subjected to BN-PAGE and complex V excised from BN-PAGE of control and MCP poisoned rat mitochondria, subjected to Tris-Tricine-SDS-PAGE, electroblotting and probed with streptavidin -HRP antibodies.

Figure 3.3.5 C Densitometric analysis of complex V sulphhydryl group labeling from mitochondria isolated from control and MCP poisoned rat skeletal muscle

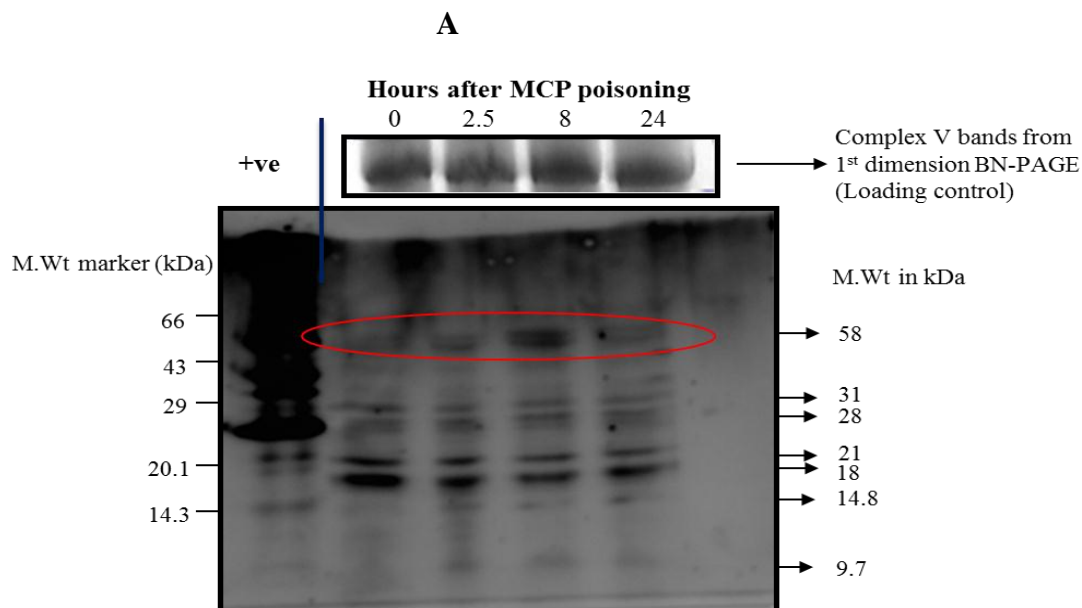


Densitometric analysis of sulphhydryl group labelling of complex V. (Mean \pm SD) * $p < 0.05$ compared to control.

Sulphydryl group modification of ATP synthase following MCP poisoning

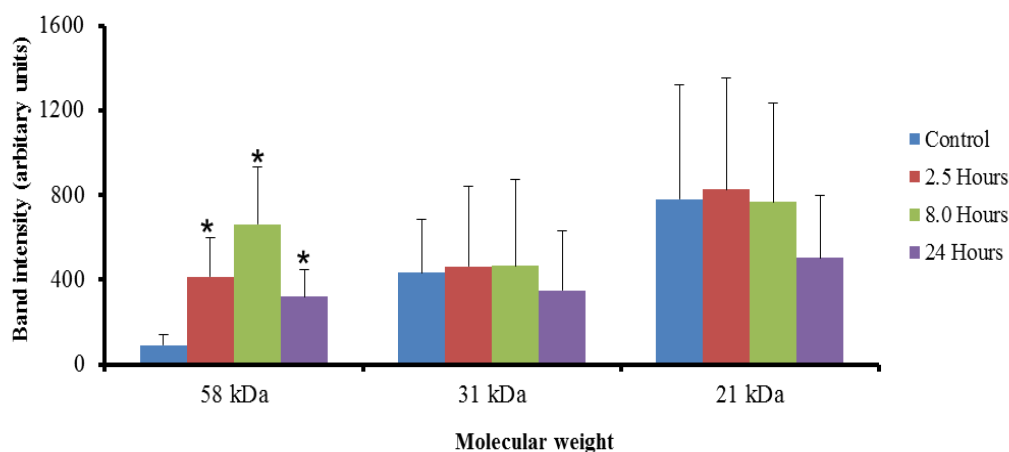
Free thiol groups react with Biotin-iodoacetamide resulting in signals on the BIAM blot membranes indicative of free thiol groups. BN-PAGE, Tris-Tricine-SDS-PAGE and western blots of ATP synthase from mitochondria treated with biotin-iodoacetamide indicated that MCP poisoning did not lead to modification of sulphydryl groups of the enzyme for one hour (n = 3) (**Figure 3.3.5A**). Free sulphydryl groups were modified i.e. not available for reaction with iodoacetamide, at 2.5, 8 and 24 hours after poisoning (n = 6). Sulphydryl group modification was identified to occur on the 58 and 36 kDa subunits of ATP synthase. Sulphydryl group modifications were reversible. The modifications were maximal 2.5 hours after poisoning and reversible (**Figure 3.3.5. A , B & C**).

Figure 3.3.6 A Representative nitro-cysteine blot of complex V from mitochondria isolated from control and MCP poisoned rat skeletal muscle



Representative nitro-cysteine blot. Mitochondrial complex V excised from BN-PAGE of control and MCP poisoned rat mitochondria were subjected to Tris-Tricine-SDS-PAGE, electroblotting and probed with anti-nitro-cysteine antibodies.

Figure 3.3.6 B Densitometric analysis of nitro-cysteine blots of complex V from mitochondria isolated from control and MCP poisoned rat skeletal muscle



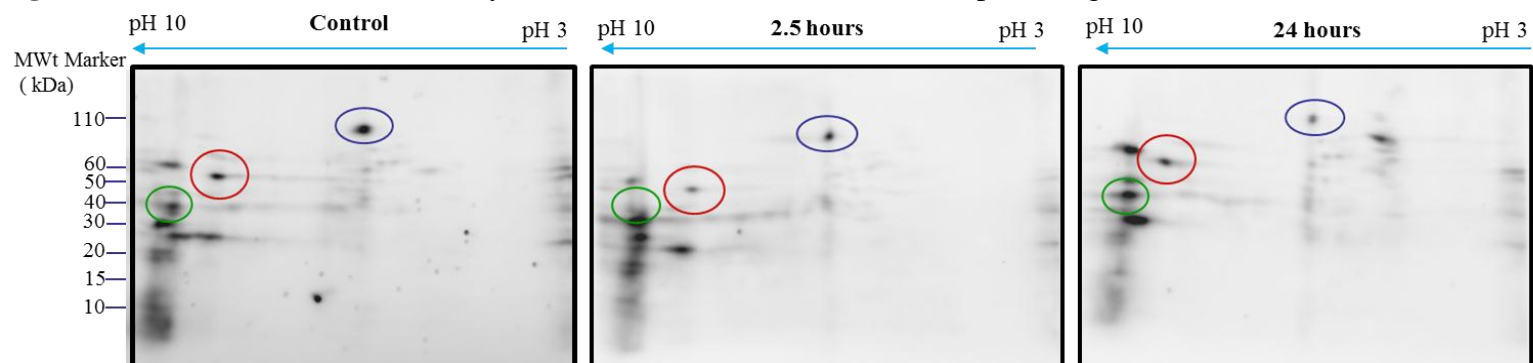
Densitometric analysis of nitro-cysteinylation of complex V. (Mean \pm SD, n = 3) * p < 0.05 compared to control.

Nitrocysteinylation of complex V

BIAM labelling indicated that free sulphhydryl groups were modified in MCP poisoning. This might be through either oxidative or nitrosative modifications. In order to evaluate NO induced modifications we examined nitrocysteinylation of ATP synthase.

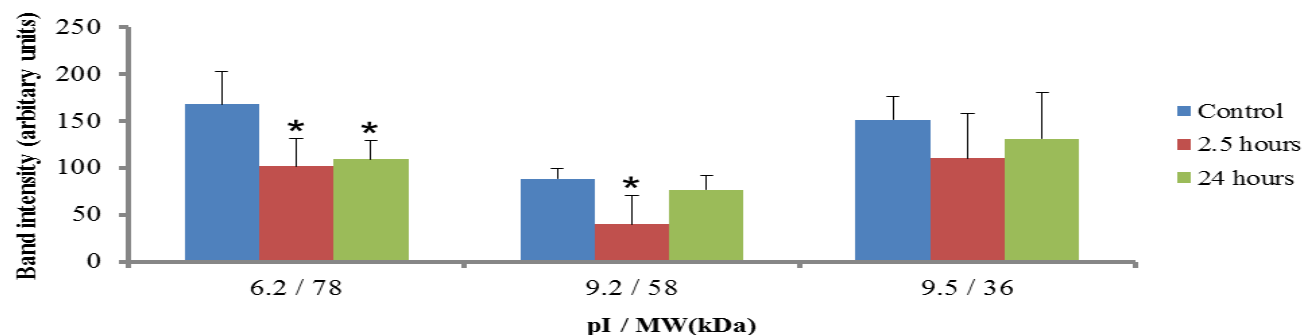
2D gel electrophoresis with BN-PAGE followed by Tris-Tricine-SDS-PAGE and western blots showed that MCP poisoning led to a 4.5, 7.2 & 3.5 fold increase in nitro-cysteinylation of the 58 kDa α subunit of complex V at 2.5 hours, 8 hours and 24 hours respectively after poisoning ($p < 0.05$). Despite the decrease in free sulphhydryl group labelling on 36 kDa, nitrocysteinylation of 36 kDa was not seen in MCP poisoned rats ($n = 3$) (**Figure 3.3.6 A & B**).

Figure 3.3.7A Identification of ATP synthase subunit modification in MCP poisoning



Representative sulphhydryl group labelled mitochondrial complex V blot. Sulphydryl group labelled control and MCP poisoned rat skeletal muscle mitochondria were subjected to BN-PAGE. Complex V proteins were extracted from the BN-PAGE and subjected to IEF in a immobilised pH gradient strips (pH 3 -10). After IEF, the strips were subjected to Tris-Tricine-SDS-PAGE and resolved proteins were transferred to PVDF membranes. Membranes were probed with streptavidin horseradish peroxidase.

Figure 3.3.7B Densitometric analysis of sulphhydryl group labelled blots of control and MCP poisoned rat

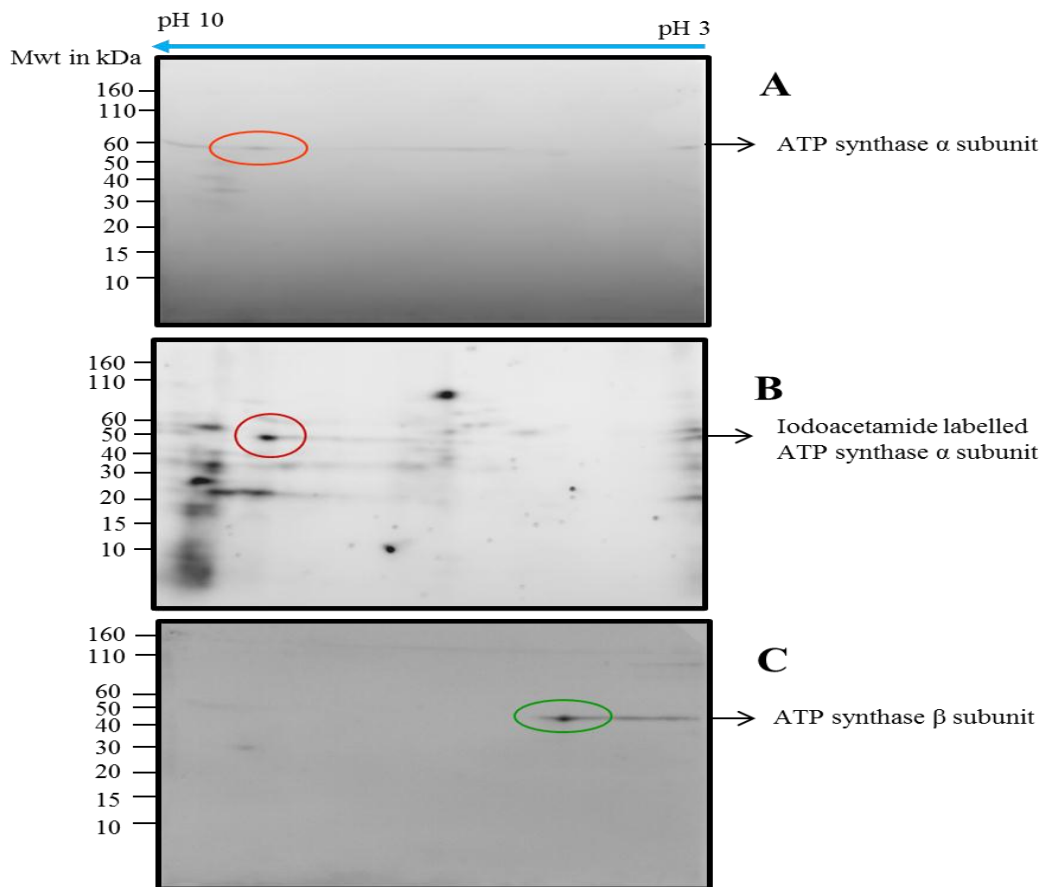


Densitometric analysis of sulphhydryl group labelled complex V blots of control and MCP poisoned rat (Mean \pm SD, n = 3). * p < 0.05 compared to control.

Identification of ATP synthase subunit modification in MCP poisoning

Western blots of ATP synthase after separation by BN-PAGE, IEF and Tris-Tricine-SDS-PAGE also showed subunits of 78 kDa at pI 6.2, 58 kDa at pI 9.2 and 36 kDa at pI 9.5 to undergo reversible sulphhydryl group modification maximally 2.5 hours after MCP poisoning in rats (n =3) (**Figure 3.3.7. A & B**).

Figure 3.3.8 ATP synthase α and β subunit blots of sulphydryl group labelled ATP synthase



Sulphydryl group labelled control rat skeletal muscle mitochondria were subjected to BN-PAGE. Complex V proteins were extracted from the BN-PAGE and subjected to IEF in a immobilised pH gradient strips (pH 3- 10). After IEF, the strips were subjected to Tris-Tricine-SDS-PAGE and resolved proteins were transferred to PVDF membranes. Membranes were probed with A) ATP synthase α subunit, B) Streptavidin horseradish peroxidase and C) ATP synthase β subunit.

Table 3.3.2 Muscle reduced glutathione levels in the control and MCP poisoned rats

Parameter	Control	Time after MCP poisoning			
		1 hour	2.5 hours	8.0 hours	24 hours
Reduced glutathione (μ moles / gram wet tissue) (Mean \pm SD) (n = 6)	0.89 \pm 0.13	1.09 \pm 0.37	0.64 \pm 0.18 (p < 0.05)	0.82 \pm 0.27	1.04 \pm 0.37
p compared to control muscle					

ATP synthase α and β subunit blots of sulphhydryl group labelled ATP synthase

Western blots probed for ATP synthase α and β subunits after separation by BN-PAGE, IEF and Tris-Tricine-SDS-PAGE resulted in detection of proteins at 58 and 52 kDa subunits. The modified 58 kDa protein (pI \rightarrow 9.2) was identified as the α subunit of ATP synthase (**Figure 3.3.8**).

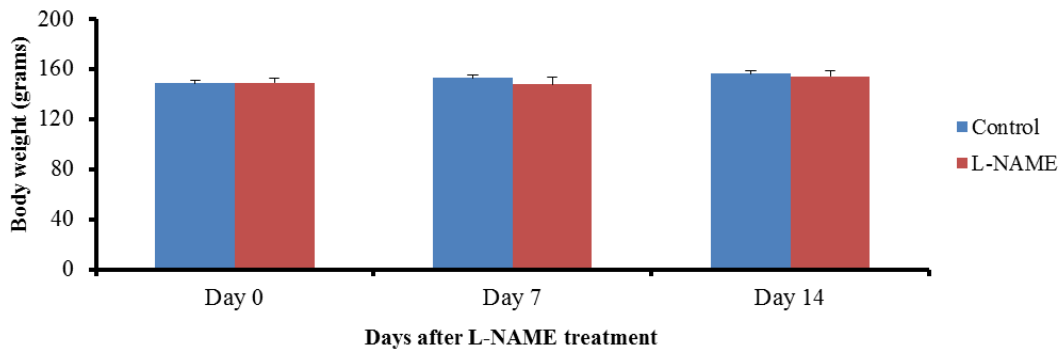
Muscle GSH levels

Muscle GSH levels are given in **Table 3.3.2**. MCP poisoning led to significant 28% decrease in GSH levels of skeletal muscle 2.5 hours after poisoning ($p < 0.05$) and returned to normal 8 hours after poisoning. Muscle GSH levels increased by 22% and 17% by 1 hour and 24 hours after poisoning respectively.

Table 3.3.3 Clinical profile of MCP poisoned rats pre-treatment with and without L-NAME

Symptom	Start of symptom (Minutes) (Mean ±SD)		Duration of symptom (Mean ±SD)	
	MCP (n = 18)	L-NAME + MCP (n = 9)	MCP (n = 18)	L-NAME + MCP (n = 9)
Chewing	3.3 ±2.1*	5.2 ±1.1* (p < 0.01)	25.0 ± 10 min	24.6 ±4.3 min
Body tremors	7.9 ± 1.9**	11.8 ± 1.5** (p < 0.0001)	3 ± 1 hour	4 ± 1 hour
Salivation	20.1 ± 5.7	28.4 ± 14.2	90 ± 30 min	68.3 ± 38.6 min
Lacrimation	20.4 ± 4.2	22.1 ± 2.6	90 ± 30 min	70.6 ± 33.4 min
Muscle power				
Grade I power	10.6 ± 1.9	12.0 ± 2.5	10 ± 5 min	12.1 ± 4.14 min
Grade II power	22.1 ± 6.5	24.1 ± 5.35	25 ± 5 min	26.2 ± 17.6 min
Grade III power	51.5 ± 22.3	50.3 ± 16.3	20 ± 5 min	18.0 ± 1.73 min
p compared to MCP poisoned rats				

Figure: 3.3.9 Effect of L-NAME on body weight of rats



Body weight of rats with and without L-NAME pre-treatment. (Mean ± SD, n = 6)

Can MCP induced ATP synthase inhibition be prevented by pre-treatment with NO synthase inhibitor L-NAME?

As ATP synthase activity was severely inhibited and ATP levels decreased 2.5 hours after MCP poisoning, we carried out our study in L-NAME pre-treated rats at 2.5 hours after MCP poisoning.

MCP poisoning – clinical profile in rats pre-treatment with and without L-NAME

Rats treated with L-NAME to inhibit NOS and subjected to severe MCP poisoning (0.8LD₅₀) manifested significant delay in the development of nicotinic signs of chewing that developed within a mean of 5.2 min and body tremors that developed within a mean of 11.8 minutes when compared to rats not treated with L-NAME (7.9 min). Muscarinic signs of salivation occurred within a mean of 28.4 minutes and lacrimation in a mean time of 22.1 minutes (20.1 & 20.4 min in MCP poisoned rats not treated with L-NAME respectively) (**Table 3.3.3**).

The development of muscle weakness, paralysis and recovery of muscle power was as seen in MCP poisoned rats not treated with L-NAME (**Table 3.3.3**).

Body weight after L-NAME treatment

Fourteen days of L-NAME treatment (20 mg/ kg) did not significantly decrease body weight of rats when compared to age matched controls. The initial body weights of control and L-NAME treated rats were 149 ± 3.0 and 149 ± 3.7 grams respectively and on day 14; 156.3 ± 2.7 and 154.3 ± 4.6 grams respectively (**Figure: 3.3.9**).

Table 3.3.4 Muscle AChE activity of control and MCP poisoned rats pre-treatment with and without L-NAME.

	Control	Control + L-NAME	Time after MCP poisoning	
			2.5 hours	L-NAME + 2.5 hours
nmoles acetylthiocholine iodide hydrolysed / min / mg protein (Mean \pm SD)	13.56 \pm 0.96	13.64 \pm 0.67	3.72 \pm 0.35	4.01 \pm 0.48
Sample size	n = 5	n = 3	n = 3	n = 3

Table 3.3.5 Adenine nucleotide levels in the muscle of control and MCP poisoned rats pre-treatment with and without L-NAME.

Adenine nucleotide	Control	Control + L-NAME	Time after MCP poisoning	
			2.5 hours	L-NAME + 2.5 hours
ATP (n moles / mg protein) (Mean \pm SD)	8.49 \pm 4.81	6.93 \pm 0.80	0.7 \pm 0.64 (p < 0.0001)	3.28 \pm 0.28 (p < 0.02)
ADP (n moles / mg protein) (Mean \pm SD)	4.37 \pm 0.93	2.74 \pm 0.55	1.6 \pm 1.5 (p < 0.01)	2.06 \pm 0.59
AMP (n moles / mg protein) (Mean \pm SD)	0.72 \pm 0.28	1.81 \pm 1.04	0.32 \pm 0.21 (p < 0.01)	1.78 \pm 0.82
Sample size	n = 9	n = 3	n = 6	n = 3
	p compared to control muscle			

Table 3.3.6 Energy charge of skeletal muscle of control and MCP poisoned rats pre-treatment with and without L-NAME.

	Control	Control + L-NAME	Time after MCP poisoning	
			2.5 hours	L-NAME + 2.5 hours
Energy charge (Mean \pm SD)	0.75 \pm 0.1	0.73 \pm 0.1	0.56 \pm 0.08 (p < 0.002)	0.62 \pm 0.1 (p < 0.05)
Sample size	n = 9	n = 3	n = 6	n = 3
	p compared to control muscle			

Skeletal muscle AChE activity of L-NAME treated rats subject to MCP poisoning

In L-NAME treated rats subject to severe MCP poisoning (0.8LD₅₀) muscle AChE inhibition was similar to that seen in rats not pre-treated with L-NAME (**Table 3.3.4**).

Adenine nucleotide levels in skeletal muscle of L-NAME treated rats subject to MCP poisoning

L-NAME treatment reduced ATP levels by 18 % and ADP levels by 37% compared to un-treated controls. The decrease in ADP levels was significant ($p < 0.02$).

Two and a half hours after MCP poisoning of L-NAME treated rats, muscle ATP levels were reduced by 52% compared to L-NAME treated control rats ($p < 0.01$), ADP levels were reduced by 25% compared to L-NAME treated control rats and AMP levels were not altered (**Table 3.3.5**).

Energy charge of skeletal muscle of L-NAME treated rats subject to MCP poisoning

The mean adenylate energy charge of skeletal muscle of L-NAME treated rats was 0.73 and did not differ from that of skeletal muscle 2.5 hours after MCP poisoning which was 0.62 (**Table 3.3.6**).

Table 3.3.7 ATP synthase activity in the muscle mitochondria of control and MCP poisoned rats pre-treatment with and without L-NAME.

Parameter	Control	Control + L-NAME	Time after MCP poisoning	
			2.5 hours	L-NAME + 2.5 hours
ATP synthase activity (μ moles NADH oxidised/min/mg protein) (Mean \pm SD)	0.31 \pm 0.05	0.3 \pm 0.01	0.14 \pm 0.09 (p < 0.0002)	0.22 \pm 0.02 (p < 0.0002)
Sample size	n = 11	n = 3	n = 9	n = 3
p compared to control muscle mitochondria				

Table 3.3.8 Lactate levels in the muscle of control and MCP poisoned rats pre-treatment with and without L-NAME.

Parameter	Control	Control + L-NAME	Time after MCP poisoning	
			2.5 hours	L-NAME + 2.5 hours
Lactate levels (μ moles / gram wet tissue) (Mean \pm SD)	3.44 \pm 1.04	4.08 \pm 0.28	2.07 \pm 0.92 (p < 0.05)	3.16 \pm 0.26
Sample size	n = 6	n = 3	n = 6	n = 3
p compared to control muscle				

Table 3.3.9 Muscle nitrate levels in the control and MCP poisoned rats pre-treatment with and without L-NAME

Parameter	Control	Control + L-NAME	Time after MCP poisoning	
			2.5 hours	L-NAME + 2.5 hours
Nitrate (nmoles / mg protein) (Mean \pm SD)	0.48 \pm 0.06	0.28 \pm 0.02 (p < 0.0001)	1.36 \pm 0.23 (p < 0.0001)	0.74 \pm 0.05 (p < 0.001)
Sample size	n = 6	n = 3	n = 6	n = 3
p compared to control muscle				

Skeletal muscle mitochondrial ATP synthase activity of L-NAME treated rats subject to MCP poisoning

In L-NAME treated rats, ATP synthase (Complex V) was significantly inhibited 27% in muscle mitochondria 2.5 hours after MCP poisoning compared to L-NAME treated control animals ($p < 0.01$) (**Table 3.3.7**).

ATP synthase activity of L-NAME treated rats was 73% 2.5 hours after MCP poisoning while it was 46% in non L-NAME treated poisoned rats ($p < 0.02$) (**Table 3.3.7**).

Lactate levels of skeletal muscle of L-NAME treated rats subject to MCP poisoning

In L-NAME treated rats, lactate levels were significantly decreased by 23% in muscle 2.5 hours after MCP poisoning compared to L-NAME treated control animals ($p < 0.02$) (**Table 3.3.8**).

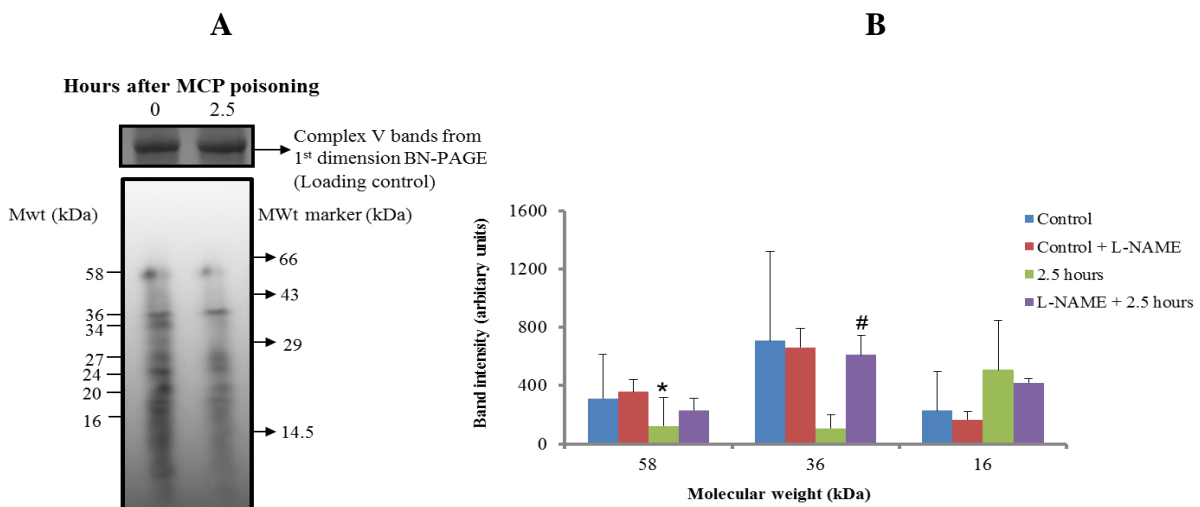
Lactate levels of skeletal muscle 2.5 hours after poisoning in L-NAME treated rats were 53% higher than un-treated poisoned control ($p < 0.02$) (**Table 3.3.8**).

Nitrate levels in the skeletal muscle of rats pre-treated with L-NAME

L-NAME treatment of rats led to a 44% decrease of nitrate levels in skeletal muscle compared to non-treated rats (**Table 3.3.9**).

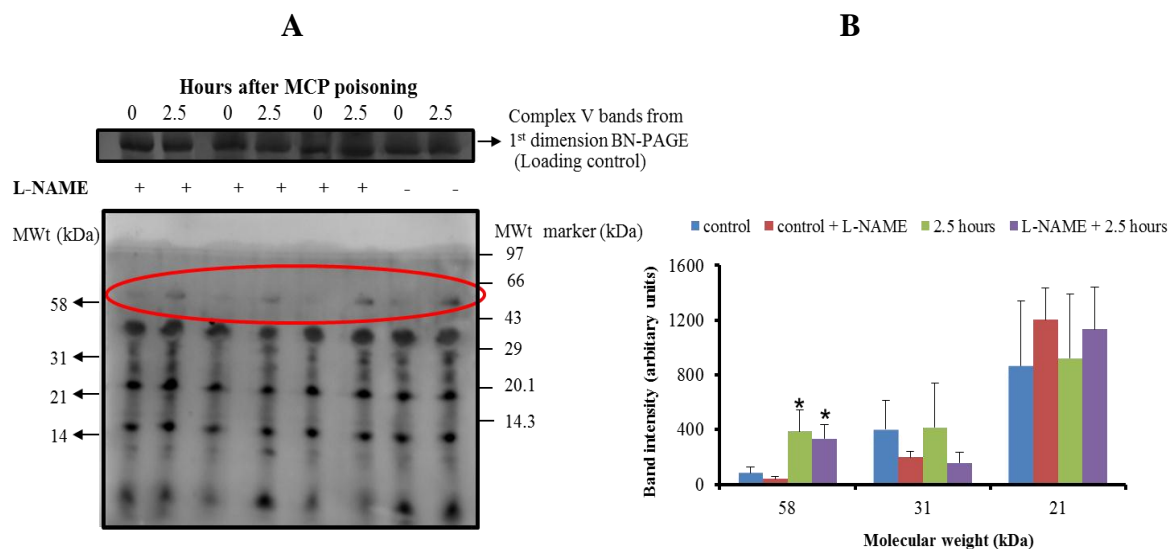
Muscle nitrate levels of L-NAME treated rats subject to MCP increased 264 % 2.5 hours after poisoning compared to non-poisoned L-NAME treated rats, but the levels were 46 % less than of poisoned rats pre-treated with L-NAME ($p < 0.001$) (**Table 3.3.9**).

Figure 3.3.10 Representative sulphhydryl group labeling of complex V from mitochondria isolated from control and MCP poisoned rat skeletal muscle pre-treatment with L-NAME.



Sulphhydryl group labelling of complex V - Mitochondrial complex V from control and MCP poisoned rats pre-treated with L-NAME. **B.** Densitometric analysis of sulphhydryl group labelling of complex V blots- (Mean \pm SD, n = 3) * p < 0.05 compare to control. # p < 0.05 compared to un-treated control.

Figure 3.3.11 Representative nitrocyysteine blot of complex V from mitochondria isolated from control and MCP poisoned rat skeletal muscle pre-treatment with and without L-NAME



A. Nitrocyysteine blot. Mitochondrial complex V from control and MCP poisoned rat skeletal muscle (2.5 hours) pre-treatment with and without L-NAME. **B.** Densitometric analysis of nitrocyysteine blot (Mean \pm SD, n = 3) * p < 0.05 compared to un-treated control.

Sulphydryl group modification of ATP synthase following MCP poisoning in rats pre-treated with L-NAME

The extent of sulphydryl group modification was less in MCP poisoned rats pre-treated with L-NAME. Sulphydryl group modification on 58 and 36 kDa subunits were less in MCP poisoned rats pre-treated with L-NAME, though only the changes on the 36 kDa subunit attained statistical significance. **(Figure 3.3.10).**

Nitrocysteinylation of complex V in MCP poisoned rats pre-treated with L-NAME

L-NAME treatment of rats reduces MCP induced nitro-cysteinylation of the 58 kDa subunit (n =3) **(Figure 3.3.11A & B).**

Table 3.3.10 Muscle reduced glutathione levels in the control and MCP poisoned rats pre-treatment with and without L-NAME

Parameter	Control	Control + L-NAME	Time after MCP poisoning	
			2.5 hours	L-NAME + 2.5 hours
Reduced glutathione (μ moles / gram wet tissue) (Mean \pm SD)	0.89 \pm 0.13	0.79 \pm 0.1	0.64 \pm 0.18 (p < 0.05)	0.71 \pm 0.03 (p < 0.05)
Sample size	n = 6	n = 3	n = 6	n = 3
p compared to control muscle				

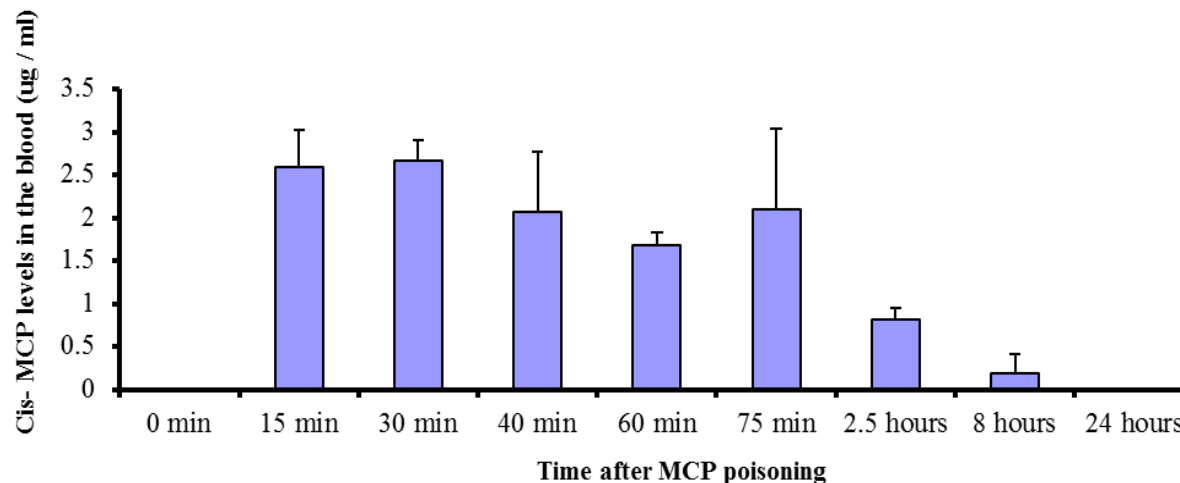
Muscle GSH levels of L-NAME treated rats subject to MCP poisoning

In L-NAME treated rats, GSH levels decreased by 10% in muscle 2.5 hours after MCP poisoning compared to L-NAME treated control animals (**Table 3.3.10**).

Table 3.4.1 Cis-MCP levels in the blood of control and MCP poisoned rats

	Control	Time after MCP poisoning							
		15 min	30 min	40 min	60 min	75 min	2.5 hours	8.0 hours	24 hours
Cis-MCP levels in the blood ($\mu\text{g/ml}$) (Mean \pm SD)	0	2.59 ± 0.4	2.66 ± 0.2	2.07 ± 0.7	1.68 ± 0.1	2.1 ± 0.9	0.81 ± 0.2	0.19 ± 0.2	0
Sample size	n = 6	n = 3	n = 3	n = 4	n = 3	n = 5	n = 7	n = 6	n = 4

Figure 3.4.1 Histogram of cis-MCP levels in the blood of control and MCP poisoned rats



Histogram shows cis –MCP levels in the blood of control and MCP poisoned rat (Mean \pm SD) .

3.4 MCP induced muscle weakness and recovery of muscle power in relation to clearance of pesticide

3.4.1 Cis-MCP levels in rat blood

MCP was administered orally by gavage into the stomach of rats.

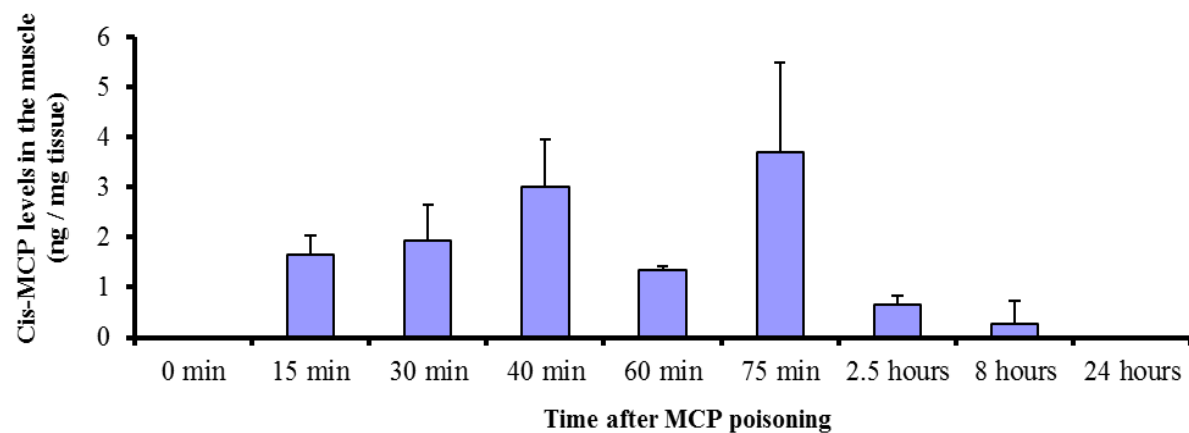
Cis-MCP was detected in the blood 15 minutes after administration at 2.59 ± 0.43 μg /ml, $1/40^{\text{th}}$ the given dose. These levels were maintained in blood for 75 minutes.

Two and half hours and 8 hours after poisoning the levels were 0.81 ± 0.2 μg /ml and 0.19 ± 0.22 μg /ml respectively. Cis-MCP was not detected in blood 24 hours after administration (**Table 3.4.1**), (**Histogram 3.4.1**).

Table 3.4.2 Cis-MCP levels in the muscle of control and MCP poisoned rats

	Control	Time after MCP poisoning							
		15 min	30 min	40 min	60 min	75 min	2.5 hours	8.0 hours	24 hours
Cis-MCP levels in the muscle (ng/mg tissue) (Mean \pm SD)	0	1.66 \pm 0.4	1.93 \pm 0.7	3.02 \pm 0.9	1.35 \pm 0.1	3.70 \pm 1.8	0.66 \pm 0.2	0.27 \pm 0.5	0
Sample size	n = 3	n = 3	n = 3	n = 3	n = 3	n = 5	n = 3	n = 7	n = 3

Figure 3.4.2 Histogram of cis-MCP levels in the muscle of control and MCP poisoned rats



Histogram shows cis –MCP levels in the muscle of control and MCP poisoned rat (Mean \pm SD)

Cis-MCP levels in rat skeletal muscle and mitochondria

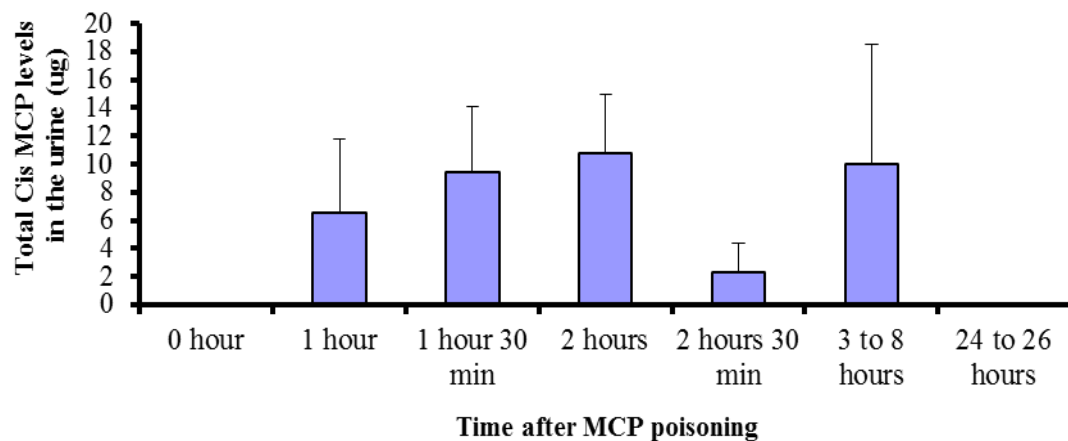
Cis-MCP was detected in skeletal muscle 15 minutes after administration at levels of 1.66 ± 0.4 ng/mg tissue. The levels increased at 40 minutes to 3.02 ± 0.9 ng/mg tissue, decreased at 60 minutes to levels noted at 15 minutes and increased at 75 minutes to 3.7 ± 1.8 ng/mg tissue. Muscle levels of cis-MCP were 0.66 ± 0.2 ng/mg tissue 2.5 hours after administration and not detected 8 and 24 hours after poisoning (**Table 3.4.2**), (**Histogram 3.4.2**).

Cis-MCP was not detected in the skeletal muscle mitochondria in MCP poisoned animals.

Table 3.4.3 Total cis-MCP levels in the urine of control and MCP poisoned rats

	Control	Time after MCP poisoning					
		1 hour	1 hour 30 min	2 hours	2 hours 30 min	3 to 8 hours	24 to 26 hours
Total cis-MCP in urine (μg) (Mean \pm SD) (n = 3)	0	6.53 \pm 5.3	9.43 \pm 4.7	10.75 \pm 4.2	2.33 \pm 2.0	9.97 \pm 8.6	0

Figure 3.4.3 Histogram of total cis-MCP levels in the urine of control and MCP poisoned rats



Histogram shows total cis –MCP levels in the urine of control and MCP poisoned rat (Mean \pm SD).

Cis-MCP levels in rat urine

As MCP is water soluble in nature, some amount escapes from biotransformation and appears in the urine (267). Rats administered a dose of 0.8 LD₅₀ (6.4mg / kg body weight) MCP excreted 4.0% of the active principle in the urine in 8 hours. Cis-MCP was not detected in the urine 24 hours after administration (**Table 3.4.3**), (**Histogram 3.4.3**).

CHAPTER 4

GENERAL DISCUSSION AND CONCLUSION

4.0 Discussion

MCP poisoning – clinical profile in rats

OPPs inhibit AChE which result in accumulation of ACh at cholinergic synaptic terminals and overactivation of ACh receptors (muscarinic and nicotinic receptors) of the parasympathetic, sympathetic and central nervous systems. Overactivation of muscarinic receptors in the parasympathetic system is characterised by salivation and lacrimation. Overactivation of nicotinic receptors is characterised by chewing, body tremors, muscle weakness and paralysis (268-270). In our study, rats subjected to severe MCP poisoning manifested cholinergic signs of chewing, body tremors, salivation, lacrimation and muscle weakness. This rapid onset of cholinergic symptoms, body tremors and weakness in the muscle characterize the acute toxicity of MCP. Inhibition of AChE followed by ACh hyper-stimulation and persistent depolarization of the muscle is the primary event of muscle weakness in severe OPP poisoning. It has been shown earlier that muscle AChE activity was significantly inhibited in OPP soman poisoning (271). The rapid onset of inhibition in our study using MCP demonstrates the rapid absorption and distribution of MCP to the muscle. Interestingly, while inhibition of AChE peaked by 75 minutes after poisoning and activity recovered by 8 hours after poisoning, this did not correlate with muscle paralysis, which occurred within 1 hour after poisoning when muscle AChE was still active. One explanation for this could be the rapid depolarisation of 'naive' muscle when it encounters a sudden onset of cholinergic hyper-stimulation. Rapid adaptation of the muscle with low AChE activity may lead to recovery from paralysis.

Recovery from muscle weakness and regaining of complete muscle power in presence of less than 50% AChE activity suggested involvement of other

mechanisms in preventing prolonged muscle weakness and enabling recovery of muscle strength. It has been shown that AChE knockout mice showed greater susceptibility to the OPP diisopropylfluorophosphate and died compared to control wild type mice which also suggesting the presence of non-cholinergic toxic mechanisms (55). Such mechanisms may also occur in pheochromocytoma (PC12) cells that are devoid of AChE but in which OPPs disrupt mitochondrial function in presence of cholinergic receptor antagonists (54).

Mitochondria are critical to normal muscle function since the muscle is a high-energy-requiring organ and muscle contraction is an energy dependent process. The mitochondria provide most of this energy through oxidative phosphorylation (133) and OPPs that disrupt mitochondrial function and ATP generation (272-274) may induce muscle injury and weakness through a bioenergetic failure. Insufficient production of energy as a cause of muscle weakness that occurs in acute severe OPP poisoning has not been analysed and is a focal points of these studies.

Do reduced ATP levels contribute to muscle paralysis?

Cellular ATP content was found to be decreased by 75% when PC12 cells were treated with the OPP mevinphos at a concentration of 4 μmol for 3 hours (54) and brain ATP content was decreased by 60% in the cortex when rats were treated with the OPP diisopropylphosphorofluoridate (1.25 mg/kg, sc) (241). In the MCP treated rats, we found that the adenine nucleotides, ATP, ADP and AMP in muscle were normal in the first hour after MCP poisoning; (i.e) during paralysis. This suggests that, inadequate energy (ATP) in the muscle *per se* did not contribute to the severe muscle weakness following MCP poisoning in rats. However, muscle ATP, ADP and AMP levels decreased significantly 2.5 hours after MCP poisoning i.e. soon after paralysis and then returned to normal 8 hours after poisoning, when

rats had regained the muscle power. In fact by 24 hours after poisoning when rats had regained complete muscle power, muscle ATP, ADP and AMP levels were higher than normal. ATP synthesis and utilisation are highly regulated processes (103). However, during recovery from stress conditions (adaptation) adenine nucleotide synthesis rates were increased in our study. This is similar to what has been observed in rats where cardiac hypertrophy was induced and adenine nucleotide (ATP, ADP and AMP) synthesis increased 2 fold 24 hours later (i.e. during recovery) (275). Adenine nucleotide synthesis has also been shown to be increased 2 fold in the rat heart during recovery from hypoxia (276). Prolonged muscle weakness is the major problem in OPP poisoned patients and the differences between temporary muscle weakness in the MCP poisoned rat and prolonged muscle weakness in humans may arise from a longer duration of insufficient ATP synthesis following the early cholinergic phase of poisoning.

Does low energy charge contribute to severe muscle weakness in MCP poisoning?

Since perturbations in levels of all adenine nucleotides were evident after MCP poisoning, the next question arose whether cellular energy charge played a role in muscle weakness. The energy charge is a measure of metabolically available energy transiently stored in the adenine nucleotide pool (104), which controls metabolism. A low energy charge leads to an increase in the ATP regenerating reactions by activating pyruvate dehydrogenase and phosphofructokinase (105) and decreases the rates of ATP consuming biosynthetic enzyme reactions in order to compensate for the low energy charge (106). In addition, ATP dependent biosynthetic enzymes such as phosphoribosyl adenosine triphosphate synthetase, aspartokinase and phosphoribosyl pyrophosphate synthetase are inhibited by low energy charge (107).

Our data from MCP treated rats indicates that the energy charge of the skeletal muscle was not decreased when rats were completely paralysed but decreased 2.5 hours after poisoning in comparison to controls. The high-energy charge of the muscle maintained over the course of poisoning, as well as during periods of both severe and persisting muscle weakness, indicate that the muscle was able to maintain sufficient ATP for energy dependent biosynthetic reactions to be carried out. The data indicate that bioenergetic failure does not seem to play a role in *initiating* muscle weakness following MCP poisoning in rats, as ATP levels and energy charge were normal in paralyzed muscle. However, it is possible that these parameters are affected as a consequence of paralysis, since low ATP levels and decreased energy charge were noted only in the immediate aftermath of poisoning and subsequently returned to normal even though muscle weakness persisted.

As humans have prolonged muscle weakness, a role for persistent inhibition of ATP synthesis and low energy charge in contributing to muscle weakness in humans cannot be ruled out. However, all the data so far indicates that the initiating trigger for muscle paralysis could be upstream of ATP levels *per se* and hence we focused on mitochondrial ATP synthesis directly to elucidate the mechanism of muscle weakness after MCP. As an initial step in this direction, the integrity of muscle mitochondria after MCP poisoning was evaluated by examination of mitochondrial swelling characteristics.

Is mitochondria integrity maintained in MCP poisoning?

It has been observed that OPP induced mitochondrial dysfunction in rodent brain where OPPs inhibit complexes I–IV, disrupt mitochondrial transmembrane potential and deplete ATP (272-274, 277). In the rodent muscle, MCP toxicity is associated with complex V inhibition, sparing the activity of respiratory complexes I–IV (160),

whereas in muscle cell cultures, dimethoate increases mitochondrial Na⁺K⁺ ATPase activity and inhibits Ca²⁺ ATPase (278). As intact mitochondria are required to maintain transmembrane potential and ATP generation (279), we evaluated muscle mitochondrial integrity in MCP poisoned rats. The mitochondrial permeability transition (MPT) pore opening (mainly induced by reactive oxygen species) with high conductance facilitates the non-selective diffusion of solutes (< 1500 Da) and results in mitochondria swelling and membrane rupture (280). Mitochondrial swelling was measured by decrease in absorbance at 540 nm (279). Since muscle mitochondrial swelling rates were similar in MCP treated animals when compared to controls, our data indicates that the decreased ATP levels were not due to the loss of membrane integrity.

Muscle mitochondrial ATP synthase activity over the course of acute severe MCP poisoning and its effect on ATP levels

Electron transport through respiratory complexes I to IV generate a proton gradient across the inner mitochondrial membrane that drives oxidative phosphorylation at ATP synthase and enables synthesis of ATP from ADP and inorganic phosphate (Pi). In MCP treated rats, ATP synthase activity was not inhibited in paralysed muscle. However, ATP synthase activity was severely decreased in muscle mitochondria 2.5 hours and 8 hours after MCP poisoning and returned to normal when rats had regained complete muscle power (24 hours). Despite complex I activity being inhibited by 64% in the cerebral cortex of immature rats during seizures, ATP levels were maintained in the control range (281). However, inhibition of ATP synthase has been shown to result in decreased ATP levels (132, 234), similar to our study where ATP levels were severely decreased when ATP synthase was inhibited.

ATP is produced by both oxidative phosphorylation (ATP synthase mediated) and substrate level phosphorylation. In order to determine whether inhibition of glycolysis contributed to the decreased ATP levels in MCP poisoning, we measured lactate levels in the muscle as an indirect indicator for glycolysis (substrate level phosphorylation). Muscle lactate levels were decreased significantly 2.5 hours after poisoning, while the levels were normal 24 hours after poisoning. It has been shown earlier that inhibition of glycolysis was observed in poisoning with the OPP, soman (282). In conclusion, reduced ATP levels in the muscle of MCP poisoned rats were a consequence of events that occurred in the initial cholinergic phase and also during paralysis that reversibly inhibited oxidative phosphorylation and substrate level phosphorylation.

The role of NO in ATP synthase inhibition following acute severe OPP poisoning

Animal studies have shown that NO is involved in OPP induced myopathy, and paraoxon induced muscle necrosis in rats is reduced by 80% when animals are administered NOS inhibitors along with the OPP (238). Increased citrulline and decreased ATP levels were observed in the rat brain after being treated with AChE inhibitors (241).

NO is endogenously synthesised by NOS enzymes, which exist as neuronal (nNOS), endothelial (eNOS), and inducible (iNOS) isoforms (165). All the isoforms use L-arginine as a substrate and citrulline is produced as a by-product (168, 169). Activation of eNOS by ACh is observed in endothelial cells under normal physiological conditions. ACh binds to the muscarinic receptor in the endothelial cell and activates the inositol triphosphate (IP₃) signalling cascade which in turn increases the release of calcium from the endoplasmic reticulum. Increased

intracellular calcium activates calmodulin and protein kinase C (PKC), stimulating eNOS which results in NO production (230, 236). Moreover, in rat retina, carbachol treatment (cholinergic agonist) also increases NOS activity by increasing the expression of nNOS messenger RNA (mRNA) (231). Increased levels of NO were also observed when rat atria and rat cerebral frontal cortex were treated with carbachol (236, 237). Thus, elevated levels of NO are a natural consequence in OPP poisoning when AChE is inhibited and ACh levels increased. Our data indicated that nitrate levels increased in MCP poisoned rat skeletal muscle and remained elevated on recovery of muscle strength.

What is the source for NO in skeletal muscle?

nNOS is the major source for NO in skeletal muscle (283, 284). nNOS is highly expressed in human skeletal muscle when compared to the brain (285). Increased nNOS and iNOS protein expression in the rostral ventrolateral medulla has been observed after administration of the OPP mevinphos to rats (286). In our study, nNOS protein is up-regulated in skeletal muscle of MCP poisoned rats, while iNOS is not induced.

What is the mechanism of ATP synthase inhibition?

Our data from rats treated with MCP indicate that NO levels in the muscle are increased in MCP poisoning. This NO can induce post-translational modifications and alter ATP synthase activity. NO modifies proteins, by direct interaction or by producing reactive nitrogen species, which then result in S-nitrosylation of reduced cysteine residues or by nitration of tyrosine residues (193, 194). Chronic exposure to NO decreases mitochondrial complex I, complex II and complex IV activity in bovine aortic endothelial cells. The decrease in enzyme activity was associated with decrease in complex I, complex II and complex IV protein expression (287).

However, data from our study indicates that ATP synthase protein expression is not altered between control and MCP poisoned rats, suggesting that ATP synthase inhibition is not due to the decreased expression of ATP synthase protein.

It is well known that there is a strong correlation between NO induced post translational modifications on ATP synthase and its inhibition (217, 226, 233-235). In Alzheimer's disease, ATP synthase is modified by NO through α subunit nitrotyrosinylation (232). Cellular excess of NO production as well as peroxynitrite, result in formation of nitro-tyrosine and inhibition of ATP synthase activity (217, 226, 233). The activity of ATP synthase decreases in aging when the β subunit of the enzyme is nitrated (234). S-nitrosylation of the α subunit of ATP synthase also leads to loss of activity (235). However, data from our study indicates tyrosine nitration was not observed in MCP poisoned rats at any time point.

Are free sulphhydryl groups of ATP synthase modified in MCP poisoning?

As mentioned earlier, NO can modify protein sulphhydryl groups and ATP synthase has more than 10 cysteine residues. Proteomic analysis using Biotin incorporated iodoacetamide (BIAM) labelling of unmodified sulphhydryl groups can provide information about post-translational modification on these groups (288, 289), where a signal on the BIAM western blot membranes indicates unmodified free thiol groups on the protein. Biotin-iodoacetamide labelling of ATP synthase indicated that MCP poisoning did not lead to modification of sulphhydryl groups of the enzyme for one hour when enzyme activity was not inhibited. However, free sulphhydryl groups were modified 2.5, 8 and 24 hours after poisoning and sulphhydryl group modification was identified as occurring on the 58 and 36 kDa subunits of ATP synthase. The modifications were maximal 2.5 hours after poisoning when ATP synthase was significantly inhibited.

This data indicates that free sulphhydryl groups on mitochondrial ATP synthase were modified during MCP poisoning. This might be through either oxidative or nitrosative modifications. In order to evaluate possible NO induced modifications, nitrocysteinylation of ATP synthase subunits were analysed in control rats and 2.5 hours, 8 hours and 24 hours after MCP poisoning. We found that MCP poisoning led to nitro-cysteinylation of the 58 kDa subunit of ATP synthase at 2.5 hours, 8 hours and 24 hours after poisoning. However, nitro-cysteinylation of the 58 kDa subunit of ATP synthase was still observed when rats had regained ATP synthase activity, suggesting that this modification may not be solely responsible for ATP synthase inhibition.

In spite of the decrease in free sulphhydryl group labelling on the 36 kDa subunit of ATP synthase, nitrocysteinylation of 36 kDa was not seen in MCP poisoned rats. This suggests that this may be an oxidative modification which is associated with enzyme inhibition.

Which subunit of ATP synthase is modified in MCP poisoning?

Western blots of ATP synthase after separation by BN-PAGE, IEF and Tris-Tricine-SDS-PAGE also demonstrated that subunits of 78 kDa at pI 6.2, 58 kDa at pI 9.2 and 36 kDa at pI 9.5 undergo reversible sulphhydryl group modification maximally 2.5 hours after MCP poisoning in rats. The 78 kDa protein does not match any of the published ATP synthase subunits and hence it is possible that this could be a protein associating with ATP synthase such as the molecular chaperone, glucose regulated protein (Hsp 70), which has a similar molecular weight and pI (290) and is involved in protein translocation across the mitochondrial membrane and protein folding (291, 292). The modified 58 kDa protein (pI → 9.2) was identified as the α subunit of ATP synthase by probing with ATP synthase α

antibody and based on the pI, which is similar to that published earlier (232, 293). The pI and molecular weight of the modified 36 kDa subunit closely correlate with the ATP synthase γ subunit (DrugBank database, ID No: 6344) suggesting that this subunit is probably the γ subunit of ATP synthase.

Does reduced glutathione have a role in ATP synthase inhibition?

Studies have shown that OPP poisoning decreased GSH levels in the liver of rat and mice (294, 295) and NO mediated mitochondrial damage was prevented by reduced glutathione (296). Prolonged mitochondrial complex I S-nitrosylation and enzyme inhibition was observed when murine macrophage cells were treated with NO donors, during which GSH levels decreased. This decrease might be due to NO removal from nitrosylated SH moieties or direct removal of NO by GSH (214). Moreover NO itself increases glutathione biosynthesis by up-regulating glutamate-cysteine ligase, which is a rate limiting enzyme in glutathione biosynthesis (297). Sulphydryl group modifications have been shown to be reversible and readily decomposable (195), and oxidative stress induced mitochondrial complex II, complex III and ATP synthase inhibition were attenuated by GSH treatment in synaptosomes isolated from rat brain cortex (298). In our study, GSH levels decreased 2.5 hours after MCP poisoning and returned to normal 8 and 24 hours after MCP poisoning. Sulphydryl group labelling of ATP synthase indicated that reversible sulphydryl group modification of ATP synthase subunits was prominent when GSH levels were depleted. ATP synthase activity was also severely inhibited when GSH levels were significantly decreased and recovery of enzyme activity correlated to recovery of GSH levels.

Thus, the data indicates that NO levels were elevated in MCP poisoning through up-regulation of nNOS while iNOS was not induced. Though nitro-tyrosinylation of

ATP synthase was not evident in MCP poisoning, iodoacetamide labeling of ATP synthase indicated that reversible sulphhydryl group modification occurred on 58 kDa and 36 kDa subunits. Of these, nitrocysteinylation analysis of ATP synthase revealed that the 58 kDa subunit was reversibly modified by NO while the 36 kDa subunit is probably modified by oxidative stress. The modified 58 kDa protein (pI → 9.2) was identified as the α subunit of ATP synthase and the 36 kDa protein is probably the γ subunit of ATP synthase. The correlation of the compromised ATP synthase activity and ATP levels in the muscle with a decrease in GSH levels further implicate oxidative stress in the process.

Can MCP induced ATP synthase inhibition be prevented by pre-treatment with NO synthase inhibitor L-NAME?

L-NAME is a general NOS inhibitor, which blocks the calcium dependent nNOS and eNOS activity (299). As ATP synthase is severely inhibited and ATP levels decreased 2.5 hours after MCP poisoning, we carried out our study in L-NAME pre-treated rats sacrificed at 2.5 hours after MCP poisoning.

L-NAME treated rats showed delayed onset of nicotinic symptoms of chewing and body tremors, but the development of muscle weakness, paralysis and recovery of muscle power and muscle AChE activity were as seen in rats not treated with L-NAME. Though it has been noted that L-NAME treatment at higher doses (100mg / kg body weight for 9 days) was associated with decreased food intake and weight loss in genetically obese mice (300), our dose of 20mg / kg body weight for 14 days did not significantly cause weight loss, suggesting that this dose does not influence a food intake and energy production in rats.

Rats pre-treated with L-NAME showed reduced muscle ATP and ADP levels compared to un-treated controls which might be due to increased ectonucleotidase activity. Ectonucleotidases are enzymes that degrade extracellular nucleotides such as ATP, ADP and AMP and it has been observed that L-NAME treatment increases ectonucleotidase activity in kidney membranes of rats (301). Despite the effect on ectonucleotidase activity, L-NAME treatment prevented severe decrease in ATP levels in MCP poisoned rats when compared to un-treated MCP poisoned rats. The energy charge was found to be increased soon after paralysis in MCP poisoned rats pre-treated with L-NAME when compared to un-treated MCP poisoned rats.

L-NAME treatment decreased nitrate levels in the muscle and protected ATP synthase activity in MCP poisoned rats. ATP synthase activity of L-NAME treated rats was 73%, 2.5 hours after MCP poisoning compared to 46% in non L-NAME treated poisoned rats. It has been noticed that rabbit muscle glycolytic enzyme glyceraldehyde-3-phosphate dehydrogenase was reversibly inhibited by S-nitrosylation when enzymes were treated with NO donor (200), suggesting that NO is involved in reversible inhibition of glyceraldehyde-3-phosphate dehydrogenase. In our study, lactate levels of skeletal muscle 2.5 hours after poisoning in L-NAME treated rats were 53% higher than un-treated poisoned rats. This is similar to what has been observed in earlier studies where glycolysis was inhibited in OPP poisoning (282). Since glycolysis has been shown to be decreased in OPP poisoning and this increase in lactate suggests that L-NAME is also able to overcome the effect of MCP on glycolysis.

Sulphydryl group modification at the 58 and 36 kDa subunits of ATP synthase were less in MCP poisoned rats pre-treated with L-NAME, though nitrocysteinylation of ATP synthase at the 58 kDa subunit was not completely abolished by L-NAME

treatment. In spite of this, ATP synthase activity was protected in MCP rats pre-treated with L-NAME, again suggesting that 58 kDa subunit modifications are not solely responsible for ATP synthase inhibition.

The reversible sulphydryl group modifications of 36 kDa subunits of ATP synthase were significantly reduced in MCP poisoned rats pre-treated with L-NAME compared to un-treated poisoned rats. It is known that L-NAME treatment not only inhibits nitrosative stress, but can also prevent oxidative stress (302) . In addition, L-NAME inhibits superoxide production (oxidative stress) by binding to the active site of NOS and decreasing the reduction of heme, thereby attenuating electron flux (303, 304). Despite the slightly lower GSH levels in L-NAME treated control rats when compared to untreated controls, maintenance of GSH levels and ATP synthase activity was seen in MCP poisoned rats pre-treated with L-NAME.

In conclusion, L-NAME treatment decreased NO levels in skeletal muscle, reduced reversible sulphydryl group modifications on 36 kDa subunit of ATP synthase and protected its activity and maintained muscle ATP levels in rats subject to MCP poisoning.

MCP induced muscle weakness and recovery of muscle power in relation to clearance of pesticide

MCP is both lipophilic and water soluble and exists in two isoforms (i.e) *cis*-MCP and *trans*-MCP (242, 267). The *cis* isoform has more biological activity than the *trans* form (242). The biotransformation of MCP includes O-methylation, N-methylation and cleavage of the vinyl phosphate bond. The main route of the biotransformation of MCP is hydrolysis of the P - O vinyl linkage, producing dimethylphosphate (DMP) and *N*-methylacetoacetamide as major metabolites.

Since MCP is water soluble, some amount escapes biotransformation and appears in the urine (267).

We estimated cis-MCP levels in the blood, muscle, muscle mitochondria and urine and correlated it with muscle weakness. The absorption of MCP was rapid and reached maximum concentrations in the blood within 30 minutes after MCP poisoning in the rat. This is faster than the rate reported for the OPP, fenitrothion, which peaked 2 hours after oral administration (305). This difference may be due to the highly lipophilic nature of MCP. As muscle is the major target tissue for muscle weakness, MCP levels were measured in the muscle. In MCP poisoned rat, accumulation of MCP peaked at 75 minutes and started to decrease by 2.5 hours and almost disappeared by 8 hours after poisoning. Interestingly, MCP levels in the muscle and blood decreased during paralysis though the reasons for this are not evident. MCP levels in the muscle almost disappeared 8 hours after poisoning. In fact, among 7 rats only 2 showed MCP in the muscle 8 hours after poisoning. This indicates that in these animals MCP may have been deposited in fat tissue and released during later periods. Cis- MCP was not detected in muscle mitochondria (detection limit 40nM) (242) in MCP poisoned rat, confirming that unlike atrazine (triazine herbicide) mediated ATP synthase inhibition, MCP mediated ATP synthase inhibition was not due to the direct binding of MCP to ATP synthase (132).

The data on MCP levels in urine after poisoning showed that rats excreted 4% of cis-MCP in the urine within 8 hours. However, this could have been affected by urine output as excessive water loss by salivation and sweating as well as decreased intake of water could have resulted in decreased urine production. Cis-MCP, either in the blood or in the muscle, was not detected by HPLC 24 hours after poisoning.

It is possible that by this time it must have either been degraded or converted to less toxic, more water soluble compounds and subsequently excreted in the urine.

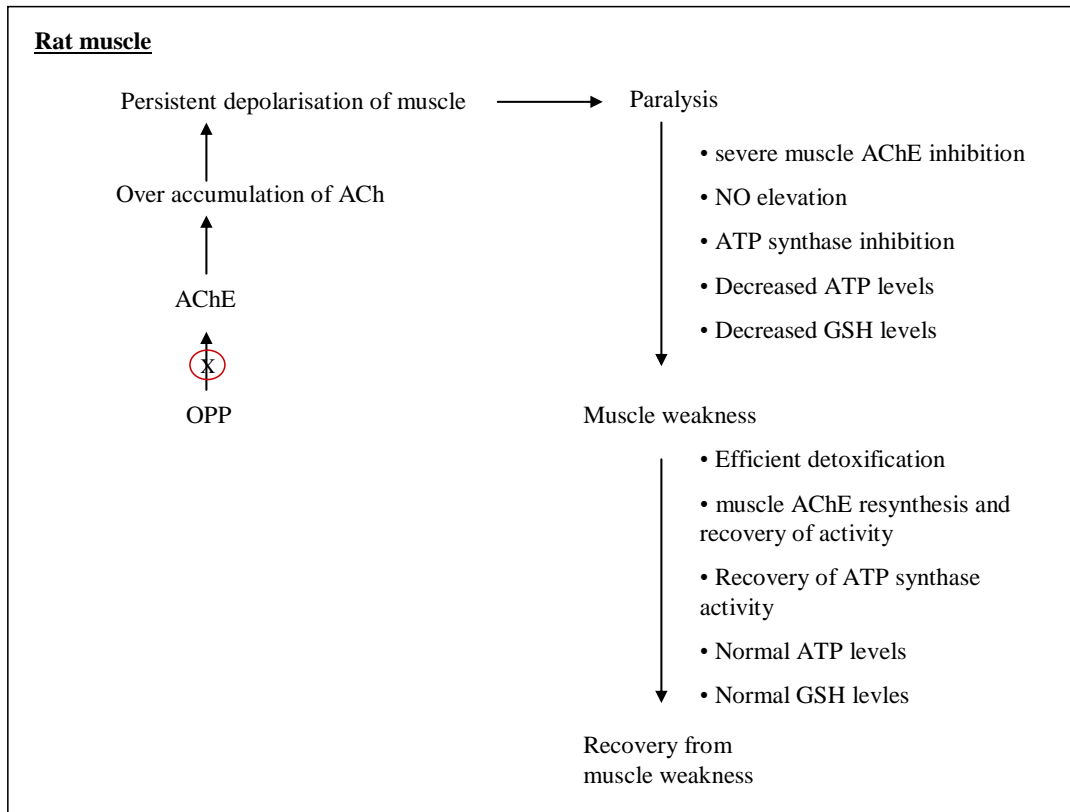
It has been observed that about 50% of the inhibition of muscle AChE induced by paraoxon (OPP) in rats was regained within 24 hours (130) and the recovery of paraoxon inhibited chick embryonic muscle AChE activity was correlated to newly synthesised AChE (131). In MCP poisoned rat, muscle AChE inhibition decreased from 80% at 75 minutes after MCP poisoning to 55% at 24 hours after poisoning, indicating a recovery of enzyme activity. Rats had regained complete muscle power by 24 hours after poisoning, when active MCP was completely absent in blood and muscle. This suggests that absence of active MCP in the muscle ensured that newly synthesised AChE was not inhibited, which would have contributed to recovery of muscle power.

Prolonged muscle weakness is a major problem in OPP poisoned patients and this may be due to the release over prolonged period of MCP stored in fat tissue. It has been noticed that prolonged OPP metabolite excretion in urine was associated with development of intermediate syndrome in OPP patients (120). If cis-MCP in the blood and urine are estimated for 3 days after poisoning, it may be possible to predict onset of intermediate syndrome in a patient.

In conclusion, MCP absorption and distribution in the muscle occurred within 15 minutes in rats subjected to MCP poisoning and correlated to the profile of muscle weakness (i.e.) ataxic gait (Grade 1 muscle weakness), which appeared within 15 minutes of MCP poisoning. Cis- MCP was not detected in blood, muscle and urine when rats had regained complete muscle power (i.e. 24 hours after poisoning).

The study demonstrated that less than 50% of muscle AChE activity was sufficient to permit muscle repolarization and complete recovery from severe muscle weakness. Maintaining these levels of AChE early in poisoning suggests their adequacy for normal muscle function. The differences between temporary muscle weakness in MCP poisoned rat and prolonged weakness in humans may arise from higher doses ingested in humans and lower metabolic clearance of OPP compounds.

Figure 5.1 MCP poisoning and mechanism of muscle weakness in rat



Overall conclusion

Acute severe MCP poisoning rapidly induced muscle weakness that progressed to paralysis in rats. The animals recovered from paralysis and regained complete muscle power within 24 hours of MCP poisoning with no treatment. Strong inhibition of muscle AChE (67%) was the primary toxicity responsible for induction of muscle weakness and recovery of enzyme activity to 45% was important for regaining of muscle power. However, regaining of muscle power in spite of incomplete recovery of AChE activity suggests the existence of other mechanisms which prevent prolonged muscle weakness and enable recovery of muscle strength in rats.

The premise of this thesis was that intense muscle activity that occurs rapidly on OPP poisoning depletes muscle ATP to levels inadequate for contraction. The finding that ATP synthase was inhibited soon after the development of muscle weakness and paralysis and the fact that recovery of muscle strength was associated with re-activation of ATP synthase supports this. A similar decline and increase of muscle lactate in concert with muscle weakness and recovery of muscle strength also suggested inadequate energy levels contributed to muscle weakness of OPP poisoning. It appears that events in the early phase of poisoning and during paralysis led to inhibition of oxidative phosphorylation and substrate level phosphorylation and subsequent reduction of ATP available for muscle function. Reversal of this inhibition allowed sufficient energy production and recovery of muscle strength. This is important in prevention of prolonged muscle weakness **(Figure 5.1)**.

The energy charge of the muscle, an index of metabolic energy available to the cell, showed that early muscle activity in poisoning depleted energy. This was in keeping

with the hypothesis of this thesis. The ability of the poisoned rat muscle to re-synthesize adenine nucleotides and normalize energy charge restored muscle function. We consider that if the energy charge was not restored muscle weakness would continue in the rat. We suggest that prolonged muscle weakness that characterizes OPP poisoning in humans may be a consequence of bioenergetic failure in the muscle. In addition, rapid metabolic clearance of the active form of an OPP pesticide from the muscle is also important in preventing prolonged muscle weakness following severe poisoning as evident in the rat. A slower clearance rate of OPP in humans could also contribute to prolonged muscle weakness.

MCP poisoning led to NO induction in the muscle due to the up-regulation of nNOS, which contributed to inhibition of ATP synthase and decreased ATP levels. Pre-treatment with L-NAME significantly protected against sulphydryl group modification at the 36 kDa subunit of ATP synthase and prevented inhibition of ATP synthase activity induced by MCP poisoning, suggesting a role of NO in the process. We conclude that efficient protection of muscle ATP synthase activity would help maintain the energy charge of the muscle and reduce muscle weakness that occurs in OPP poisoning.

BIBLIOGRAPHY

Bibliography

1. Pesticide News. Towards a reduction in pesticide use 1990;43. 17-20.
2. Gunnell D, Eddleston M, Phillips MR, Konradsen F. The global distribution of fatal pesticide self-poisoning: systematic review. BMC Public Health. 2007;7:357.
3. Gunnell D, Eddleston M. Suicide by intentional ingestion of pesticides: a continuing tragedy in developing countries. Int J Epidemiol. 2003 Dec;32(6):902-9.
4. World Health Organization. Mental Health and Substance Abuse Facts and Figures Suicide Prevention: Emerging from Darkness.2006. (http://www.searo.who.int/en/Section1174/Section1199/Section1567/Section1824_8078)
5. Karalliedde L, Senanayake N. Acute organophosphorus insecticide poisoning in Sri Lanka. Forensic Sci Int. 1988 Jan;36(1-2):97-100.
6. Zhao DL, Li LJ. [The emergency treatment of organophosphorus pesticides poisoning]. Zhonghua Nei Ke Za Zhi. 1994 Sep;33(9):630-2.
7. Jang SW, Lin JL, Chuang FR. Electrocardiographic findings of organophosphate intoxication in emergency department as predictors of prognosis: a retrospective analysis. Changgeng Yi Xue Za Zhi. 1995 Jun;18(2):120-5.
8. Ozturk MA, Kelestimur F, Kurtoglu S, Guven K, et al. Anticholinesterase poisoning in Turkey--clinical, laboratory and radiologic evaluation of 269 cases. Hum Exp Toxicol. 1990 Sep;9(5):273-9.
9. Balali-Mood M, Shariat M. Treatment of organophosphate poisoning. Experience of nerve agents and acute pesticide poisoning on the effects of oximes. J Physiol Paris. 1998 Oct-Dec;92(5-6):375-8.
10. Zamir DL, Novis BN. Organophosphate poisoning and necrotizing pancreatitis. Isr J Med Sci. 1994 Nov;30(11):855-6.
11. Batra AK, Keoliya AN, Jadhav GU. Poisoning: an unnatural cause of morbidity and mortality in rural India. J Assoc Physicians India. 2003 Oct;51:955-9.
12. Bardin PG, van Eeden SF, Joubert JR. Intensive care management of acute organophosphate poisoning. A 7-year experience in the western Cape. S Afr Med J. 1987 Nov 7;72(9):593-7.

13. Abebe M. Organophosphate pesticide poisoning in 50 Ethiopian patients. *Ethiop Med J.* 1991 Jul;29(3):109-18.
14. Hayes MM, van der Westhuizen NG, Gelfand M. Organophosphate poisoning in Rhodesia. A study of the clinical features and management of 105 patients. *S Afr Med J.* 1978 Aug 5;54(6):230-4.
15. da Silva OA, Lopez M. [Acute poisoning treated in intensive care (author's transl)]. *AMB Rev Assoc Med Bras.* 1980 Jan;26(1):4-6.
16. Delgado M, Suazo M. [Poisoning by organo-phosphorate compounds (author's transl)]. *Rev Med Chil.* 1981 Sep;109(9):837-40.
17. Wessler I, Kirkpatrick CJ, Racke K. Non-neuronal acetylcholine, a locally acting molecule, widely distributed in biological systems: expression and function in humans. *Pharmacol Ther.* 1998 Jan;77(1):59-79.
18. Cooper JR, Bloom, F.E., and Roth, R.H.2003. *Acetylcholine. 8th ed ed.: The Biochemical Basis of Neuropharmacology*, Oxford University Press; New York.151-80
19. Eyer P. The role of oximes in the management of organophosphorus pesticide poisoning. *Toxicol Rev.* 2003;22(3):165-90.
20. Peter JV, Moran JL, Graham P. Oxime therapy and outcomes in human organophosphate poisoning: an evaluation using meta-analytic techniques. *Crit Care Med.* 2006 Feb;34(2):502-10.
21. Antonijevic B, Stojilkovic MP. Unequal efficacy of pyridinium oximes in acute organophosphate poisoning. *Clin Med Res.* 2007 Mar;5(1):71-82.
22. Marrs TC. Organophosphate poisoning. *Pharmacol Ther.* 1993;58(1):51-66.
23. Jokanovic M. Biotransformation of organophosphorus compounds. *Toxicology.* 2001 Sep 25;166(3):139-60.
24. Lucier GW, Menzer RE. Nature of oxidative metabolites of dimethoate formed in rats, liver microsomes, and bean plants. *J Agric Food Chem.* 1970 Jul-Aug;18(4):698-704.
25. Fukuto TR. Mechanism of action of organophosphorus and carbamate insecticides. *Environ Health Perspect.* 1990 Jul;87:245-54.
26. Dauterman WC. Biological and non biological modification of organophosphorus compounds. *Bull. WHO.* 1971;44:133 -50.

27. Eto M, Casida JE, Eto T. Hydroxylation and cyclization reactions involved in the metabolism of tri-o-cresyl phosphate. *Biochem Pharmacol.* 1962 Apr-May;11:337-52.
28. Hodgson E, Silver, I.S., Butler, L.E., Lawton, M.P., Levi,P.E.,. 1991. Metabolism In: Series Hayes WJJ, Laws, E.R. Jr. series Metabolism Academic Press, San Diego; 107-67.
29. Miyamoto J. Non-enzymatic conversion of Dipterex into DDVP and their inhibitory action on enzymes. *Botyu - Kagaku.* 1959;24:130 -7.
30. Walker CH. The classification of esterases which hydrolyse organophosphates: recent developments. *Chem Biol Interact.* 1993 Jun;87(1-3):17-24.
31. Li WF, Costa LG, Furlong CE. Serum paraoxonase status: a major factor in determining resistance to organophosphates. *J Toxicol Environ Health.* 1993 Oct-Nov;40(2-3):337-46.
32. Li WF, Furlong CE, Costa LG. Paraoxonase protects against chlorpyrifos toxicity in mice. *Toxicol Lett.* 1995 Apr;76(3):219-26.
33. Furlong CE, Li WF, Brophy VH, Jarvik GP, et al. The PON1 gene and detoxication. *Neurotoxicology.* 2000 Aug;21(4):581-7.
34. Silman I, Sussman JL. Acetylcholinesterase: how is structure related to function? *Chem Biol Interact.* 2008 Sep 25;175(1-3):3-10.
35. Fukuto TR, Metcalf RL. Metabolism of insecticides in plants and animals. *Ann N Y Acad Sci.* 1969;160(1):97-113.
36. Jokanovic M. Role of carboxylesterase in soman, sarin and tabun poisoning in rats. *Pharmacol Toxicol.* 1989 Sep;65(3):181-4.
37. Nachmansohn D, Wilson IB. The enzymic hydrolysis and synthesis of acetylcholine. *Adv Enzymol Relat Subj Biochem.* 1951;12:259-339.
38. Leuzinger W, Baker AL. Acetylcholinesterase, I. Large-scale purification, homogeneity, and amino Acid analysis. *Proc Natl Acad Sci U S A.* 1967 Feb;57(2):446-51.
39. Sussman JL, Harel M, Frolow F, Oefner C, et al. Atomic structure of acetylcholinesterase from *Torpedo californica*: a prototypic acetylcholine-binding protein. *Science.* 1991 Aug 23;253(5022):872-9.

40. Bon S, Vigny M, Massoulie J. Asymmetric and globular forms of acetylcholinesterase in mammals and birds. *Proc Natl Acad Sci U S A*. 1979 Jun;76(6):2546-50.
41. Steitz TA, Shulman RG. Crystallographic and NMR studies of the serine proteases. *Annu Rev Biophys Bioeng*. 1982;11:419-44.
42. Heide EA. 2007. Agency for Toxic Substances and Disease Registry Case Studies in Environmental Medicine Cholinesterase Inhibitors: Including Pesticides and Chemical Warfare Nerve Agents Atlanta, GA 30341.1-153
43. Dvir H, Silman I, Harel M, Rosenberry TL, et al. Acetylcholinesterase: from 3D structure to function. *Chem Biol Interact*. Sep 6;187(1-3):10-22.
44. Shinitzky M, Dudai Y, Silman I. Spectral evidence for the presence of tryptophan in the binding site of acetylcholinesterase. *FEBS Lett*. 1973 Feb 15;30(1):125-8.
45. Goeldner MP, Hirth CG. Specific photoaffinity labeling induced by energy transfer: application to irreversible inhibition of acetylcholinesterase. *Proc Natl Acad Sci U S A*. 1980 Nov;77(11):6439-42.
46. Weise C, Kreienkamp HJ, Raba R, Pedak A, et al. Anionic subsites of the acetylcholinesterase from *Torpedo californica*: affinity labelling with the cationic reagent N,N-dimethyl-2-phenyl-aziridinium. *Embo J*. 1990 Dec;9(12):3885-8.
47. Harel M, Sonoda LK, Silman I, Sussman JL, et al. Crystal structure of thioflavin T bound to the peripheral site of *Torpedo californica* acetylcholinesterase reveals how thioflavin T acts as a sensitive fluorescent reporter of ligand binding to the acylation site. *J Am Chem Soc*. 2008 Jun 25;130(25):7856-61.
48. Auletta JT, Johnson JL, Rosenberry TL. Molecular basis of inhibition of substrate hydrolysis by a ligand bound to the peripheral site of acetylcholinesterase. *Chem Biol Interact*. 2010 Sep 6;187(1-3):135-41.
49. Coult DB, Marsh DJ, Read G. Dealkylation studies on inhibited acetylcholinesterase. *Biochem J*. 1966 Mar;98(3):869-73.
50. Mason HJ, Sams C, Stevenson AJ, Rawbone R. Rates of spontaneous reactivation and aging of acetylcholinesterase in human erythrocytes after inhibition by organophosphorus pesticides. *Hum Exp Toxicol*. 2000 Sep;19(9):511-6.

51. Zilker T, Felgenhauer N, Hibler A, Pfab R, et al. Factors influencing the efficacy of obidoxime in organophosphate pesticides poisoning. *Przegl Lek.* 1997;54(10):662-4.
52. Willson BH, Hooper, M. J., Hansen, M. E., and Nieberg, P. S. 1992. Reactivation of organophosphorus inhibited AChE with oximes. J.E. Chambers and P.E. Levi. ed.: *Organophosphates - Chemistry, Fate and effects* Academic Press, San Diego.; 107 - 37
53. Vale JA. Toxicokinetic and toxicodynamic aspects of organophosphorus (OP) insecticide poisoning. *Toxicol Lett.* 1998 Dec 28;102-103:649-52.
54. Chan JY, Chan SH, Dai KY, Cheng HL, et al. Cholinergic-receptor-independent dysfunction of mitochondrial respiratory chain enzymes, reduced mitochondrial transmembrane potential and ATP depletion underlie necrotic cell death induced by the organophosphate poison mevinphos. *Neuropharmacology.* 2006 Dec;51(7-8):1109-19.
55. Duysen EG, Li B, Xie W, Schopfer LM, et al. Evidence for nonacetylcholinesterase targets of organophosphorus nerve agent: supersensitivity of acetylcholinesterase knockout mouse to VX lethality. *J Pharmacol Exp Ther.* 2001 Nov;299(2):528-35.
56. Pope CN. Organophosphorus pesticides: do they all have the same mechanism of toxicity? *J Toxicol Environ Health B Crit Rev.* 1999 Apr-Jun;2(2):161-81.
57. Shah N, Khurana S, Cheng K, Raufman JP. Muscarinic receptors and ligands in cancer. *Am J Physiol Cell Physiol.* 2009 Feb;296(2):C221-32.
58. Changeux JP, Taly A. Nicotinic receptors, allosteric proteins and medicine. *Trends Mol Med.* 2008 Mar;14(3):93-102.
59. Tsetlin V, Kuzmin D, Kasheverov I. Assembly of nicotinic and other Cys-loop receptors. *J Neurochem.* 2011 Mar;116(5):734-41.
60. Wu J, Lukas RJ. Naturally-expressed nicotinic acetylcholine receptor subtypes. *Biochem Pharmacol.* 2011 Oct 15;82(8):800-7.
61. Hammer R, Berrie CP, Birdsall NJ, Burgen AS, et al. Pirenzepine distinguishes between different subclasses of muscarinic receptors. *Nature.* 1980 Jan 3;283(5742):90-2.
62. Bonner TI, Buckley NJ, Young AC, Brann MR. Identification of a family of muscarinic acetylcholine receptor genes. *Science.* 1987 Jul 31;237(4814):527-32.

63. Wess J. Molecular biology of muscarinic acetylcholine receptors. *Crit Rev Neurobiol.* 1996;10(1):69-99.
64. Abrams P, Andersson KE, Buccafusco JJ, Chapple C, et al. Muscarinic receptors: their distribution and function in body systems, and the implications for treating overactive bladder. *Br J Pharmacol.* 2006 Jul;148(5):565-78.
65. Gil DW, Krauss HA, Bogardus AM, WoldeMussie E. Muscarinic receptor subtypes in human iris-ciliary body measured by immunoprecipitation. *Invest Ophthalmol Vis Sci.* 1997 Jun;38(7):1434-42.
66. Wang Z, Shi H, Wang H. Functional M3 muscarinic acetylcholine receptors in mammalian hearts. *Br J Pharmacol.* 2004 Jun;142(3):395-408.
67. Islam MA, Nojima H, Kimura I. Muscarinic M1 receptor activation reduces maximum upstroke velocity of action potential in mouse right atria. *Eur J Pharmacol.* 1998 Apr 10;346(2-3):227-36.
68. Stengel PW, Gomeza J, Wess J, Cohen ML. M(2) and M(4) receptor knockout mice: muscarinic receptor function in cardiac and smooth muscle in vitro. *J Pharmacol Exp Ther.* 2000 Mar;292(3):877-85.
69. Kitazawa T, HIRAMA R, Masunaga K, Nakamura T, et al. Muscarinic receptor subtypes involved in carbachol-induced contraction of mouse uterine smooth muscle. *Naunyn Schmiedebergs Arch Pharmacol.* 2008 Jun;377(4-6):503-13.
70. Gillberg PG, Sundquist S, Nilvebrant L. Comparison of the in vitro and in vivo profiles of tolterodine with those of subtype-selective muscarinic receptor antagonists. *Eur J Pharmacol.* 1998 May 22;349(2-3):285-92.
71. Ikeda K, Kobayashi S, Suzuki M, Miyata K, et al. M(3) receptor antagonism by the novel antimuscarinic agent solifenacin in the urinary bladder and salivary gland. *Naunyn Schmiedebergs Arch Pharmacol.* 2002 Aug;366(2):97-103.
72. CK. A. 2001. Organophosphates and carbamates In: Series Ford MD DK, Ling LJ, Erickson T. series Organophosphates and carbamates WB Saunders Company; 819–28.
73. AR E. 2004. Insecticides In: Series Dart RC CE, McGuigan MA, et al., series Insecticides 3rd edn Lippincott Williams & Wilkins; 1475–96.
74. RF C. 2002. organic phosphorus compounds and carbamates.: Goldfrank's Toxicological Emergencies McGraw-Hill Professional; New York. 1346–60

75. Wadia RS, Sadagopan C, Amin RB, Sardesai HV. Neurological manifestations of organophosphorous insecticide poisoning. *J Neurol Neurosurg Psychiatry*. 1974 Jul;37(7):841-7.
76. Senanayake N, Karalliedde L. Neurotoxic effects of organophosphorus insecticides. An intermediate syndrome. *N Engl J Med*. 1987 Mar 26;316(13):761-3.
77. Johnson MK. A phosphorylation site in brain and the delayed neurotoxic effect of some organophosphorus compounds. *Biochem J*. 1969 Feb;111(4):487-95.
78. Abdollahi M, Karami-Mohajeri S. A comprehensive review on experimental and clinical findings in intermediate syndrome caused by organophosphate poisoning. *Toxicol Appl Pharmacol*. 2012 Feb 1;258(3):309-14.
79. Eddleston M, Singh S, Buckley N. Organophosphorus poisoning (acute). *Clin Evid*. 2005 Jun(13):1744-55.
80. Thiermann H, Szinicz L, Eyer P, Zilker T, et al. Correlation between red blood cell acetylcholinesterase activity and neuromuscular transmission in organophosphate poisoning. *Chem Biol Interact*. 2005 Dec 15;157-158:345-7.
81. Brown JH TP. 2001. Muscarinic receptor agonists and antagonists In: Series Hardman JG LL. seriesMuscarinic receptor agonists and antagonists 10th edn McGraw-Hill; 155–73.
82. Kventzel I, Berkovitch M, Reiss A, Bulkowstein M, et al. Scopolamine treatment for severe extra-pyramidal signs following organophosphate (chlorpyrifos) ingestion. *Clin Toxicol (Phila)*. 2005;43(7):877-9.
83. Heath AJW MT. 1992. Atropine in the management of anticholinesterase poisoning In: Series Ballantyne B MT. seriesAtropine in the management of anticholinesterase poisoning Butterworth Heinemann; 543–54.
84. Namba T, Hiraki K. PAM (pyridine-2-aldoxime methiodide) therapy for alkyl-phosphate poisoning. *J Am Med Assoc*. 1958 Apr 12;166(15):1834-9.
85. Eddleston M, Eyer P, Worek F, Mohamed F, et al. Differences between organophosphorus insecticides in human self-poisoning: a prospective cohort study. *Lancet*. 2005 Oct 22-28;366(9495):1452-9.
86. Eddleston M, Szinicz L, Eyer P, Buckley N. Oximes in acute organophosphorus pesticide poisoning: a systematic review of clinical trials. *Qjm*. 2002 May;95(5):275-83.

87. Thiermann H, Szinicz L, Eyer F, Worek F, et al. Modern strategies in therapy of organophosphate poisoning. *Toxicol Lett.* 1999 Jun 30;107(1-3):233-9.
88. Wadia RS, Bhirud RH, Gulavani AV, Amin RB. Neurological manifestations of three organophosphate poisons. *Indian J Med Res.* 1977 Sep;66(3):460-8.
89. FR S. 2006. Nerve agents In: Series Sidell FR TE, Franz DR. series Nerve agents Borden Institute, Walter Reed Army Medical Center; 129–79.
90. Murphy MR, Blick DW, Dunn MA, Fanton JW, et al. Diazepam as a treatment for nerve agent poisoning in primates. *Aviat Space Environ Med.* 1993 Feb;64(2):110-5.
91. Dickson EW, Bird SB, Gaspari RJ, Boyer EW, et al. Diazepam inhibits organophosphate-induced central respiratory depression. *Acad Emerg Med.* 2003 Dec;10(12):1303-6.
92. Singh G, Avasthi G, Khurana D, Whig J, et al. Neurophysiological monitoring of pharmacological manipulation in acute organophosphate (OP) poisoning. The effects of pralidoxime, magnesium sulphate and pancuronium. *Electroencephalogr Clin Neurophysiol.* 1998 Aug;107(2):140-8.
93. Pajoumand A, Shadnia S, Rezaie A, Abdi M, et al. Benefits of magnesium sulfate in the management of acute human poisoning by organophosphorus insecticides. *Hum Exp Toxicol.* 2004 Dec;23(12):565-9.
94. Chambers J, Oppenheimer SF. Organophosphates, serine esterase inhibition, and modeling of organophosphate toxicity. *Toxicol Sci.* 2004 Feb;77(2):185-7.
95. Raushel FM. Bacterial detoxification of organophosphate nerve agents. *Curr Opin Microbiol.* 2002 Jun;5(3):288-95.
96. Sogorb MA, Vilanova E, Carrera V. Future applications of phosphotriesterases in the prophylaxis and treatment of organophosphorus insecticide and nerve agent poisonings. *Toxicol Lett.* 2004 Jun 15;151(1):219-33.
97. McGinnis P. 1999. *Biomechanics of Sport and Exercise.* Champaign, IL: Human Kinetics; 256
98. Keynes RD AD. 2001. *Nerve and Muscle.* Cambridge: Cambridge University Press; 143

99. Vander SaL.1994. Human Physiology. 6th ed.: McGraw-Hill; 312-3
100. Dulhunty AF. Excitation-contraction coupling from the 1950s into the new millennium. *Clin Exp Pharmacol Physiol*. 2006 Sep;33(9):763-72.
101. Hellsten-Westing Y, Sollevi A, Sjodin B. Plasma accumulation of hypoxanthine, uric acid and creatine kinase following exhausting runs of differing durations in man. *Eur J Appl Physiol Occup Physiol*. 1991;62(5):380-4.
102. Sahlin K, Broberg S. Adenine nucleotide depletion in human muscle during exercise: causality and significance of AMP deamination. *Int J Sports Med*. 1990 May;11 Suppl 2:S62-7.
103. Ataullakhanov FI, Vitvitsky VM. What determines the intracellular ATP concentration. *Biosci Rep*. 2002 Oct-Dec;22(5-6):501-11.
104. Atkinson DE, Walton GM. Adenosine triphosphate conservation in metabolic regulation. Rat liver citrate cleavage enzyme. *J Biol Chem*. 1967 Jul 10;242(13):3239-41.
105. Shen LC, Fall L, Walton GM, Atkinson DE. Interaction between energy charge and metabolite modulation in the regulation of enzymes of amphibolic sequences. Phosphofructokinase and pyruvate dehydrogenase. *Biochemistry*. 1968 Nov;7(11):4041-5.
106. Atkinson DE. The energy charge of the adenylate pool as a regulatory parameter. Interaction with feedback modifiers. *Biochemistry*. 1968 Nov;7(11):4030-4.
107. Klungsoyr L, Hagemen JH, Fall L, Atkinson DE. Interaction between energy charge and product feedback in the regulation of biosynthetic enzymes. Aspartokinase, phosphoribosyladenosine triphosphate synthetase, and phosphoribosyl pyrophosphate synthetase. *Biochemistry*. 1968 Nov;7(11):4035-40.
108. Newsholme EA, and Start, C.1973. Regulation in Metabolism. John Wiley and Sons,; London.34-87
109. Hardie DG, Carling D. The AMP-activated protein kinase--fuel gauge of the mammalian cell? *Eur J Biochem*. 1997 Jun 1;246(2):259-73.
110. Green HJ. Mechanisms of muscle fatigue in intense exercise. *J Sports Sci*. 1997 Jun;15(3):247-56.

111. Meriggioli MN. Myasthenia gravis with anti-acetylcholine receptor antibodies. *Front Neurol Neurosci.* 2009;26:94-108.
112. Tarnopolsky MA, Raha S. Mitochondrial myopathies: diagnosis, exercise intolerance, and treatment options. *Med Sci Sports Exerc.* 2005 Dec;37(12):2086-93.
113. Allen DG, Lannergren J, Westerblad H. Muscle cell function during prolonged activity: cellular mechanisms of fatigue. *Exp Physiol.* 1995 Jul;80(4):497-527.
114. Jones DA. High-and low-frequency fatigue revisited. *Acta Physiol Scand.* 1996 Mar;156(3):265-70.
115. Westerblad H, Bruton JD, Allen DG, Lannergren J. Functional significance of Ca²⁺ in long-lasting fatigue of skeletal muscle. *Eur J Appl Physiol.* 2000 Oct;83(2-3):166-74.
116. Fitts RH. Cellular mechanisms of muscle fatigue. *Physiol Rev.* 1994 Jan;74(1):49-94.
117. De Bleecker J, Van Den Neucker K, Willems J. The intermediate syndrome in organophosphate poisoning: presentation of a case and review of the literature. *J Toxicol Clin Toxicol.* 1992;30(3):321-9; discussion 31-2.
118. De Wilde V, Vogelaers D, Colardyn F, Vanderstraeten G, et al. Postsynaptic neuromuscular dysfunction in organophosphate induced intermediate syndrome. *Klin Wochenschr.* 1991 Feb 26;69(4):177-83.
119. Jin YH, Jeong TO, Lee JB. Isolated bilateral vocal cord paralysis with intermediate syndrome after organophosphate poisoning. *Clin Toxicol (Phila).* 2008 Jun;46(5):482-4.
120. De Bleecker J, Van den Neucker K, Colardyn F. Intermediate syndrome in organophosphorus poisoning: a prospective study. *Crit Care Med.* 1993 Nov;21(11):1706-11.
121. Jayawardane P, Dawson AH, Weerasinghe V, Karalliedde L, et al. The spectrum of intermediate syndrome following acute organophosphate poisoning: a prospective cohort study from Sri Lanka. *PLoS Med.* 2008 Jul 15;5(7):e147.
122. Good JL, Khurana RK, Mayer RF, Cintra WM, et al. Pathophysiological studies of neuromuscular function in subacute organophosphate poisoning induced by phosmet. *J Neurol Neurosurg Psychiatry.* 1993 Mar;56(3):290-4.

123. Aaron CK. Organophosphate poisoning-induced intermediate syndrome: can electrophysiological changes help predict outcome? *PLoS Med.* 2008 Jul 15;5(7):e154.
124. De Bleecker JL. The intermediate syndrome in organophosphate poisoning: an overview of experimental and clinical observations. *J Toxicol Clin Toxicol.* 1995;33(6):683-6.
125. Jayawardane P, Senanayake N, Dawson A. Electrophysiological correlates of intermediate syndrome following acute organophosphate poisoning. *Clin Toxicol (Phila).* 2009 Mar;47(3):193-205.
126. Karalliedde L, Baker D, Marrs TC. Organophosphate-induced intermediate syndrome: aetiology and relationships with myopathy. *Toxicol Rev.* 2006;25(1):1-14.
127. Dandapani M, Zachariah A, Kavitha MR, Jeyaseelan L, et al. Oxidative damage in intermediate syndrome of acute organophosphorous poisoning. *Indian J Med Res.* 2003 Jun;117:253-9.
128. Xiao C, He FS, Zheng YX, Leng SG, et al. [Genetic susceptibility to intermediate myasthenia syndrome following organophosphate insecticides poisoning]. *Zhonghua Yu Fang Yi Xue Za Zhi.* 2003 Jul;37(4):259-62.
129. Singh AK, Zeleznikar RJ, Jr., Drewes LR. Analysis of soman and sarin in blood utilizing a sensitive gas chromatography-mass spectrometry method. *J Chromatogr.* 1985 May 17;324(1):163-72.
130. Wecker L, Dettbarn WD. Paraoxon-induced myopathy: muscle specificity and acetylcholine involvement. *Exp Neurol.* 1976 May;51(2):281-91.
131. Cisson CM, Wilson BW. Paraoxon increases the rate of synthesis of acetylcholinesterase in cultured muscle. *Toxicol Lett.* 1981 Oct;9(2):131-5.
132. Hase Y, Tatsuno M, Nishi T, Kataoka K, et al. Atrazine binds to F1F0-ATP synthase and inhibits mitochondrial function in sperm. *Biochem Biophys Res Commun.* 2008 Feb 1;366(1):66-72.
133. Pagliarini DJ, Dixon JE. Mitochondrial modulation: reversible phosphorylation takes center stage? *Trends Biochem Sci.* 2006 Jan;31(1):26-34.
134. Rich PR, Marechal A. The mitochondrial respiratory chain. *Essays Biochem.* 2010;47:1-23.

135. Carroll J, Fearnley IM, Skehel JM, Shannon RJ, et al. Bovine complex I is a complex of 45 different subunits. *J Biol Chem*. 2006 Oct 27;281(43):32724-7.
136. Zickermann V, Drose S, Tocilescu MA, Zwicker K, et al. Challenges in elucidating structure and mechanism of proton pumping NADH:ubiquinone oxidoreductase (complex I). *J Bioenerg Biomembr*. 2008 Oct;40(5):475-83.
137. Cecchini G. Function and structure of complex II of the respiratory chain. *Annu Rev Biochem*. 2003;72:77-109.
138. Walker JE, Dickson VK. The peripheral stalk of the mitochondrial ATP synthase. *Biochim Biophys Acta*. 2006 May-Jun;1757(5-6):286-96.
139. Crofts AR. The cytochrome bc₁ complex: function in the context of structure. *Annu Rev Physiol*. 2004;66:689-733.
140. DePierre JW, Ernster L. Enzyme topology of intracellular membranes. *Annu Rev Biochem*. 1977;46:201-62.
141. Tsukihara T, Aoyama H, Yamashita E, Tomizaki T, et al. Structures of metal sites of oxidized bovine heart cytochrome c oxidase at 2.8 Å. *Science*. 1995 Aug 25;269(5227):1069-74.
142. Walker JE, Lutter R, Dupuis A, Runswick MJ. Identification of the subunits of F₁F₀-ATPase from bovine heart mitochondria. *Biochemistry*. 1991 Jun 4;30(22):5369-78.
143. Wallace DC. A mitochondrial paradigm of metabolic and degenerative diseases, aging, and cancer: a dawn for evolutionary medicine. *Annu Rev Genet*. 2005;39:359-407.
144. Houstek J, Pickova A, Vojtiskova A, Mracek T, et al. Mitochondrial diseases and genetic defects of ATP synthase. *Biochim Biophys Acta*. 2006 Sep-Oct;1757(9-10):1400-5.
145. Rubinstein JL, Walker JE, Henderson R. Structure of the mitochondrial ATP synthase by electron cryomicroscopy. *Embo J*. 2003 Dec 1;22(23):6182-92.
146. Cox GB, Jans DA, Fimmel AL, Gibson F, et al. Hypothesis. The mechanism of ATP synthase. Conformational change by rotation of the beta-subunit. *Biochim Biophys Acta*. 1984 Dec 17;768(3-4):201-8.
147. Boyer PD, and Kohlbrenner, W. E.1981. The present status of the binding-change mechanism and its relation to ATP formation by chloroplasts. *Energy Coupling in Photosynthesis* Elsevier; Amsterdam.231–40

148. Abrahams JP, Leslie AG, Lutter R, Walker JE. Structure at 2.8 Å resolution of F₁-ATPase from bovine heart mitochondria. *Nature*. 1994 Aug 25;370(6491):621-8.
149. Devenish RJ, Prescott M, Rodgers AJ. The structure and function of mitochondrial F₁F₀-ATP synthases. *Int Rev Cell Mol Biol*. 2008;267:1-58.
150. Ganti S, Vik SB. Chemical modification of mono-cysteine mutants allows a more global look at conformations of the epsilon subunit of the ATP synthase from *Escherichia coli*. *J Bioenerg Biomembr*. 2007 Feb;39(1):99-107.
151. Feniouk BA, Suzuki T, Yoshida M. Regulatory interplay between proton motive force, ADP, phosphate, and subunit epsilon in bacterial ATP synthase. *J Biol Chem*. 2007 Jan 5;282(1):764-72.
152. Suzuki T, Murakami T, Iino R, Suzuki J, et al. F₀F₁-ATPase/synthase is geared to the synthesis mode by conformational rearrangement of epsilon subunit in response to proton motive force and ADP/ATP balance. *J Biol Chem*. 2003 Nov 21;278(47):46840-6.
153. Tsunoda SP, Rodgers AJ, Aggeler R, Wilce MC, et al. Large conformational changes of the epsilon subunit in the bacterial F₁F₀ ATP synthase provide a ratchet action to regulate this rotary motor enzyme. *Proc Natl Acad Sci U S A*. 2001 Jun 5;98(12):6560-4.
154. Klein G, Satre M, Dianoux AC, Vignais PV. Photoaffinity labeling of mitochondrial adenosine triphosphatase by an azido derivative of the natural adenosine triphosphate inhibitor. *Biochemistry*. 1981 Mar 3;20(5):1339-44.
155. Hashimoto T, Negawa Y, Tagawa K. Binding of intrinsic ATPase inhibitor to mitochondrial ATPase--stoichiometry of binding of nucleotides, inhibitor, and enzyme. *J Biochem*. 1981 Oct;90(4):1151-7.
156. Pullman ME, Monroy GC. A Naturally Occurring Inhibitor of Mitochondrial Adenosine Triphosphatase. *J Biol Chem*. 1963 Nov;238:3762-9.
157. Van Heeke G, Deforce L, Schnizer RA, Shaw R, et al. Recombinant bovine heart mitochondrial F₁-ATPase inhibitor protein: overproduction in *Escherichia coli*, purification, and structural studies. *Biochemistry*. 1993 Sep 28;32(38):10140-9.
158. Kartha GK, Moshal KS, Sen U, Joshua IG, et al. Renal mitochondrial damage and protein modification in type-2 diabetes. *Acta Diabetol*. 2008 Feb 22.

159. Kaur P, Radotra B, Minz RW, Gill KD. Impaired mitochondrial energy metabolism and neuronal apoptotic cell death after chronic dichlorvos (OP) exposure in rat brain. *Neurotoxicology*. 2007 Nov;28(6):1208-19.
160. Venkatesh S, Ramachandran A, Zachariah A, Oommen A. Mitochondrial ATP synthase inhibition and nitric oxide are involved in muscle weakness that occurs in acute exposure of rats to monocrotophos. *Toxicol Mech Methods*. 2009 Mar;19(3):239-45.
161. Lowenstein CJ, Dinerman JL, Snyder SH. Nitric oxide: a physiologic messenger. *Ann Intern Med*. 1994 Feb 1;120(3):227-37.
162. Mitka M. 1998 Nobel Prize winners are announced: three discoverers of nitric oxide activity. *Jama*. 1998 Nov 18;280(19):1648.
163. Chiueh CC. Neuroprotective properties of nitric oxide. *Ann N Y Acad Sci*. 1999;890:301-11.
164. Abe K, Hayashi N, Terada H. Effect of endogenous nitric oxide on energy metabolism of rat heart mitochondria during ischemia and reperfusion. *Free Radic Biol Med*. 1999 Feb;26(3-4):379-87.
165. Alderton WK, Cooper CE, Knowles RG. Nitric oxide synthases: structure, function and inhibition. *Biochem J*. 2001 Aug 1;357(Pt 3):593-615.
166. Ghafourifar P, Richter C. Nitric oxide synthase activity in mitochondria. *FEBS Lett*. 1997 Dec 1;418(3):291-6.
167. Giulivi C, Poderoso JJ, Boveris A. Production of nitric oxide by mitochondria. *J Biol Chem*. 1998 May 1;273(18):11038-43.
168. Bryan NS, Bian K, Murad F. Discovery of the nitric oxide signaling pathway and targets for drug development. *Front Biosci*. 2009;14:1-18.
169. Murad F. Shattuck Lecture. Nitric oxide and cyclic GMP in cell signaling and drug development. *N Engl J Med*. 2006 Nov 9;355(19):2003-11.
170. Martinez-Ruiz A, Cadenas S, Lamas S. Nitric oxide signaling: classical, less classical, and nonclassical mechanisms. *Free Radic Biol Med*. Jul 1;51(1):17-29.
171. Mujoo K, Krumenacker JS, Murad F. Nitric oxide-cyclic GMP signaling in stem cell differentiation. *Free Radic Biol Med*. 2011 Dec 15;51(12):2150-7.

172. Lucas KA, Pitari GM, Kazerounian S, Ruiz-Stewart I, et al. Guanylyl cyclases and signaling by cyclic GMP. *Pharmacol Rev.* 2000 Sep;52(3):375-414.
173. Biel M, Seeliger M, Pfeifer A, Kohler K, et al. Selective loss of cone function in mice lacking the cyclic nucleotide-gated channel CNG3. *Proc Natl Acad Sci U S A.* 1999 Jun 22;96(13):7553-7.
174. Boolell M, Allen MJ, Ballard SA, Gepi-Attee S, et al. Sildenafil: an orally active type 5 cyclic GMP-specific phosphodiesterase inhibitor for the treatment of penile erectile dysfunction. *Int J Impot Res.* 1996 Jun;8(2):47-52.
175. Humbert P, Niroomand F, Fischer G, Mayer B, et al. Purification of soluble guanylyl cyclase from bovine lung by a new immunoaffinity chromatographic method. *Eur J Biochem.* 1990 Jun 20;190(2):273-8.
176. Lee YC, Martin E, Murad F. Human recombinant soluble guanylyl cyclase: expression, purification, and regulation. *Proc Natl Acad Sci U S A.* 2000 Sep 26;97(20):10763-8.
177. Federico A, Filippelli A, Falciani M, Tuccillo C, et al. Platelet aggregation is affected by nitrosothiols in patients with chronic hepatitis: in vivo and in vitro studies. *World J Gastroenterol.* 2007 Jul 21;13(27):3677-83.
178. Abiru T, Watanabe Y, Kamata K, Miyata N, et al. Decrease in endothelium-dependent relaxation and levels of cyclic nucleotides in aorta from rabbits with alloxan-induced diabetes. *Res Commun Chem Pathol Pharmacol.* 1990 Apr;68(1):13-25.
179. Huang PL, Huang Z, Mashimo H, Bloch KD, et al. Hypertension in mice lacking the gene for endothelial nitric oxide synthase. *Nature.* 1995 Sep 21;377(6546):239-42.
180. Wimalawansa SJ. Age-related changes in tissue contents of immunoreactive calcitonin gene-related peptide. *Aging (Milano).* 1992 Sep;4(3):211-7.
181. Wimalawansa SJ. Calcitonin gene-related peptide and its receptors: molecular genetics, physiology, pathophysiology, and therapeutic potentials. *Endocr Rev.* 1996 Oct;17(5):533-85.
182. Wimalawansa SJ, De Marco G, Gangula P, Yallampalli C. Nitric oxide donor alleviates ovariectomy-induced bone loss. *Bone.* 1996 Apr;18(4):301-4.
183. Yallampalli C, Dong YL, Wimalawansa SJ. Calcitonin gene-related peptide reverses the hypertension and significantly decreases the fetal mortality in

- pre-eclampsia rats induced by N(G)-nitro-L-arginine methyl ester. *Hum Reprod.* 1996 Apr;11(4):895-9.
184. Wimalawansa SJ. Antihypertensive effects of oral calcium supplementation may be mediated through the potent vasodilator CGRP. *Am J Hypertens.* 1993 Dec;6(12):996-1002.
 185. Leon L, Jeannin JF, Bettaieb A. Post-translational modifications induced by nitric oxide (NO): implication in cancer cells apoptosis. *Nitric Oxide.* 2008 Sep;19(2):77-83.
 186. Wimalawansa SJ. Amylin, calcitonin gene-related peptide, calcitonin, and adrenomedullin: a peptide superfamily. *Crit Rev Neurobiol.* 1997;11(2-3):167-239.
 187. Alonso MJ, Salaices M, Sanchez-Ferrer CF, Marin J. Predominant role for nitric oxide in the relaxation induced by acetylcholine in cat cerebral arteries. *J Pharmacol Exp Ther.* 1992 Apr;261(1):12-20.
 188. Kelly PA, Ritchie IM, Collins FM. Cerebrovascular consequences of repeated exposure to NG-nitro-L-arginine methyl ester. *Br J Pharmacol.* 1995 Nov;116(6):2771-7.
 189. Gustafsson LE, Wiklund CU, Wiklund NP, Persson MG, et al. Modulation of autonomic neuroeffector transmission by nitric oxide in guinea pig ileum. *Biochem Biophys Res Commun.* 1990 Nov 30;173(1):106-10.
 190. Sanders KM, Ward SM, Thornbury KD, Dalziel HH, et al. Nitric oxide as a non-adrenergic, non-cholinergic neurotransmitter in the gastrointestinal tract. *Jpn J Pharmacol.* 1992;58 Suppl 2:220P-5P.
 191. Martinez-Ruiz A, Lamas S. Detection and proteomic identification of S-nitrosylated proteins in endothelial cells. *Arch Biochem Biophys.* 2004 Mar 1;423(1):192-9.
 192. Wiseman H, Halliwell B. Damage to DNA by reactive oxygen and nitrogen species: role in inflammatory disease and progression to cancer. *Biochem J.* 1996 Jan 1;313 (Pt 1):17-29.
 193. Handy DE, Loscalzo J. Nitric oxide and posttranslational modification of the vascular proteome: S-nitrosation of reactive thiols. *Arterioscler Thromb Vasc Biol.* 2006 Jun;26(6):1207-14.
 194. Ischiropoulos H. Biological tyrosine nitration: a pathophysiological function of nitric oxide and reactive oxygen species. *Arch Biochem Biophys.* 1998 Aug 1;356(1):1-11.

195. Hess DT, Matsumoto A, Kim SO, Marshall HE, et al. Protein S-nitrosylation: purview and parameters. *Nat Rev Mol Cell Biol.* 2005 Feb;6(2):150-66.
196. Jeannin JF, Leon L, Cortier M, Sassi N, et al. Nitric oxide-induced resistance or sensitization to death in tumor cells. *Nitric Oxide.* 2008 Sep;19(2):158-63.
197. Ischiropoulos H. Biological selectivity and functional aspects of protein tyrosine nitration. *Biochem Biophys Res Commun.* 2003 Jun 6;305(3):776-83.
198. Aulak KS, Koeck T, Crabb JW, Stuehr DJ. Dynamics of protein nitration in cells and mitochondria. *Am J Physiol Heart Circ Physiol.* 2004 Jan;286(1):H30-8.
199. Radi R. Nitric oxide, oxidants, and protein tyrosine nitration. *Proc Natl Acad Sci U S A.* 2004 Mar 23;101(12):4003-8.
200. Mohr S, Stamler JS, Brune B. Posttranslational modification of glyceraldehyde-3-phosphate dehydrogenase by S-nitrosylation and subsequent NADH attachment. *J Biol Chem.* 1996 Feb 23;271(8):4209-14.
201. Whiteman M, Chua YL, Zhang D, Duan W, et al. Nitric oxide protects against mitochondrial permeabilization induced by glutathione depletion: role of S-nitrosylation? *Biochem Biophys Res Commun.* 2006 Jan 6;339(1):255-62.
202. Mannick JB, Schonhoff C, Papeta N, Ghafourifar P, et al. S-Nitrosylation of mitochondrial caspases. *J Cell Biol.* 2001 Sep 17;154(6):1111-6.
203. MacMillan-Crow LA, Crow JP, Kerby JD, Beckman JS, et al. Nitration and inactivation of manganese superoxide dismutase in chronic rejection of human renal allografts. *Proc Natl Acad Sci U S A.* 1996 Oct 15;93(21):11853-8.
204. Jenkins DC, Charles IG, Thomsen LL, Moss DW, et al. Roles of nitric oxide in tumor growth. *Proc Natl Acad Sci U S A.* 1995 May 9;92(10):4392-6.
205. Liu CY, Wang CH, Chen TC, Lin HC, et al. Increased level of exhaled nitric oxide and up-regulation of inducible nitric oxide synthase in patients with primary lung cancer. *Br J Cancer.* 1998 Aug;78(4):534-41.
206. Puhakka AR, Harju TH, Paakko PK, Soini YM, et al. Nitric oxide synthases are associated with bronchial dysplasia. *Lung Cancer.* 2006 Mar;51(3):275-82.

207. Ekmekcioglu S, Ellerhorst J, Smid CM, Prieto VG, et al. Inducible nitric oxide synthase and nitrotyrosine in human metastatic melanoma tumors correlate with poor survival. *Clin Cancer Res.* 2000 Dec;6(12):4768-75.
208. Bancel B, Esteve J, Souquet JC, Toyokuni S, et al. Differences in oxidative stress dependence between gastric adenocarcinoma subtypes. *World J Gastroenterol.* 2006 Feb 21;12(7):1005-12.
209. Vickers SM, MacMillan-Crow LA, Green M, Ellis C, et al. Association of increased immunostaining for inducible nitric oxide synthase and nitrotyrosine with fibroblast growth factor transformation in pancreatic cancer. *Arch Surg.* 1999 Mar;134(3):245-51.
210. Schapira AH, Cooper JM. Mitochondrial function in neurodegeneration and ageing. *Mutat Res.* 1992 Sep;275(3-6):133-43.
211. Beal MF. Mitochondria, NO and neurodegeneration. *Biochem Soc Symp.* 1999;66:43-54.
212. Kosel S, Hofhaus G, Maassen A, Vieregge P, et al. Role of mitochondria in Parkinson disease. *Biol Chem.* 1999 Jul-Aug;380(7-8):865-70.
213. Cleeter MW, Cooper JM, Darley-Usmar VM, Moncada S, et al. Reversible inhibition of cytochrome c oxidase, the terminal enzyme of the mitochondrial respiratory chain, by nitric oxide. Implications for neurodegenerative diseases. *FEBS Lett.* 1994 May 23;345(1):50-4.
214. Clementi E, Brown GC, Feelisch M, Moncada S. Persistent inhibition of cell respiration by nitric oxide: crucial role of S-nitrosylation of mitochondrial complex I and protective action of glutathione. *Proc Natl Acad Sci U S A.* 1998 Jun 23;95(13):7631-6.
215. Riobo NA, Clementi E, Melani M, Boveris A, et al. Nitric oxide inhibits mitochondrial NADH:ubiquinone reductase activity through peroxynitrite formation. *Biochem J.* 2001 Oct 1;359(Pt 1):139-45.
216. Jekabsone A, Ivanoviene L, Brown GC, Borutaite V. Nitric oxide and calcium together inactivate mitochondrial complex I and induce cytochrome c release. *J Mol Cell Cardiol.* 2003 Jul;35(7):803-9.
217. Cassina A, Radi R. Differential inhibitory action of nitric oxide and peroxynitrite on mitochondrial electron transport. *Arch Biochem Biophys.* 1996 Apr 15;328(2):309-16.
218. Welter R, Yu L, Yu CA. The effects of nitric oxide on electron transport complexes. *Arch Biochem Biophys.* 1996 Jul 1;331(1):9-14.

219. Hederstedt LO. 1992. Progress in succinate:quinone oxidoreductase research. In: Series Ernster L. seriesProgress in succinate:quinone oxidoreductase research. Elsevier Science B.V; 199 –216.
220. Rubbo H, Denicola A, Radi R. Peroxynitrite inactivates thiol-containing enzymes of Trypanosoma cruzi energetic metabolism and inhibits cell respiration. Arch Biochem Biophys. 1994 Jan;308(1):96-102.
221. Babcock GT, Wikstrom M. Oxygen activation and the conservation of energy in cell respiration. Nature. 1992 Mar 26;356(6367):301-9.
222. Brown GC, Cooper CE. Nanomolar concentrations of nitric oxide reversibly inhibit synaptosomal respiration by competing with oxygen at cytochrome oxidase. FEBS Lett. 1994 Dec 19;356(2-3):295-8.
223. Takehara Y, Kanno T, Yoshioka T, Inoue M, et al. Oxygen-dependent regulation of mitochondrial energy metabolism by nitric oxide. Arch Biochem Biophys. 1995 Oct 20;323(1):27-32.
224. Poderoso JJ, Carreras MC, Lisdero C, Riobo N, et al. Nitric oxide inhibits electron transfer and increases superoxide radical production in rat heart mitochondria and submitochondrial particles. Arch Biochem Biophys. 1996 Apr 1;328(1):85-92.
225. Poderoso JJ, Peralta JG, Lisdero CL, Carreras MC, et al. Nitric oxide regulates oxygen uptake and hydrogen peroxide release by the isolated beating rat heart. Am J Physiol. 1998 Jan;274(1 Pt 1):C112-9.
226. Radi R, Rodriguez M, Castro L, Telleri R. Inhibition of mitochondrial electron transport by peroxynitrite. Arch Biochem Biophys. 1994 Jan;308(1):89-95.
227. Borutaite V, Budriunaite A, Brown GC. Reversal of nitric oxide-, peroxynitrite- and S-nitrosothiol-induced inhibition of mitochondrial respiration or complex I activity by light and thiols. Biochim Biophys Acta. 2000 Aug 15;1459(2-3):405-12.
228. Pearce LL, Epperly MW, Greenberger JS, Pitt BR, et al. Identification of respiratory complexes I and III as mitochondrial sites of damage following exposure to ionizing radiation and nitric oxide. Nitric Oxide. 2001 Apr;5(2):128-36.
229. Zhang Y, Marcillat O, Giulivi C, Ernster L, et al. The oxidative inactivation of mitochondrial electron transport chain components and ATPase. J Biol Chem. 1990 Sep 25;265(27):16330-6.

230. Knowles RG, Moncada S. Nitric oxide synthases in mammals. *Biochem J*. 1994 Mar 1;298 (Pt 2):249-58.
231. Borda E, Berra A, Saravia M, Ganzinelli S, et al. Correlations between neuronal nitric oxide synthase and muscarinic M3/M1 receptors in the rat retina. *Exp Eye Res*. 2005 Mar;80(3):391-9.
232. Sultana R, Poon HF, Cai J, Pierce WM, et al. Identification of nitrated proteins in Alzheimer's disease brain using a redox proteomics approach. *Neurobiol Dis*. 2006 Apr;22(1):76-87.
233. Aulak KS, Miyagi M, Yan L, West KA, et al. Proteomic method identifies proteins nitrated in vivo during inflammatory challenge. *Proc Natl Acad Sci U S A*. 2001 Oct 9;98(21):12056-61.
234. Haynes V, Traaseth NJ, Elfering S, Fujisawa Y, et al. Nitration of specific tyrosines in FoF1 ATP synthase and activity loss in aging. *Am J Physiol Endocrinol Metab*. 2010 May;298(5):E978-87.
235. Sun J, Morgan M, Shen RF, Steenbergen C, et al. Preconditioning results in S-nitrosylation of proteins involved in regulation of mitochondrial energetics and calcium transport. *Circ Res*. 2007 Nov 26;101(11):1155-63.
236. Sterin-Borda L, Echague AV, Leiros CP, Genaro A, et al. Endogenous nitric oxide signalling system and the cardiac muscarinic acetylcholine receptor- inotropic response. *Br J Pharmacol*. 1995 Aug;115(8):1525-31.
237. Borda T, Genaro A, Sterin-Borda L, Cremaschi G. Involvement of endogenous nitric oxide signalling system in brain muscarinic acetylcholine receptor activation. *J Neural Transm*. 1998;105(2-3):193-204.
238. Jeyarasasingam G, Yeluashvili M, Quik M. Nitric oxide is involved in acetylcholinesterase inhibitor-induced myopathy in rats. *J Pharmacol Exp Ther*. 2000 Oct;295(1):314-20.
239. Gupta RC, Milatovic D, Dettbarn WD. Involvement of nitric oxide in myotoxicity produced by diisopropylphosphorofluoridate (DFP)-induced muscle hyperactivity. *Arch Toxicol*. 2002 Dec;76(12):715-26.
240. Kim YB, Hur GH, Lee YS, Han BG, et al. A role of nitric oxide in organophosphate-induced convulsions. *Environ Toxicol Pharmacol*. 1997 Feb 15;3(1):53-6.
241. Gupta RC, Milatovic D, Dettbarn WD. Depletion of energy metabolites following acetylcholinesterase inhibitor-induced status epilepticus: protection by antioxidants. *Neurotoxicology*. 2001 Apr;22(2):271-82.

242. Ismail N, Vairamani M, Rao RN. Determination of cis and trans isomers of monocrotophos in technical products by reversed-phase column liquid chromatography. *J Chromatogr A*. 2000 Dec;903(1-2):255-60.
243. Srinivas Rao C, Venkateswarlu V, Surender T, Eddleston M, et al. Pesticide poisoning in south India: opportunities for prevention and improved medical management. *Trop Med Int Health*. 2005 Jun;10(6):581-8.
244. Chanda SM, Mortensen SR, Moser VC, Padilla S. Tissue-specific effects of chlorpyrifos on carboxylesterase and cholinesterase activity in adult rats: an in vitro and in vivo comparison. *Fundam Appl Toxicol*. 1997 Aug;38(2):148-57.
245. Gupta RC. 2006. Classification and uses of organophosphates and carbamates In: Series series Classification and uses of organophosphates and carbamates Academic Press/Elsevier, Amsterdam;
246. De Bleecker J, Willems J, De Reuck J, Santens P, et al. Histological and histochemical study of paraoxon myopathy in the rat. *Acta Neurol Belg*. 1991;91(5):255-70.
247. Ribeiro MO, Antunes E, de Nucci G, Lovisolo SM, et al. Chronic inhibition of nitric oxide synthesis. A new model of arterial hypertension. *Hypertension*. 1992 Sep;20(3):298-303.
248. Hebeda CB, Teixeira SA, Muscara MN, Vinolo MA, et al. In vivo blockade of Ca(+2)-dependent nitric oxide synthases impairs expressions of L-selectin and PECAM-1. *Biochem Biophys Res Commun*. 2008 Dec 12;377(2):694-8.
249. Haynes LW, Smith ME, Li CH. Structural requirements and species specificity of the inhibition by beta-endorphin of heavy acetylcholinesterase from vertebrate skeletal muscle. *Mol Pharmacol*. 1984 Jul;26(1):45-50.
250. Ellman GL, Courtney KD, Andres V, Jr., Feather-Stone RM. A new and rapid colorimetric determination of acetylcholinesterase activity. *Biochem Pharmacol*. 1961 Jul;7:88-95.
251. Lowry OH, Rosebrough NJ, Farr AL, Randall RJ. Protein measurement with the Folin phenol reagent. *J Biol Chem*. 1951 Nov;193(1):265-75.
252. Pennington RJ. Biochemistry of dystrophic muscle. Mitochondrial succinate-tetrazolium reductase and adenosine triphosphatase. *Biochem J*. 1961 Sep;80:649-54.

253. Takeyama N, Matsuo N, Tanaka T. Oxidative damage to mitochondria is mediated by the Ca(2+)-dependent inner-membrane permeability transition. *Biochem J.* 1993 Sep 15;294 (Pt 3):719-25.
254. Soper JW, Pedersen PL. Isolation of an oligomycin-sensitive ATPase complex from rat liver mitochondria. *Methods Enzymol.* 1979;55:328-33.
255. Gutmann I, Wahlefeld, A.W.,. 1974. L-(+)-Lactate: determination with lactate dehydrogenase and NAD. In: Series In: Bergmeyer HUE. series L-(+)-Lactate: determination with lactate dehydrogenase and NAD. 3, 2nd ed. Academic Press, New York; 1464 -8.
256. Furst W, Hallstrom S. Simultaneous determination of myocardial nucleotides, nucleosides, purine bases and creatine phosphate by ion-pair high-performance liquid chromatography. *J Chromatogr.* 1992 Jul 1;578(1):39-44.
257. Sastry KV, Moudgal RP, Mohan J, Tyagi JS, et al. Spectrophotometric determination of serum nitrite and nitrate by copper-cadmium alloy. *Anal Biochem.* 2002 Jul 1;306(1):79-82.
258. Planitzer G, Miethke A, Baum O. Nitric oxide synthase-1 is enriched in fast-twitch oxidative myofibers. *Cell Tissue Res.* 2001 Nov;306(2):325-33.
259. Laemmli UK. Cleavage of structural proteins during the assembly of the head of bacteriophage T4. *Nature.* 1970 Aug 15;227(5259):680-5.
260. Towbin H, Staehelin T, Gordon J. Electrophoretic transfer of proteins from polyacrylamide gels to nitrocellulose sheets: procedure and some applications. *Proc Natl Acad Sci U S A.* 1979 Sep;76(9):4350-4.
261. Schagger H, von Jagow G. Blue native electrophoresis for isolation of membrane protein complexes in enzymatically active form. *Anal Biochem.* 1991 Dec;199(2):223-31.
262. Schagger H, Cramer WA, von Jagow G. Analysis of molecular masses and oligomeric states of protein complexes by blue native electrophoresis and isolation of membrane protein complexes by two-dimensional native electrophoresis. *Anal Biochem.* 1994 Mar;217(2):220-30.
263. Brookes PS, Pinner A, Ramachandran A, Coward L, et al. High throughput two-dimensional blue-native electrophoresis: a tool for functional proteomics of mitochondria and signaling complexes. *Proteomics.* 2002 Aug;2(8):969-77.

264. Schagger H, von Jagow G. Tricine-sodium dodecyl sulfate-polyacrylamide gel electrophoresis for the separation of proteins in the range from 1 to 100 kDa. *Anal Biochem.* 1987 Nov 1;166(2):368-79.
265. Voordijk S, Walther, D., Bouchet, G., Appel, R.D.2003. Image Analysis Tools in Proteomics. *Encyclopedia of the human genome* Macmillan Publishers Ltd, Nature Publishing Group; London.404 - 10
266. Messina S, Altavilla D, Aguenouz M, Seminara P, et al. Lipid peroxidation inhibition blunts nuclear factor-kappaB activation, reduces skeletal muscle degeneration, and enhances muscle function in mdx mice. *Am J Pathol.* 2006 Mar;168(3):918-26.
267. Mucke W. Metabolism of monocrotophos in animals. *Rev Environ Contam Toxicol.* 1994;139:59-65.
268. Eddleston M, Buckley NA, Eyer P, Dawson AH. Management of acute organophosphorus pesticide poisoning. *Lancet.* 2008 Feb 16;371(9612):597-607.
269. Bardin PG, van Eeden SF, Moolman JA, Foden AP, et al. Organophosphate and carbamate poisoning. *Arch Intern Med.* 1994 Jul 11;154(13):1433-41.
270. Tafuri J, Roberts J. Organophosphate poisoning. *Ann Emerg Med.* 1987 Feb;16(2):193-202.
271. Vanneste Y, Lison D. Biochemical changes associated with muscle fibre necrosis after experimental organophosphate poisoning. *Hum Exp Toxicol.* 1993 Sep;12(5):365-70.
272. Yen DH, Chan JY, Tseng HP, Huang CI, et al. Depression of mitochondrial respiratory enzyme activity in rostral ventrolateral medulla during acute mevinphos intoxication in the rat. *Shock.* 2004 Apr;21(4):358-63.
273. Yen DH, Chan JY, Huang CI, Lee CH, et al. Coenzyme q10 confers cardiovascular protection against acute mevinphos intoxication by ameliorating bioenergetic failure and hypoxia in the rostral ventrolateral medulla of the rat. *Shock.* 2005 Apr;23(4):353-9.
274. Carlson K, Ehrich M. Organophosphorus compound-induced modification of SH-SY5Y human neuroblastoma mitochondrial transmembrane potential. *Toxicol Appl Pharmacol.* 1999 Oct 1;160(1):33-42.
275. Zimmer HG, Trendelenburg C, Gerlach E. Acceleration of adenine nucleotide synthesis de novo during development of cardiac hypertrophy. *J Mol Cell Cardiol.* 1972 Jun;4(3):279-82.

276. Zimmer HG, Trendelenburg C, Kammermeier H, Gerlach E. De novo synthesis of myocardial adenine nucleotides in the rat. Acceleration during recovery from oxygen deficiency. *Circ Res.* 1973 May;32(5):635-42.
277. Li FC, Tseng HP, Chang AY. Neuroprotective role of coenzyme Q10 against dysfunction of mitochondrial respiratory chain at rostral ventrolateral medulla during fatal mevinphos intoxication in the rat. *Ann N Y Acad Sci.* 2005 May;1042:195-202.
278. Yang D, Lu X, Zhang W, He F. Biochemical changes in primary culture of skeletal muscle cells following dimethoate exposure. *Toxicology.* 2002 May 24;174(2):79-85.
279. Armstrong JS, Yang H, Duan W, Whiteman M. Cytochrome bc(1) regulates the mitochondrial permeability transition by two distinct pathways. *J Biol Chem.* 2004 Nov 26;279(48):50420-8.
280. Kroemer G. Mitochondrial control of apoptosis: an introduction. *Biochem Biophys Res Commun.* 2003 May 9;304(3):433-5.
281. Folbergrova J, Jesina P, Drahota Z, Lisy V, et al. Mitochondrial complex I inhibition in cerebral cortex of immature rats following homocysteic acid-induced seizures. *Exp Neurol.* 2007 Apr;204(2):597-609.
282. Nguyen N, Gonzalez SV, Rise F, Hassel B. Cerebral metabolism of glucose and pyruvate in soman poisoning. A ¹³C nuclear magnetic resonance spectroscopic study. *Neurotoxicology.* 2007 Jan;28(1):13-8.
283. Brenman JE, Chao DS, Xia H, Aldape K, et al. Nitric oxide synthase complexed with dystrophin and absent from skeletal muscle sarcolemma in Duchenne muscular dystrophy. *Cell.* 1995 Sep 8;82(5):743-52.
284. Kobzik L, Reid MB, Bredt DS, Stamler JS. Nitric oxide in skeletal muscle. *Nature.* 1994 Dec 8;372(6506):546-8.
285. Nakane M, Schmidt HH, Pollock JS, Forstermann U, et al. Cloned human brain nitric oxide synthase is highly expressed in skeletal muscle. *FEBS Lett.* 1993 Jan 25;316(2):175-80.
286. Chan JY, Chan SH, Chang AY. Differential contributions of NOS isoforms in the rostral ventrolateral medulla to cardiovascular responses associated with mevinphos intoxication in the rat. *Neuropharmacology.* 2004 Jun;46(8):1184-94.
287. Ramachandran A, Ceaser E, Darley-Usmar VM. Chronic exposure to nitric oxide alters the free iron pool in endothelial cells: role of mitochondrial

- respiratory complexes and heat shock proteins. *Proc Natl Acad Sci U S A*. 2004 Jan 6;101(1):384-9.
288. Choi KS, Park SY, Baek SH, Dey-Rao R, et al. Analysis of protein redox modification by hypoxia. *Prep Biochem Biotechnol*. 2006;36(1):65-79.
289. Kim JR, Yoon HW, Kwon KS, Lee SR, et al. Identification of proteins containing cysteine residues that are sensitive to oxidation by hydrogen peroxide at neutral pH. *Anal Biochem*. 2000 Aug 1;283(2):214-21.
290. Takashima M, Kuramitsu Y, Yokoyama Y, Iizuka N, et al. Proteomic profiling of heat shock protein 70 family members as biomarkers for hepatitis C virus-related hepatocellular carcinoma. *Proteomics*. 2003 Dec;3(12):2487-93.
291. Webster TJ, Naylor DJ, Hartman DJ, Hoj PB, et al. cDNA cloning and efficient mitochondrial import of pre-mtHSP70 from rat liver. *DNA Cell Biol*. 1994 Dec;13(12):1213-20.
292. Kang PJ, Ostermann J, Shilling J, Neupert W, et al. Requirement for hsp70 in the mitochondrial matrix for translocation and folding of precursor proteins. *Nature*. 1990 Nov 8;348(6297):137-43.
293. Eaton P, Jones ME, McGregor E, Dunn MJ, et al. Reversible cysteine-targeted oxidation of proteins during renal oxidative stress. *J Am Soc Nephrol*. 2003 Aug;14(8 Suppl 3):S290-6.
294. Celik I, Suzek H. Subacute effects of methyl parathion on antioxidant defense systems and lipid peroxidation in rats. *Food Chem Toxicol*. 2008 Aug;46(8):2796-801.
295. Khan SM, Sobti RC, Kataria L. Pesticide-induced alteration in mice hepato-oxidative status and protective effects of black tea extract. *Clin Chim Acta*. 2005 Aug;358(1-2):131-8.
296. Bolanos JP, Heales SJ, Peuchen S, Barker JE, et al. Nitric oxide-mediated mitochondrial damage: a potential neuroprotective role for glutathione. *Free Radic Biol Med*. 1996;21(7):995-1001.
297. Moellering D, McAndrew J, Patel RP, Cornwell T, et al. Nitric oxide-dependent induction of glutathione synthesis through increased expression of gamma-glutamylcysteine synthetase. *Arch Biochem Biophys*. 1998 Oct 1;358(1):74-82.
298. Cardoso SM, Pereira C, Oliveira R. Mitochondrial function is differentially affected upon oxidative stress. *Free Radic Biol Med*. 1999 Jan;26(1-2):3-13.

299. Monica FZ, Bricola AA, Bau FR, Freitas LL, et al. Long-term nitric oxide deficiency causes muscarinic supersensitivity and reduces beta(3)-adrenoceptor-mediated relaxation, causing rat detrusor overactivity. *Br J Pharmacol.* 2008 Apr;153(8):1659-68.
300. Morley JE, Flood JF. Effect of competitive antagonism of NO synthetase on weight and food intake in obese and diabetic mice. *Am J Physiol.* 1994 Jan;266(1 Pt 2):R164-8.
301. Furstenau CR, Ramos DB, Vuaden FC, Casali EA, et al. L-NAME-treatment alters ectonucleotidase activities in kidney membranes of rats. *Life Sci.* 2010 Aug 28;87(9-10):325-32.
302. Delwing D, Delwing D, Bavaresco CS, Wyse AT. Protective effect of nitric oxide synthase inhibition or antioxidants on brain oxidative damage caused by intracerebroventricular arginine administration. *Brain Res.* 2008 Feb 8;1193:120-7.
303. Pritchard KA, Jr., Groszek L, Smalley DM, Sessa WC, et al. Native low-density lipoprotein increases endothelial cell nitric oxide synthase generation of superoxide anion. *Circ Res.* 1995 Sep;77(3):510-8.
304. Abu-Soud HM, Feldman PL, Clark P, Stuehr DJ. Electron transfer in the nitric-oxide synthases. Characterization of L-arginine analogs that block heme iron reduction. *J Biol Chem.* 1994 Dec 23;269(51):32318-26.
305. Ecobichon DJ, Zelt D. The acute toxicity of fenitrothion in weanling rats and effects on tissue esterases and mono-oxygenases. *Toxicology.* 1979 Aug;13(3):287-96.

Publication

1. **Raghupathy V**, Poornima S, Sivaguru J, Ramachandran A, A.Zachariah, A. Oommen. Monocrotophos toxicity and bioenergetics of muscle weakness in the rat. **Toxicology**. Nov 9: 277 (1 -3): 6 – 10.